HYDRODYNAMICS OF THREE-PHASE FLUIDIZED BEDS

OAK RIDGE NATIONAL LAB., TN

JUL 1978

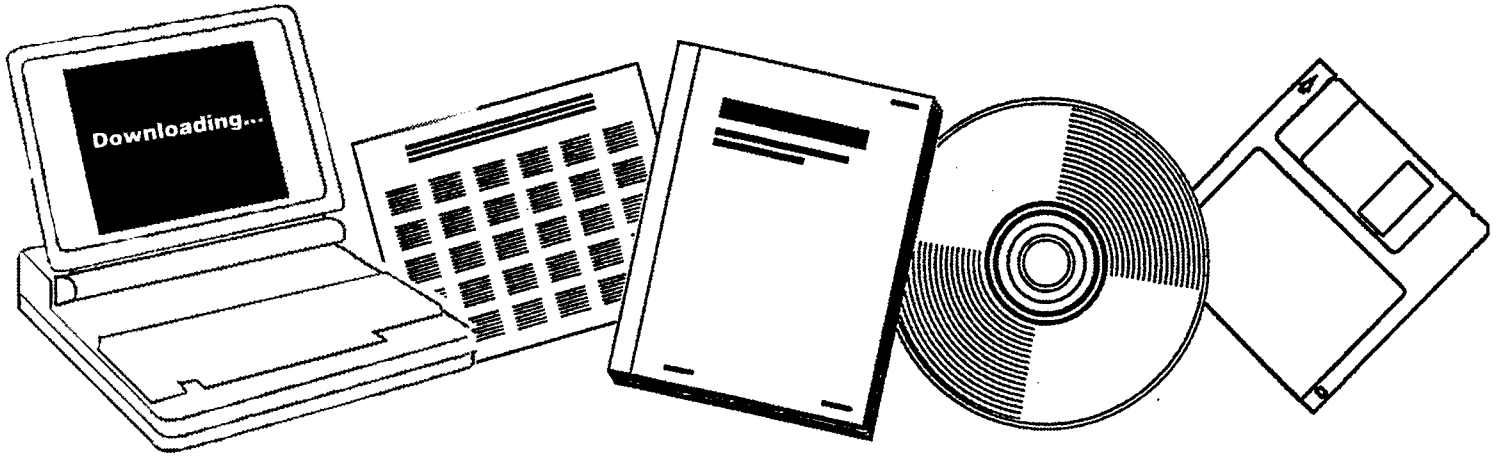

ORNL/TM-6448

Contract No. W-7405-eng-26

CHEMICAL TECHNOLOGY DIVISION

HYDRODYNAMICS OF THREE-PHASE FLUIDIZED BEDS

J. M. Begovich

This report was prepared as a thesis and submitted to the Faculty of the Graduate School of The University of Tennessee in partial fulfillment of the degree of Master of Science in the Department of Chemical, Metallurgical, and Polymer Engineering.

Date Published: July 1978

OAK RIDGE NATIONAL LABORATORY
Oak Ridge, Tennessee 37830
operated by
UNION CARBIDE CORPORATION
for the
DEPARTMENT OF ENERGY

ACKNOWLEDGMENTS

This research was sponsored by the Department of Energy under contract with the Union Carbide Corporation.

The writer wishes to acknowledge the support and numerous helpful suggestions of Dr. J. S. Watson of the Chemical Technology Division, Oak Ridge National Laboratory and the Chemical, Metallurgical, and Polymer Engineering Department, University of Tennessee.

The writer is grateful to K. J. Beach of the Tennessee Technological University, J. D. Cohill and M. R. McClure of the University of Tennessee, D. Sellinger of the Georgia Institute of Technology, and J. D. Hewitt of the Chemical Technology Division for their assistance in the collection of data.

The writer is particularly indebted to C. L. Begovich, his wife and a member of the Computer Sciences Division of the Oak Ridge National Laboratory. She not only was constantly supportive and understanding, but she was also responsible for a large part of the typing and computer analysis presented herein.

Special appreciation is expressed to M. G. Stewart of the Chemical Technology Division for editing this manuscript. The line drawings were prepared under the supervision of R. P. Edwards of the Engineering Division, Oak Ridge National Laboratory.

ABSTRACT

The hydrodynamics of three-phase (gas-liquid-solid) fluidized beds has been studied in two columns with inside diameters of 7.62 and 15.2 cm respectively. The minimum gas and liquid velocities necessary to fluidize various types of solids were determined and correlated as a function of the particle size and density and the liquid viscosity; no effect of the initial bed height or column diameter was found.

Overall phase holdups, or volume fractions, determined from a homogeneous bed model were combined with similar literature data to yield correlations for the overall gas and solid phase holdups. The overall gas holdup increased as the gas velocity was increased, while the overall solid holdup was decreased by increased liquid velocity and was increased by increased particle diameter or solid/liquid density difference.

An electroconductivity technique was developed for use in the three-phase fluidized beds which allowed each of the phase holdups to be determined at any point in the column. The technique has shown the existence of a transition region as the bed goes from a three-phase to a two-phase system. The holdup profiles were fitted using the error function, and the mean and standard deviation of the solid holdup profile, along with the gas and solid holdups in the regions where they were constant, were measured for each set of run

conditions. Use of these five parameters, which were correlated with the physical parameters of the systems studied, permits each of the three phase holdup profiles to be predicted. This gives the reactor designer more information concerning phase distributions than was available previously; thus it will aid in the design of reactors where local conditions throughout the bed must be considered.

TABLE OF CONTENTS

APPENDIXES PAGE

LIST OF TABLES

LIST OF FIGURES

FIGURE PAGE

FIGURE PAGE

FIGURE PAGE

LIST OF SYMBOLS

A	cross-sectional column area, L^2
Ar	Archimedes number, $d_p^3 \rho_L (\rho_S - \rho_L) g / \mu_L^2$
a-g	constants used in data correlations
c	solids concentration, M/L^3
C_D	Drag coefficient, $(\rho_S - \rho_L) d_p / U_G^2 \rho_L$
D_c	column diameter, L
d_p	particle diameter, L
$\bar{d}_p$	average particle diameter, L
erf(x)	error function, $\frac{2}{\sqrt{\pi}} \int_0^x e^{-z^2} dz$
Fr	Froude number, U^2/gL
Fr_H	Froude number based on bed height, U^2/gH
g	acceleration due to gravity, L/T^2
Ga	Galileo number, $d_p^3 \rho^2 g / \mu^2$
h	axial column position, L
Δh	difference in manometer readings, pressure drop, L
H	expanded bed height, L
H_L	dynamic liquid height, L
$H_{L,o}$	settled liquid height, L
I	inflection point in local holdup versus height curve, L
k	fluid consistency index
K	ratio of wake volume to bubble volume,
M	mass, M
m	mamometer reading, L
ΔP	pressure drop across bed, M/LT^2

P curve-fitting parameter, defined in Eqs. (32)-(35)

Re Reynolds number,

T pressure tap height above bottom of column, L

U superficial velocity, L/T

$\bar{U}$ actual velocity, L/T

U_t terminal free-fall particle velocity, L/T

v_S slip velocity, L/T

We Weber number, $U\mu/\sigma_{LV}$

W_{SLV} work of adhesion, M/T^2

Greek Letters

γ conductivity in the bed

γ_o conductivity in liquid alone

ε bed porosity

ε_i phase holdup (volume fraction)

$\bar{\varepsilon}$ average holdup

Θ liquid contact angle on a solid surface, rad

μ phase viscosity, M/LT

ρ phase density, M/L^3

σ standard deviation, L

σ_{LV} interfacial tension, M/T^2

$\Phi(x)$ probability integral, $\frac{1}{\sqrt{2\pi}} \int_o^x e^{-w^2/2} dw$

Ψ contraction/expansion characteristics, defined in Eq. (17), L/T

Subscripts

Bed	across bed
C	conductivity method
G	gas phase
L	liquid phase
mf	minimum fluidization
ΔP	pressure gradient method
S	solid phase
W	bubble wake phase

Superscripts

'''	three-phase
''	two-phase

Dimension

L	length, cm
M	mass, g
T	time, sec

CHAPTER 1

INTRODUCTION AND SIGNIFICANCE

A three-phase fluidized bed consists of solid phase particles fluidized by a gas and liquid flow. Although many schemes for contacting the three phases are possible [Ostergaard, 1971], a common approach is to fluidize the solid phase by the upward cocurrent flow of gas and liquid. The liquid forms the continuous phase, while the gas and solids are discontinuous phases. Applications for this type of system include the hydrogenation of liquid petroleum fractions [Pichler et al., 1957], the hydrogenation of unsaturated fats, liquid-phase methanation [Blum and Toman, 1977], coal conversion processes, and some biological reactors [Scott et al., 1976].

Of particular interest is the coal liquefaction process known as the "H-Coal process" [Hellwig et al., 1968], which involves cocurrent contact of hydrogen with a slurry of dried and pulverized coal in a coal-derived liquid in a reactor containing fluidized catalyst particles. Since the use and importance of three-phase fluidized beds are expected to increase with development of coal conversion processes, a program was initiated in the Advanced Technology Section (formerly the Experimental Engineering Section) of the Chemical Technology Division of Oak Ridge National Laboratory to study the operating characteristics of these contactors. Although some mass transfer experiments had been conducted in three-phase fluidized beds

[Saad et al., 1975; Burck et al., 1975], it became apparent that the hydrodynamics of these reactors was not understood well enough to permit meaningful interpretation of the mass transfer data. In addition, accurate design of three-phase fluidized bed reactors is complicated by such factors as (a) knowledge of the minimum fluid velocities required to achieve fluidization, and (b) axial variations in reactor properties, particularly distribution of the solid phase. No published data or equations are available for predicting reactor performance under high fluid flow rates where axial variations are important, and only a limited amount of data exists for predicting minimum fluidization velocities in three-phase fluidized beds. Once these hydrodynamic characteristics are known, mass transfer experiments can then be intelligently planned and the results accurately interpreted.

CHAPTER 2

THEORY

Measurement of Holdups and Minimum Fluidization Velocities

The holdup of one phase in a multiphase system is defined as the fraction of the system volume occupied by that phase. Thus, a three-phase fluidized bed has three such volume fractions related by the following equation:

$$\varepsilon_L + \varepsilon_G + \varepsilon_S = 1 \ , \qquad (1)$$

where

ε = holdup,

and subscripts

G = gas phase,

L = liquid phase,

S = solid phase.

If wall shear effects are neglected, the volume fractions are also related to the pressure drop over the bed [Ostergaard, 1971]:

$$\Delta P = gH(\varepsilon_L\rho_L + \varepsilon_G\rho_G + \varepsilon_S\rho_S) \ , \qquad (2)$$

where

ΔP = pressure drop over the bed,

g = acceleration due to gravity,

H = expanded bed height,

ρ = density.

The solids volume fraction can be calculated from the expanded bed height using Eq.(3):

$$\varepsilon_S = M_S/\rho_S AH \quad , \tag{3}$$

where

M_S = total mass of solids,

A = cross-sectional area of the bed.

Equations (1)-(3) are sufficient to solve for the three holdups, provided the pressure drop and expanded bed height measurements are accurate. Gas holdup can also be determined by simultaneously stopping all flows and measuring the settled liquid height, $H_{L,o}$. The gas volume fraction is then calculated since

$$\varepsilon_G = (H_L - H_{L,o})/H_L \quad , \tag{4}$$

where

H_L = dynamic height of the liquid in the column.

The gas and liquid holdups could be determined from measurements of the mean residence times of the fluid phases using tracer techniques. These techniques measure the actual linear velocities in the bed. The volume fractions are then easily calculated:

$$\varepsilon_G = U_G/\overline{U}_G \quad , \tag{5}$$

$$\varepsilon_L = U_L/\overline{U}_L \quad , \tag{6}$$

where

U = superficial velocity based on an empty column,

$\bar{U}$ = actual velocity in the bed.

The minimum fluid velocities required to achieve fluidization are determined by measuring the pressure drop across the bed. At the minimum fluidization velocities, the upward inertial and drag forces exerted on the solid particles by the fluids balance the buoyant weight of the solids. There is no further change in pressure drop across the bed at velocities above minimum fluidization until entrainment occurs.

Discussion of Holdup Measurement Techniques

Use of Eqs. (1)-(3) to determine the three phase holdups requires an accurate measurement of the expanded bed height and assumes that each phase volume fraction is constant over this bed height. This is, in general, true for heavy or large solid particles and moderate flow rates. Virtually all the data from the literature have been reported for such systems. While some processes are expected to operate with distinct bed heights, it is quite likely that the flow rates and solid particle densities in many processes will be in operating regions where the bed heights are not clearly defined and the volume fractions are not uniform over the entire bed.

An example is shown in Fig. 1, where -8+10 mesh alumina was fluidized by water and air in a 7.62-cm-ID plexiglass column. The water and gas velocities were 2.5

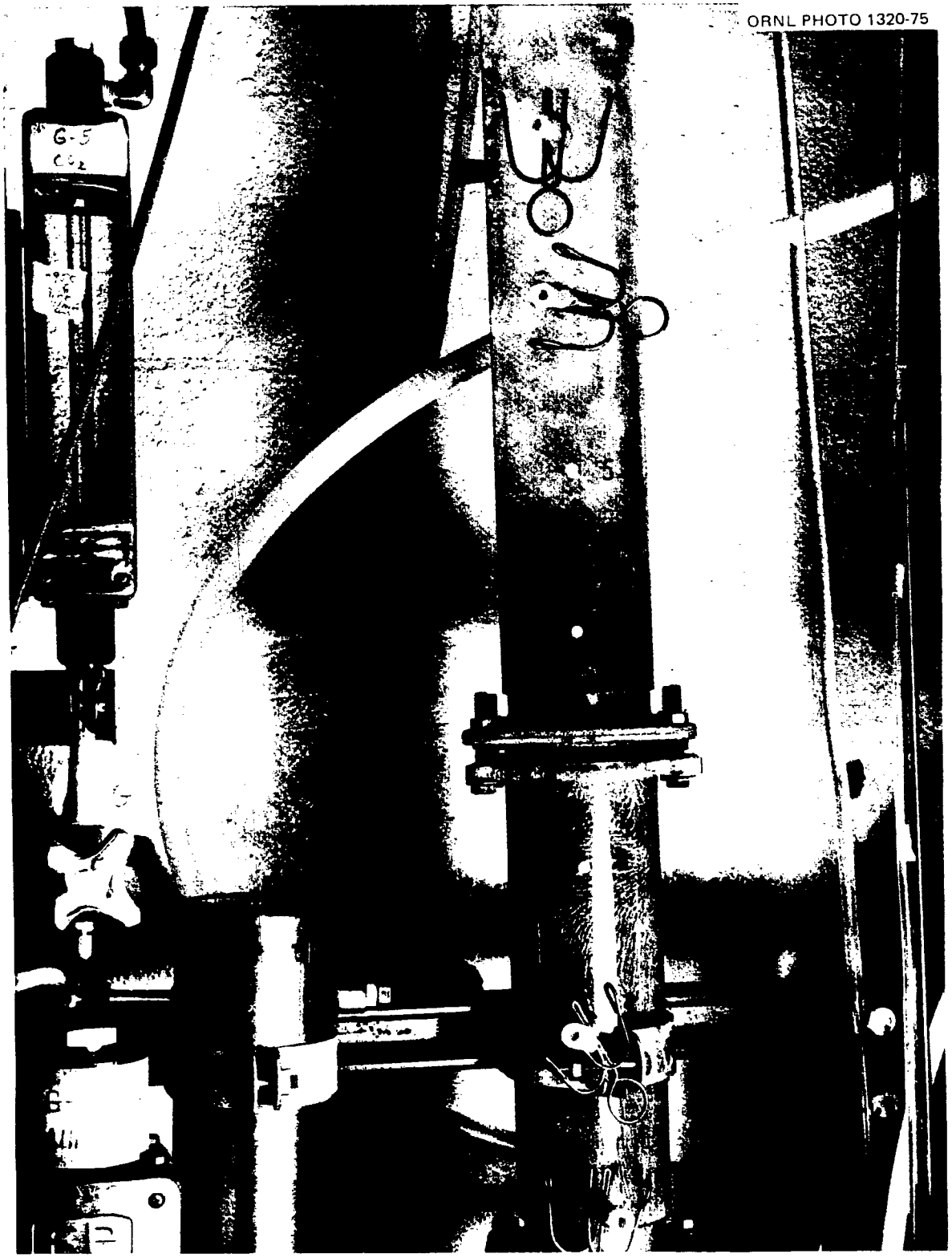

Figure 1. Fluidization of -8+12 mesh molecular sieves with air and water.

and 3.8 cm/sec, respectively. Alumina, which has a density of approximately 1.8 g/cm^3, is the most likely catalyst support for a coal liquefaction process. As can be seen in the figure, the fluidized bed does not occupy the entire column. The concentration of solids appears to be uniform in the lower section of the column, while a more dilute region exists in the middle. Above sample port 5, the column is essentially a bubble column with no solids present. The bed height is certainly not distinct; therefore, Eq. (3) could not be used.

A bed height could be obtained from the measured pressure gradient as suggested by Kim et al. [1972] and Bhatia and Epstein [1974]. The bed height obtained in this manner, however, is that height at which the pressure gradients in the two- and three-phase regions intersect, as shown in Fig. 2, and is based on a uniform bed. As shown in Fig. 1, this is an unrealistic assumption at high fluid flow rates.

By simultaneously shutting off all flows, one could use Eq. (4) to obtain an average gas volume fraction over the entire column. The gas holdup in the fluidized-bed region could be separated from that in the bubble column region by using two different bed heights. This results in two simultaneous equations which can be solved for the holdups in the fluidized bed and in the bubble column. Unfortunately, this method also requires distinct bed heights.

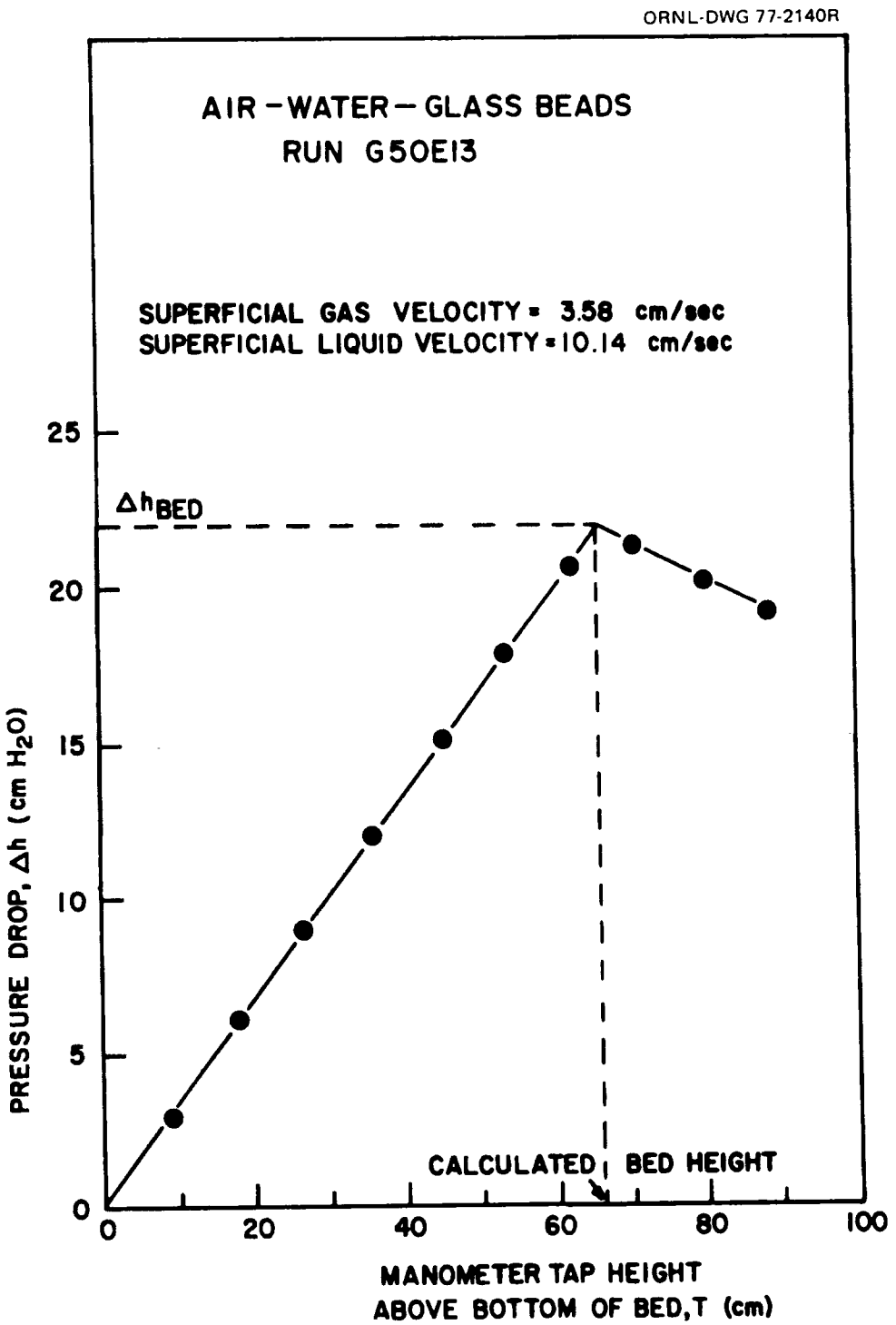

Figure 2. Use of the pressure drop profile over the column to obtain the bed height and bed pressure drop.

Another possible method for obtaining the solid holdup as a function of height (and thus the remaining holdups using Eqs. (1) and (2)) is a photographic technique [Watson, 1975]. Pictures taken of a bed with a known ratio of particles distinguishable from the remainder of the solid particles in the bed can be statistically evaluated for the incremental solids volume fraction.

Use of a tracer technique and Eqs. (5) and (6) yields an average value for the liquid and gas holdups over the measurement interval. Consequently, the holdups could be obtained at various bed heights by selecting sufficiently small measurement intervals. However, since the fluids flow cocurrently, the measuring devices would need to have shorter (faster) response times than those presently available.

An electrical conductivity method for obtaining the liquid holdup in two-phase packed beds has been described by Achwal and Stepanek [1975]. Although these investigators applied the method only to a packed column with no liquid flow, it could also be utilized for incremental sections of a three-phase fluidized bed. Their method involves measuring the conductivity of a liquid between two electrodes. The conductivity of a liquid system with a fixed ion concentration at constant conditions is proportional to the cross-sectional area of the conducting liquid and inversely proportional to the length of the path between electrodes. Thus, if the tortuosity factor remains

approximately constant, the conductivity should vary in proportion to the liquid volume fraction between the electrodes:

$$\varepsilon_L = \gamma/\gamma_o \quad , \tag{7}$$

where

γ = conductivity in the bed,

γ_o = conductivity in the liquid alone.

Similar procedures based on the same principle have been reported by several investigators. Turner [1976] measured the conductivity of liquid fluidized beds of both conducting and nonconducting solids. He found that his data for nonconducting solids followed the Maxwell [1881] equation, simplified for the case of nonconducting particles, as follows:

$$\gamma/\gamma_o = (1 - \varepsilon_S)/(1 + \varepsilon_S/2) \quad . \tag{8}$$

For two-phase fluidization, Eq. (8) can be presented in terms of liquid holdup as:

$$\varepsilon_L = (3\gamma/\gamma_o)/(2 + \gamma/\gamma_o) \quad . \tag{9}$$

Other investigators have proposed equations which yield results similar to those given by the Maxwell equation; these have been reviewed by Meredith and Tobias [1962].

Buyevich [1974] and Francl and Kingery [1954] measured the thermal conductivity of granular beds and, through the mathematical analogy between thermal and electrical

conductivity, arrived at Eq. (7). Our own measurements on two- and three-phase fluidized beds, as will be shown later, also indicate that Eq. (7) was more applicable.

Once the liquid holdup is determined as a function of height in the bed, Eq. (1) as well as a modification of Eq. (2),

$$dP/dh = g(\varepsilon_L \rho_L + \varepsilon_G \rho_G + \varepsilon_S \rho_S) \quad , \qquad (10)$$

where

h = axial column position,

can be used to obtain the solid and gas holdups as functions of height. This method does not require a distinct bed height and hence allows the study of systems with high fluid flow rates, which are of particular commercial interest.

CHAPTER 3

LITERATURE SURVEY

Three-phase fluidization has only recently become the subject of systematic research. Thus, the relevant information available in the literature is scattered and incomplete. This review will consider each hydrodynamic variable separately and will include the overall holdup of each phase and minimum fluidization velocities.

Gas Holdup

Adlington and Thompson [1965] reported results from experiments on two systems. In the first system, alumina particles with diameters ranging from 0.3 to 2.7 mm were fluidized by white spirit in a 7.62-cm-diam column. The bed height varied from 0 to 610 cm. In the second system, 0.3-mm-diam sand particles were fluidized by water in a 25.4-cm-diam column with bed heights ranging from 0 to 244 cm. Qualitatively, their results showed that the gas holdup (a) increased with height up the column, (b) increased markedly with gas rate, (c) was independent of liquid flow rate over the range investigated, and (d) was independent of the settled bed height. They also found that the presence of solids had little influence on gas holdup below superficial gas velocities of 1.5 cm/sec. At higher gas velocities, the presence of solids caused a decrease in gas holdup as compared to a solids-free system, particularly in

the denser beds prevailing at lower liquid flow rates.

Viswanathan et al. [1964] measured gas holdup in a 5.08-cm-diam column using air, water, and both glass beads and quartz particles. The glass beads were 4 mm in diameter, while the quartz particles had diameters of either 0.928 or 0.649 mm. The holdup was determined by simultaneous closing of two valves within the fluidized bed. In comparing the three-phase fluidized bed with a bubble column, they found that the presence of the glass beads increased the gas holdup, whereas the presence of the quartz particles decreased the gas holdup.

Sherrard [1966] estimated the gas holdup by measurements of gamma-ray transmission immediately above the bed surface in a column that was 6.35 cm square and 183 cm long. Water and air were used as the fluidizing media. Sherrard's results showed that gas holdup decreased with increasing liquid flow rate in beds of 6.35-mm glass spheres, 6.35-mm acrylic spheres, and 12-14 mesh lead shot, whereas it was independent of liquid flow rate in beds of 12-14 mesh and 36-44 mesh glass beads.

Schugerl [1967] measured gas holdup in an air-water fluidized bed of 0.25-mm solid particles in a 13.5-cm-diam column by simultaneously stopping all flows. Although the amount of solids used was low (2 kg of solids in a 46-liter column), it was observed that the gas holdup was smaller in the three-phase fluidized bed than in a cocurrent bubble column. Also, the difference in gas holdup between the two

systems increased with air flow rate and decreased with water flow rate.

Vail et al. [1970] studied an air-water-solids system in a 14.6-cm-diam column using a range of solid concentrations and two gas distributors. Gas holdup was determined by simultaneously stopping all flows and using Eq. (4). Three solids were used: (a) 0.73-mm-diam glass beads, (b) 0.77-mm-diam alumino-silicate particles, and (c) 0.740-mm alumino-cobalt-molybdenum particles. The gas distributors were perforated plates with free cross sections of 1.03 and 0.26% of the vessel's free cross section. These investigators found that the gas holdup was directly proportional to the gas/liquid velocity ratio, inversely proportional to the solids concentration, and independent of the free cross section of the distributors used.

Efremov and Vakhrushev [1970] studied air, water, and glass spheres in 10-cm-diam fluidized beds. Five sizes of glass spheres, with diameters ranging from 0.32 to 2.15 mm, were used. The amount of solids used varied from 1 to 9 kg. The gas holdup was determined by using the difference of the change in manometer readings of the entire column and the bubble column region divided by the bed height. They found that the gas holdup increased with gas flow rate and decreased with increasing solids concentration.

Ostergaard and Michelsen [1968] measured gas holdup for air-water fluidized beds of 0.25- ,1- , and 6-mm glass spheres contained in a 21.6-cm-diam column using a tracer

method over the entire bed. They found that gas holdup increased with increasing gas velocity for all solids used. For beds of 6-mm spheres and a bubble column, gas holdup decreased with increasing liquid velocity. However, for beds of smaller particles, gas holdup increased with increasing liquid velocity. The gas holdup was also found to be markedly lower for beds of small particles (0.25 and 1 mm) than for solids-free systems; the reverse was true for beds of 6-mm particles. However, as the liquid velocity was increased, all three solids systems tended to approximate to the values for gas holdup in a bubble column.

Bhatia and Epstein [1974] utilized two methods in measuring gas holdup for air-water fluidized beds of 1-mm glass spheres and 2-mm lead shot in a 5.08-cm-diam column. These were: (a) the simultaneous shutoff of all flows, and (b) measurement of the pressure gradient. Although their bed heights were not distinct, an experimental bed height was determined by finding the intersection of the pressure gradient over the three-phase region with that over the bubble column region. Bed heights obtained in this manner represent the height of the three-phase region for uniform solids distribution, whereas the visual upper limit of solids may be considerably higher. Gas holdup in beds of 1-mm glass spheres increased with increasing gas flow rate but was unaffected by liquid flow rate. Gas holdup was slightly less in the three-phase system than in a bubble column. Using beds of 2-mm lead shot, these investigators

found that the gas holdup decreased with increasing liquid flow rate and was proportional to the gas flow rate.

Kim et al. [1972] studied gas holdup in a "two-dimensional" bed of 6-mm glass spheres fluidized by air and water. The column was 244 cm high by 66 cm wide by 2.54 cm thick. They found that the presence of the solids decreased the gas holdup as compared with a bubble column. Gas holdup again increased with increasing gas flow rate and decreased slightly with increasing liquid flow rate.

Bloxom et al. [1975] studied gas holdup in a 7.62-cm-diam column using air, water-glycerol solutions, and 4.6-mm glass spheres. They found that the gas holdup was unaffected by the viscosity of the liquid in the range 1 to 11.5 cP and was only slightly influenced by the liquid velocity. Their data fit the following correlation:

$$\bar{\varepsilon}_G = 0.150(U_G^5 \rho_L / U_L \sigma_{LV} g)^{0.100} , \qquad (11)$$

where

$\bar{\varepsilon}$ = overall phase holdup,

σ_{LV} = liquid-gas interfacial tension.

Solid Holdup and Bed Porosity

Bed porosity is defined as the volume fraction of the bed not occupied by the solid phase. Thus, bed porosity, ε, is the sum of the gas and liquid volume fractions. Using Eq. (1):

$$\varepsilon = \varepsilon_G + \varepsilon_L = 1 - \varepsilon_S . \qquad (12)$$

An examination of Eq. (12) shows that a discussion of bed porosity is actually a discussion of solid holdup.

When a bed of particles is fluidized by a liquid, the porosity of the bed is proportional to the liquid flow rate and has been empirically correlated by Richardson and Zaki [1954]:

$$\varepsilon = (U_L/U_t)^{1/n} \quad , \tag{13}$$

where

U_t = terminal free fall velocity of the particle,

n = a function of the particle Reynolds number at U_t.

However, if the liquid flow is maintained at a constant level, the introduction of gas can sometimes decrease the bed porosity. This unique phenomenon has been the subject of considerable study.

Stewart and Davidson [1964] have advanced the following explanation based on experiments with 0.046-cm-diam glass, iron, and lead beads in a 0.635-cm x 6.35-cm two-dimensional column. As an air bubble rises through the water-fluidized bed, it is followed by water which is almost particle-free. They described this water as a wake and assumed that it traveled at a velocity similar to the bubble velocity, which may be much greater than the average liquid velocity. For the same superficial liquid velocity, the actual liquid velocity in the liquid fluidized phase is therefore reduced and the bed porosity decreases in the manner indicated by Eq. (13).

Efremov and Vakhrushev [1970], using the system described earlier, found that the bed porosity decreased with increasing gas and decreasing liquid flow rates in beds of 0.61-mm-diam glass spheres. The effect of liquid flow rates was observed to be the same, in beds of 2.15-mm glass spheres; however gas flow rates had essentially no effect on the bed porosity. These results were found to be in good agreement with the data of Ostergaard and Thiesen [1966].

Rigby and Capes [1970] reported similar results using three sizes of glass beads (0.29, 0.47, and 0.775 mm diam) in a 10-cm-diam column. They defined another volume fraction, ε_W, as the fractional bed volume occupied by bubble wakes and studied the ratio $\varepsilon_W/\varepsilon_G$. This ratio was directly proportional to the particle diameter and the liquid flow rate but inversely proportional to the gas bubble diameter and gas flow rate. From a photographic study of the 0.775-mm particles in a two-dimensional column (15 x 45 x 0.7 cm), they also concluded that the contraction of a liquid fluidized bed upon injection of a gas is caused by the presence of wakes and that these wakes consist of a stable portion carried with the bubbles as well as vortices shed by the bubbles.

Ostergaard and Michelsen [1968], using the system described previously, found bed porosity to be strongly affected by particle size. Their results showed that the porosity of a bed of 6-mm glass spheres was proportional to both liquid and gas flow rates for a superficial gas

velocity less than 15 cm/sec. At higher gas velocities, gas slugs formed which increased the bubble rise velocity and decreased the bed porosity. In beds of 3-mm particles, flow changed from a bubble breakup regime for high liquid flow rates and low gas flow rates to a bubble-coalescence regime for high gas flow rates. They observed that, as the liquid velocity was reduced, the transition from the bubble breakup regime to the coalescence regime took place at lower gas velocities; finally, at very low liquid velocities, coalescence occurred at all gas velocities. During operation in the bubble breakup regime, the bed porosity increased with increasing gas velocity; however, during operation in the coalescence regime, the bed porosity decreased with increasing gas velocity. Thus, in beds of 1-mm particles, where coalescence occurred even at low gas flow rates, the bed porosity decreased with increasing gas velocity.

Dakshinamurty et al. [1971] studied the effects of particle size, d_p, and density, liquid-gas interfacial tension, and fluid flow rates on bed porosity in a 5.6-cm-diam column. They observed a reduction in bed porosity upon injection of air into liquid fluidized beds of 0.13-cm rock wool shot and 0.33-cm glass beads in water and beds of 0.106- and 0.22-cm sand particles in water. These systems correspond to operation in the bubble coalescence regime. For systems operating in the bubble breakup regime (0.49-cm and 0.68-cm glass beads in both water and kerosene,

0.3-cm iron shot in both water and kerosene, and the above rock wool shot and glass beads in kerosene), the bed porosity increased with increasing gas flow rate. They correlated their results as follows:

for $Re_t > 500$,

$$\bar{\varepsilon} = 2.65(U_L/U_t)^{0.6} (\mu_L U_G/\sigma_{LV})^{0.08} , \qquad (14)$$

for $Re_t < 500$,

$$\bar{\varepsilon} = 2.12(U_L/U_t)^{0.41} (\mu_L U_G/\sigma_{LV})^{0.08} , \qquad (15)$$

where

Re_t = Reynolds number = $\rho_L U_t d_p/\mu_L$,

μ_L = liquid viscosity.

In a later publication [Dakshinamurty et al., 1972], these investigators changed the coefficient in Eq. (14) from 2.65 to 2.85. They claimed that the porosity can be estimated with an average deviation between 3.7 and 5.6% by using Eqs. (14) and (15).

Bruce and Revel-Chion [1974] tested Eqs. (14) and (15) for 2- , 4- , 6- , and 8-mm-diam glass spheres in a 4.63-cm-diam column. They concluded that the correlations of Dakshinamurty were limited to gas flow rates of less than 7.5 cm/sec. In addition, they observed that contraction of the bed upon injection of a gas occurred only when the 2-mm-diam particles were used and when the liquid velocity was less than 14 cm/sec.

Bhatia et al. [1972], in a comment upon the paper by Dakshinamurty et al. [1971], reported bed porosity experiments in a 5.08-cm-diam column using 1-mm glass beads and 1-mm Teflon-coated glass beads. At each liquid velocity used, the beds of clean glass beads contracted with the injection of gas, whereas the beds of Teflon-coated beads expanded. They explain these results in terms of the "work of adhesion," W_{SLV}:

$$W_{SLV} = \sigma_{LV} (1 + \cos \Theta) \quad , \tag{16}$$

where

W_{SLV} = the energy that must be expended per unit interfacial area to separate a solid phase and a liquid phase in the presence of a gas,

Θ = contact angle of the liquid on the solid surface in the presence of the gas.

Thus, the increase of Θ from 0 for glass to almost π for Teflon particles brings about a continuous decrease in $\cos\Theta$ and hence W_{SLV}. Therefore, bed expansion, instead of an expected contraction, may occur upon introduction of gas flow.

Using their previously described system, Kim et al. [1972] concluded that a critical particle size existed which determined the type of three-phase fluidization--either bubble coalescence or bubble breakup. For particles having a density similar to glass (2.5 g/cm^3), this critical size was about 2.5 mm. In a later paper [Kim et al., 1975], they

report results using the same equipment with various solutions to test the effects of liquid viscosity and surface tension. From an analysis of literature and their data, they found that solids having a minimum fluidizing velocity in the liquid phase alone of less than 1.28 cm/sec initially contracted upon injection of gas into the bed but expanded otherwise. A notable exception to this was the results of Bhatia et al. [1972]. Two correlations are presented for the bed porosity, depending on whether the bed initially expands or contracts upon introduction of the gas phase. The correlations, in terms of the Weber and Froude numbers, have standard errors of estimate equal to 0.040.

Using continuity considerations, Epstein [1976] showed that the inital contraction or expansion of a liquid fluidized bed upon introduction of gas could be predicted by the following:

$$\Psi = \left(\frac{n}{n-1} + K\right)\bar{U}_L - \left[(1 + K)U_L + \frac{Kv_S}{n-1}\right] \quad , \qquad (17)$$

where

Ψ = criteria for expansion or contraction of bed upon injection of gas,

K = ratio of wake volume to bubble volume,

v_S = relative slip velocity between gas and liquid.

A positive value of ψ signifies a bed expansion, while a negative value denotes contraction. An estimate of K for zero gas holdup is obtained from:

$$K = 3.5(1 - \varepsilon_S)^3 \quad . \qquad (18)$$

For bubbly flow, the slip velocity is the rising bubble velocity, as determined experimentally, while the following is used in slug flow:

$$v_S = 0.2\ U_L + 0.35\ \sqrt{gD_c} \quad , \tag{19}$$

where

D_c = column diameter.

Epstein applied Eq. (17) to the data of Bhatia and Epstein [1974] and correctly matched the experimental results in all of the 31 runs conducted.

Razumov et al. [1973] measured the solid holdup in a 30-cm-diam column using a capacitance probe. For these measurements a wide size distribution of quartz sand with an equivalent mean diameter of 0.82 mm was fluidized by air and water. Their data yielded the following dimensional correlation:

$$\bar{\varepsilon}_S = 0.578 - 0.03198\ U_L - 0.00538\ U_G \quad . \tag{20}$$

Saad et al. [1975] fluidized 6.2-mm alumina beads by air and water in a 7.62-cm-diam column and found that the bed porosity increased for both increasing liquid and gas flow rates. However, Burck et al. [1975] used the same system and found the bed porosity to be independent of gas flow rate. In addition, results obtained by Burck using 6.3-mm plexiglass and 1.9-mm alumina beads led him to conclude that the bed porosity was inversely proportional to the particle density.

Bloxom et al. [1975] combined their data obtained for bed porosity on the system previously described with data obtained by Khosrowshahi et al. [1975], who used the same system with 1.9-mm and 6.2-mm alumina beads, and found the following correlation:

$$\bar{\varepsilon} = 1 - \bar{\varepsilon}_S = 1.027\ Fr_L^{0.094}\ Ga_L^{-0.026} \quad , \qquad (21)$$

where

Fr = Froude number = U^2/gd_p ,

Ga = Galileo number = $d_p^3 \rho_L g/\mu_L^2$.

Bloxom also abstracted more than 1200 points from the literature and, after combining all the data, obtained the following correlation:

$$\bar{\varepsilon} = 1 - \bar{\varepsilon}_S = 0.427\ Re_L^{0.275}\ Ga_L^{-0.171} \quad . \qquad (22)$$

Liquid Holdup

Razumov et al. [1973] studied liquid holdup in a 9-cm-diam column using sand and slag beads for the solid phase, with the average diameter ranging from 0.57 to 1.275 mm. The method used was simultaneous stoppage of all flows. This required that the solid phase be evenly and completely distributed over the entire column prior to flow stoppage. Their results yielded the following correlation:

$$\bar{\varepsilon}_L = 0.422 + 0.0180\ U_L/\bar{d}_p^{0.562} - 0.0182\ U_G \quad , \qquad (23)$$

where

$\bar{d}_p$ = average particle diameter, cm,

$1 \leq U_L \leq 4$ cm/sec,

$1 \leq U_G \leq 5$ cm/sec.

The difference between the experimental data and the values calculated by Eq. (23) did not exceed 10%.

Mukherjee et al. [1974] measured liquid holdup in a 5.2-cm-diam column using the method based on determination of the pressure drop over the bed. Particles of four sizes, 0.287, 1.4, 2.8, and 4.12 mm with densities of 2.92, 2.86, 2.92, and 2.78 g/cm^3 respectively, were used as the solid phase. Liquid holdup was found to increase with increasing liquid velocity and decreasing gas velocity. At the same time, liquid holdup decreased with an increase in particle size until it reached a critical value (2.8 mm) beyond which it increased with further increase in particle size.

Michelsen and Ostergaard [1970] measured liquid holdup in beds of 1- , 3- , and 6-mm-diam glass spheres in a 15-cm-diam column using a radioactive tracer. They found that the liquid holdup increased with increased liquid flow rate, decreased gas flow rate, and decreased particle size. The same investigators [Ostergaard and Michelsen, 1968] found similar results in a 21.6-cm-diam column for beds of 0.25- , 1- , and 6-mm glass spheres.

Kim et al. [1972] studied liquid holdup in their previously described system using the pressure drop over the bed and the bed height to calculate the liquid holdup. The solid phase was either 6-mm glass beads or 2.6-mm irregular gravel. They observed that the liquid holdup increased with

increasing gas and liquid velocity, and that it was greater in the bed of gravel than in the bed of glass beads. Under the same experimental conditions, they found that the presence of solids reduced the liquid holdup, as compared with a bubble column. In a related study [Kim et al., 1975], the investigators found that the liquid holdup increased with viscosity, the effect being more marked as the particle size decreased. The liquid holdup decreased with increasing surface tension (40 to 73 dynes/cm), in beds of 1-mm glass beads, but was proportional to the surface tension in beds of 2.6-mm gravel. The following dimensionless correlation was obtained:

$$\bar{\varepsilon}_L = 1.504\ Fr_L^{0.234}\ Fr_G^{-0.086}\ Re_L^{-0.082}\ We^{0.092}\ , \qquad (24)$$

where

Re = Reynolds number = $U^{2-n} d_p^{\,n} \rho / V$,

We = Weber number = $U_G V / \sigma_{LV}$,

V = generalized viscosity constant = $k 8^{n-1}$,

k = fluid consistency index,

standard error of estimate = 0.039.

In a comparison of Eqs. (24) and (23), Kim found that the correlation of Razumov slightly underestimates the liquid holdup. However, it should be noted that Eq. (23) was derived from experiments in which the only liquid phase used was water.

Bloxom et al. [1975], using the system described previously, found liquid holdup to be directly proportional to the liquid viscosity and velocity. They obtained the following dimensional correlation:

$$\bar{\varepsilon}_L = 0.451\ U_L^{0.269}\ U_G^{-0.146}\ (\rho_S - \rho_L)^{-1.072} \quad , \qquad (25)$$

where the velocities are in cm/sec and the densities are in g/cm^3. They were unsuccessful in finding a correlation which combined their own data with data from the literature.

Minimum Fluidization Velocities

Wen and Yu [1966] combined experimental and literature data on two-phase fluidized beds and arrived at the following correlation, which is applicable to both liquid and gas fluidized beds:

$$Re_{mf} = \sqrt{(33.7)^2 + 0.0408\ Ar} - 33.7 \quad , \qquad (26)$$

where

$$Re_{mf} = \rho_L U_{mf} d_p / \mu_L \quad ,$$

$$Ar = d_p^3 \rho_L (\rho_S - \rho_L) g / \mu_L^2 \quad .$$

Burck et al. [1975], in their system described previously, presented the minimum fluidization velocities for three-phase fluidized beds as a function of packing and initial bed height. These results are shown in Fig. 3. It can be seen that $U_{L,mf}$ decreased with increasing gas flow rate, particle size, and particle density. The differences due to initial bed height were explained as end effects

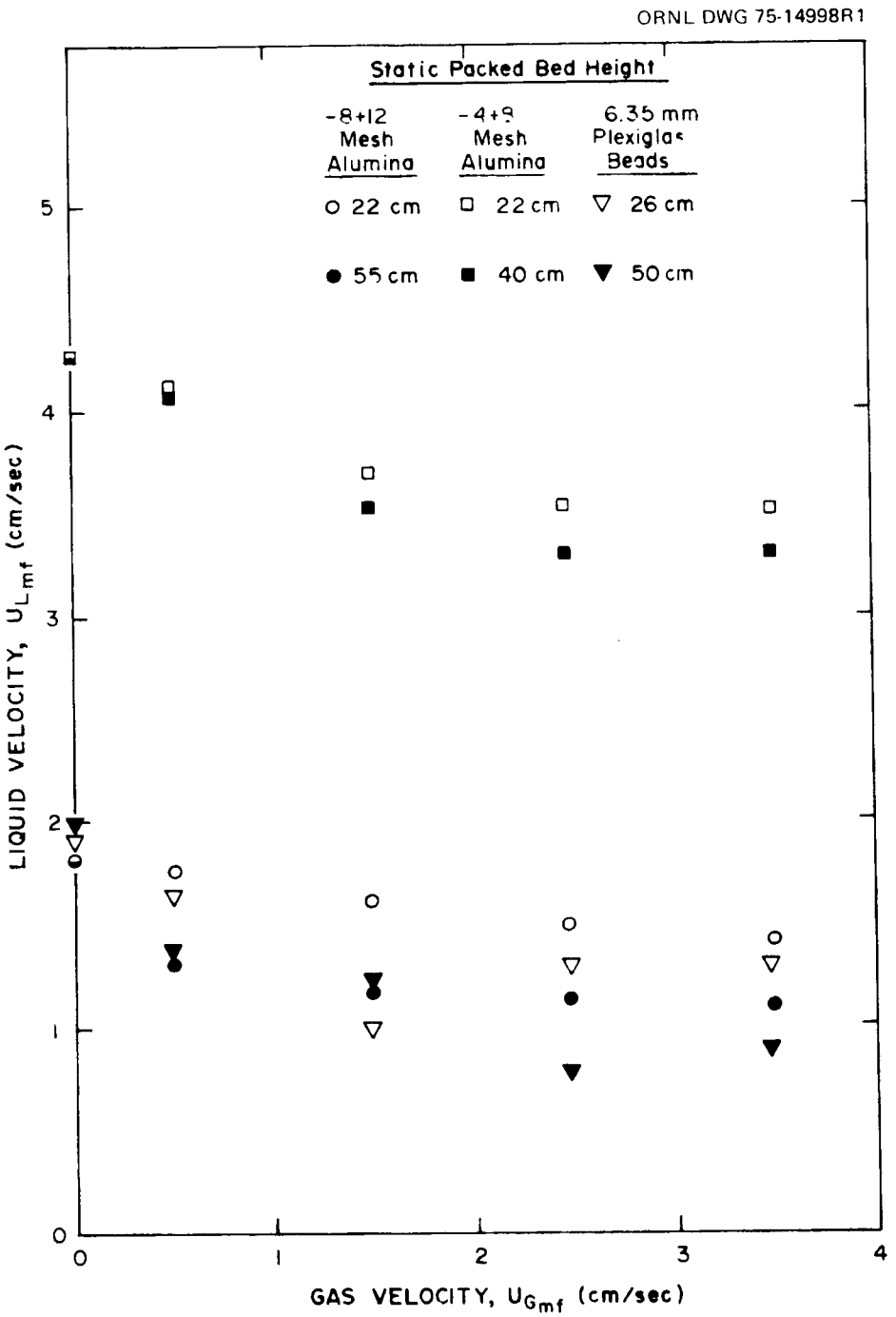

Figure 3. Incipient fluidization velocities as a function of packing and initial bed height.

since the gas and liquid distributors were separated by a distance of 3.8 cm.

Using 4.6-mm glass spheres and aqueous glycerol solutions in a 7.62-cm-diam column, Bloxom et al. [1975], found that, for a given gas velocity, the minimum liquid fluidization velocity decreased as the liquid viscosity increased. Bloxom et al. presented their results based on a computer analysis of their pressure drop-versus-liquid velocity data. However, Begovich [1978] compared the computer analysis with analysis by hand and found that the minimum fluidization velocities obtained by the computer method were too high. The corrected results are shown in Fig. 4. The conclusions reported by Bloxom et al. have not been altered. For a given gas velocity, the minimum liquid fluidization velocity decreased as the liquid viscosity increased; however, the influence of the liquid viscosity appeared to decrease for the higher viscosities. Also, the gas velocity did not appreciably affect the minimum liquid fluidization velocity for the more viscous aqueous glycerol solutions studied.

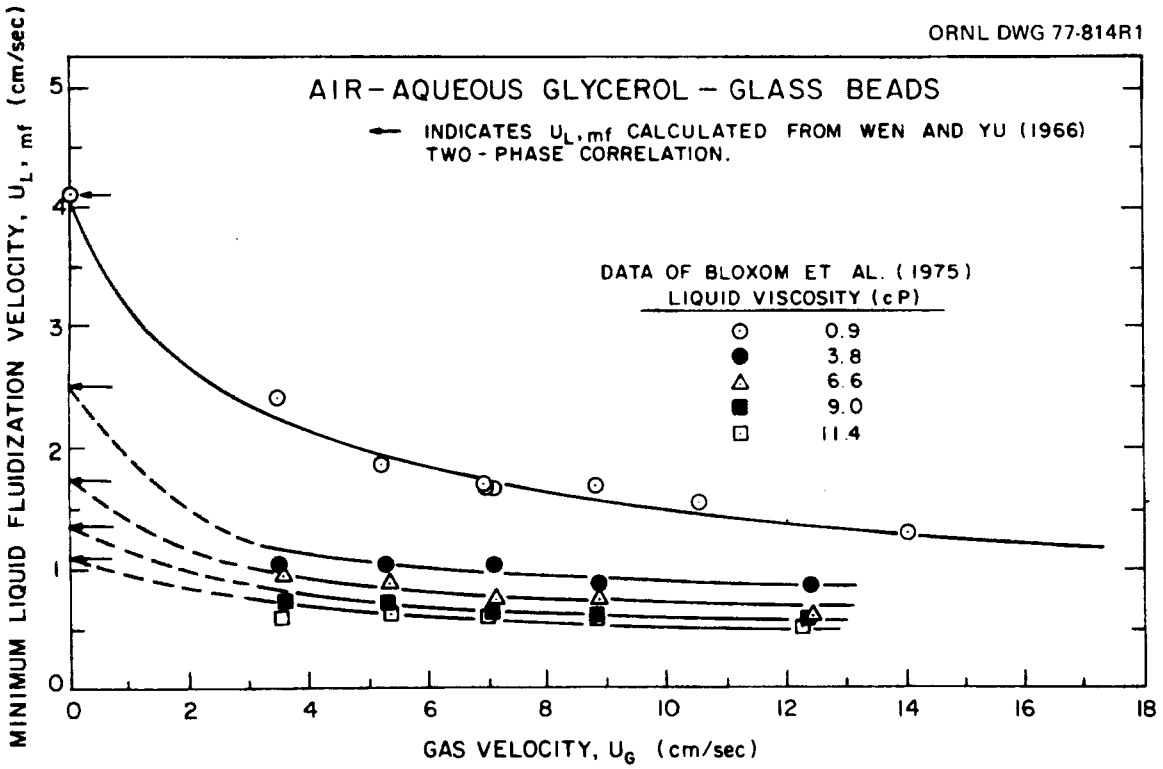

Figure 4. Effect of liquid viscosity on the minimum fluidization velocities.

CHAPTER 4

EXPERIMENTAL

Experimental Apparatus

The experimental apparatus shown in Fig. 5 was located in Laboratory 38 of Building 4505 at the Oak Ridge National Laboratory. Various solids were fluidized by air and liquid in either a 7.62- or a 15.2-cm-ID plexiglass column.

Liquid was pumped from one or both 55-gal feed tanks by centrifugal pumps through an appropriate rotameter to the bottom of one of the two columns which were connected in parallel. Process air was fed through the desired rotameter to the side of the fluid distributor through two 6.35-mm-diam channels forming a cross and then passed upward into the column through seventeen 1.59-mm-diam holes. Approximately thirty-six 1.59-mm-diam holes were drilled entirely through the distributor, as shown in Fig. 6, in each quadrant (between cross arms) to allow liquid to enter the bed. Thus, the gas and liquid phases were intimately mixed at the top of this fluid distributor, which also acted as the packing support. The air was vented to the atmosphere, while the water exited through a glass tee and returned to the feed tanks. A wire-mesh screen across the glass tee prevented solids from flowing out of the column. The physical characteristics of the solids and the range of experimental conditions used in this study are detailed in Tables 1 and 2. A series of liquid manometers located at

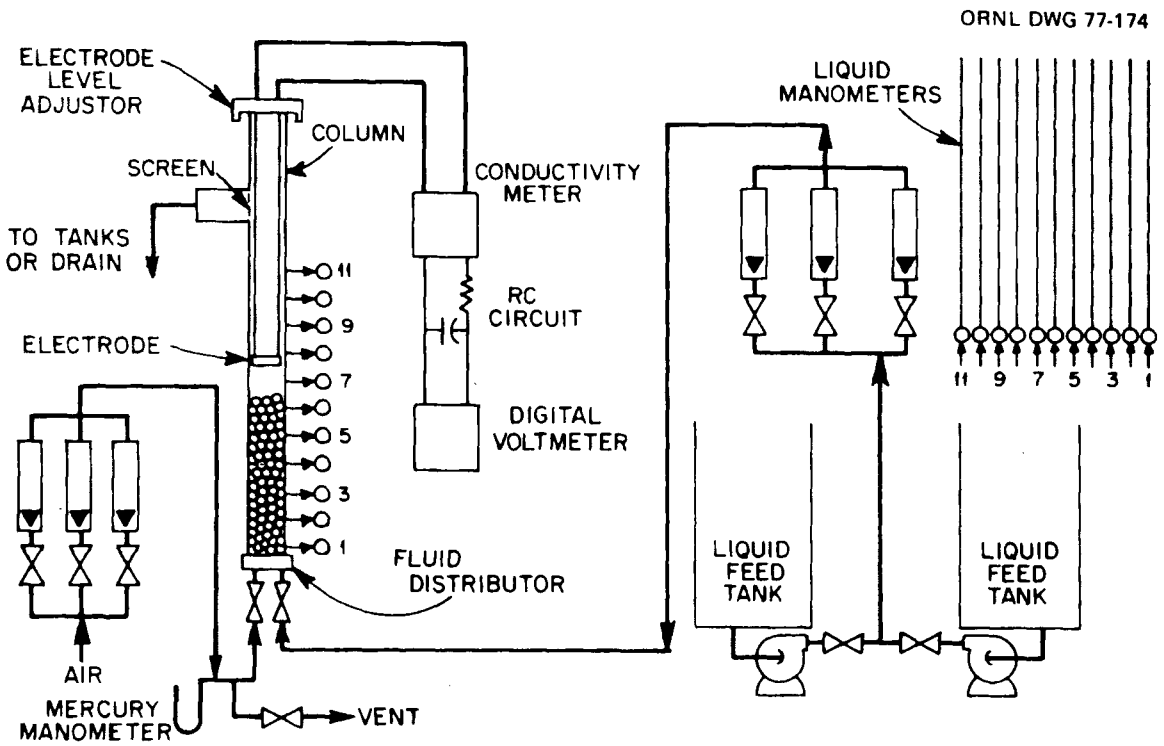

Figure 5. Three-phase fluidization and electroconductivity apparatus.

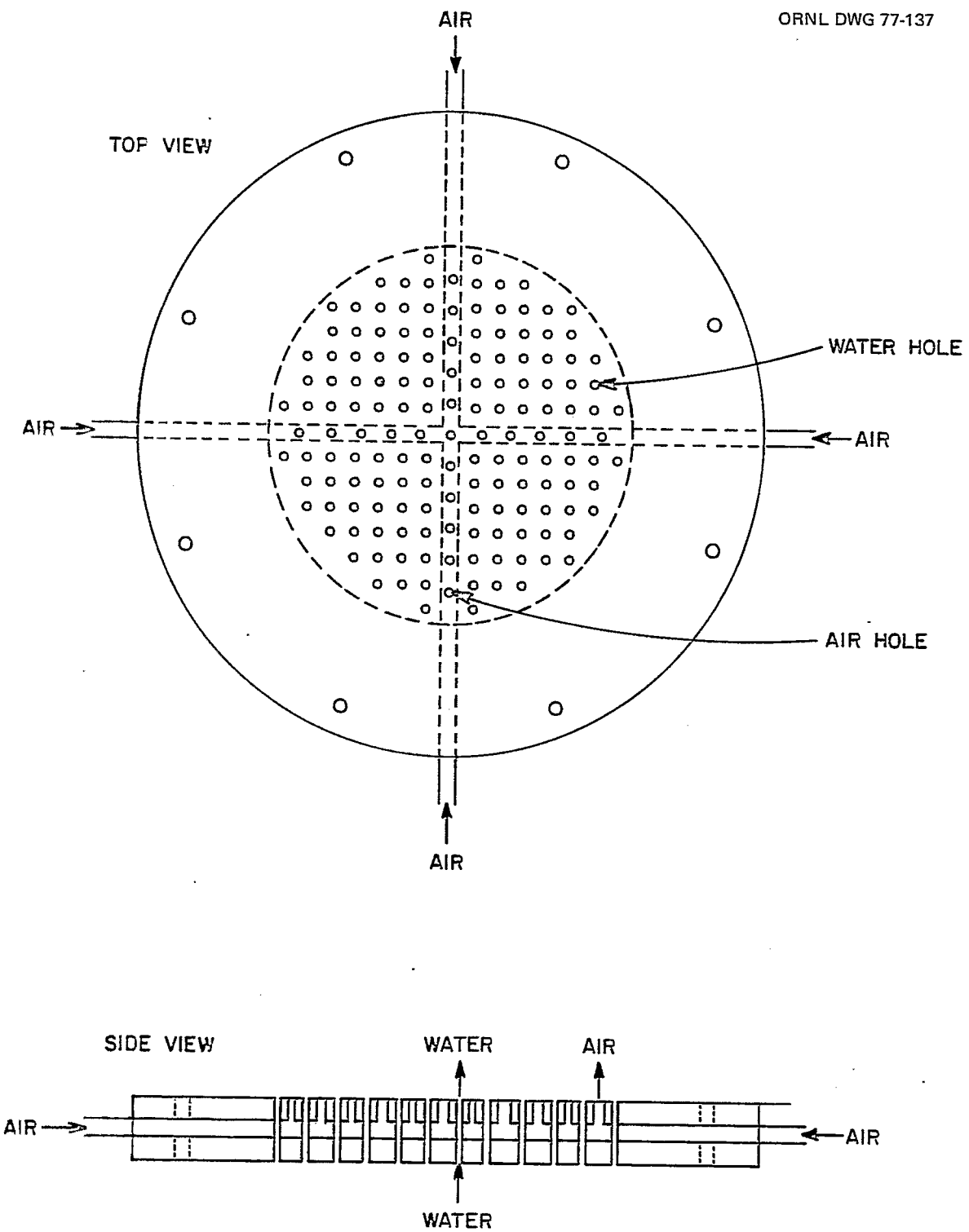

Figure 6. Air-water fluids distributor and bed support.

Table 1. Physical characteristics of solid beads used in three-phase fluidization studies

Solid	Diameter (cm)	Density (g/cm^3)
Glass [1]	0.32	2.24
Glass	0.46	2.24
Glass [1]	0.62	2.20
Plexiglass	0.63	1.17
Alumina	0.62	1.99
Alumino-silicate [1]	0.19	1.72

[1]Used only in minimum fluidization experiments.

Table 2. Range of experimental conditions used in three-phase fluidization studies

Superficial gas velocity, U_G, cm/sec	0 - 17.3
Superficial liquid velocity, U_L, cm/sec	0 - 12.0
Column diameter, D_c, cm	7.62, 15.2
Initial bed height, H_o, cm	22 - 45

9-cm intervals (8-cm intervals for the 15.2-cm-ID column) along the column wall provided the pressure gradient in the column.

Two platinum electrodes, each with an area of approximately 1.5 cm^2, were attached 180° apart on the inside of a movable plexiglass ring. The ring, which had a radial thickness of 4.7 mm and an axial width of 19 mm, was lowered or raised by two 3.2-mm-OD stainless steel tubes threaded into the ring. Insulated wires were passed through the tubing and soldered to the electrodes. These wires were then connected by coaxial cable to a Radiometer Copenhagen Type CDM2e conductivity meter. A digital millivoltmeter and a resistor-capacitor circuit (15-sec time constant) connected to the conductivity meter permitted a time-averaged digital readout. Potassium chloride was added to the water in the feed tanks to allow readings on the 5-mmho scale of the conductivity meter.

Experimental Procedure

The electrical conductivity was first measured above the bed in the liquid alone. After the liquid and gas velocities had been adjusted to their desired flow rates, the liquid manometer heights were recorded. Then the conductivity between adjacent pressure taps was also recorded. The liquid manometer heights were recorded a second time with the conductivity probe positioned in the middle of the bed. Equations (1), (7), and (10) could then

be solved to yield values for each of the three phase holdups as a function of position in the column.

The minimum fluidization velocities required to achieve fluidization were determined from the intersection of the fixed- and fluidized-bed pressure drop curves on the plot of bed pressure drop versus superficial liquid velocity at a constant gas flow rate.

Runs were numbered according to the system shown in Table 3. Thus, the fifth run using the 4.6-mm-diam glass beads in the 7.62-cm-ID column and water with no air flow would be numbered G05A13. A two-letter code, either IN or AB, was added to the run number to distinguish between parameters calculated using the pressure gradient as measured with the conductivity probe either in or above the bed, respectively.

Table 3. System for numbering runs made in three-phase fluidization studies

Runs were numbered based on a six-digit system:

Digits

1 Type of particle:

Glass, diam: C = 0.32 cm, G = 0.46 cm, K = 0.62 cm

Plexiglass: P

Alumina: A

Alumino-silicate: S

2-3 Experiment number with particular solid in column

4 Gas flow rate (percent of maximum)

0	A	50	H
2.5	B	60	I
5	C	70	J
10	D	80	K
20	E	90	L
30	F	100	M
40	G		

5 Liquid viscosity (cP)

6 Column diameter (in.)

CHAPTER 5

EXPERIMENTAL RESULTS

Minimum Fluidization

The minimum fluid flow rates required to achieve fluidization were determined by a plot of the pressure drop across the bed versus the superficial liquid velocity at a constant gas flow rate. The flow rates at which a break in the curve occurred correspond to the minimum fluidization (MF) velocities.

Effect of column diameter and static bed height. The effects of column diameter and static bed height (or bed mass) on the MF velocities for the air-water-glass beads and the air-water-plexiglass beads systems are shown in Figs. 7 and 8, respectively. In each system, the minimum liquid velocity required to fluidize the bed with no gas phase present is indicated by the arrow on the ordinate of the plot as calculated from the two-phase correlation of Wen and Yu [1966]. Excellent agreement between the calculated and experimental points for each system can be observed, as was the case for each system studied.

Neither the column diameter nor the mass of solids present in the column appeared to have any significant effect upon the MF velocities. A slight dependence on column diameter might be indicated for the air-water-plexiglass beads system; however, the small

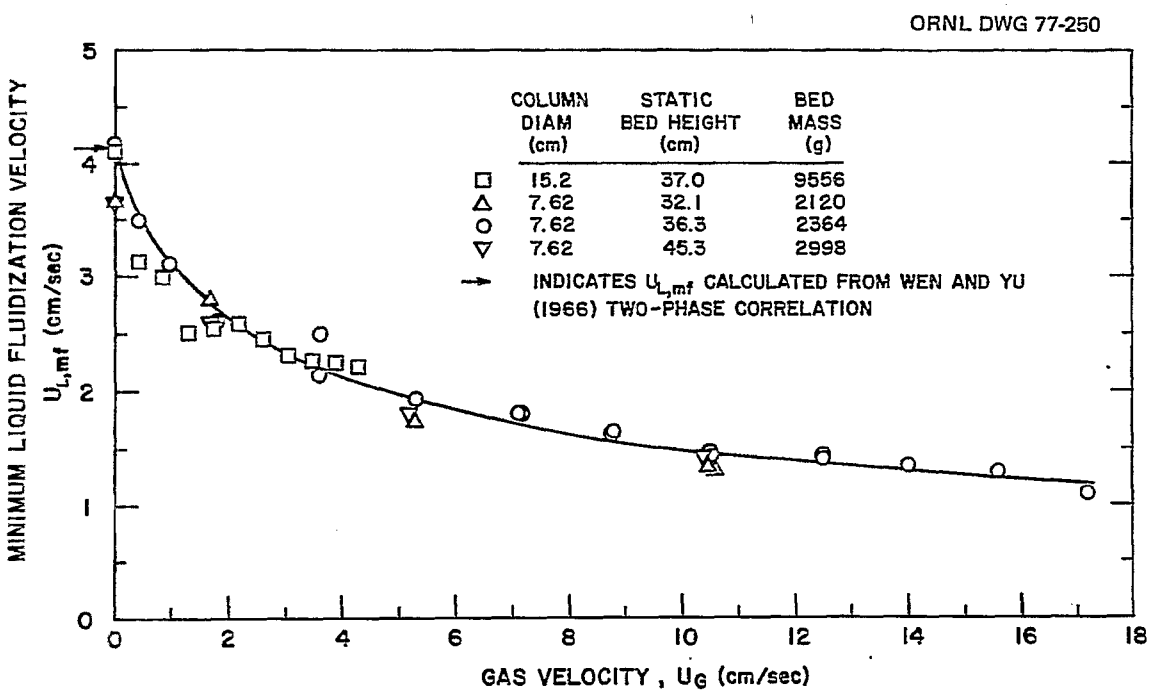

Figure 7. Minimum fluidization velocities for the air-water-glass beads.

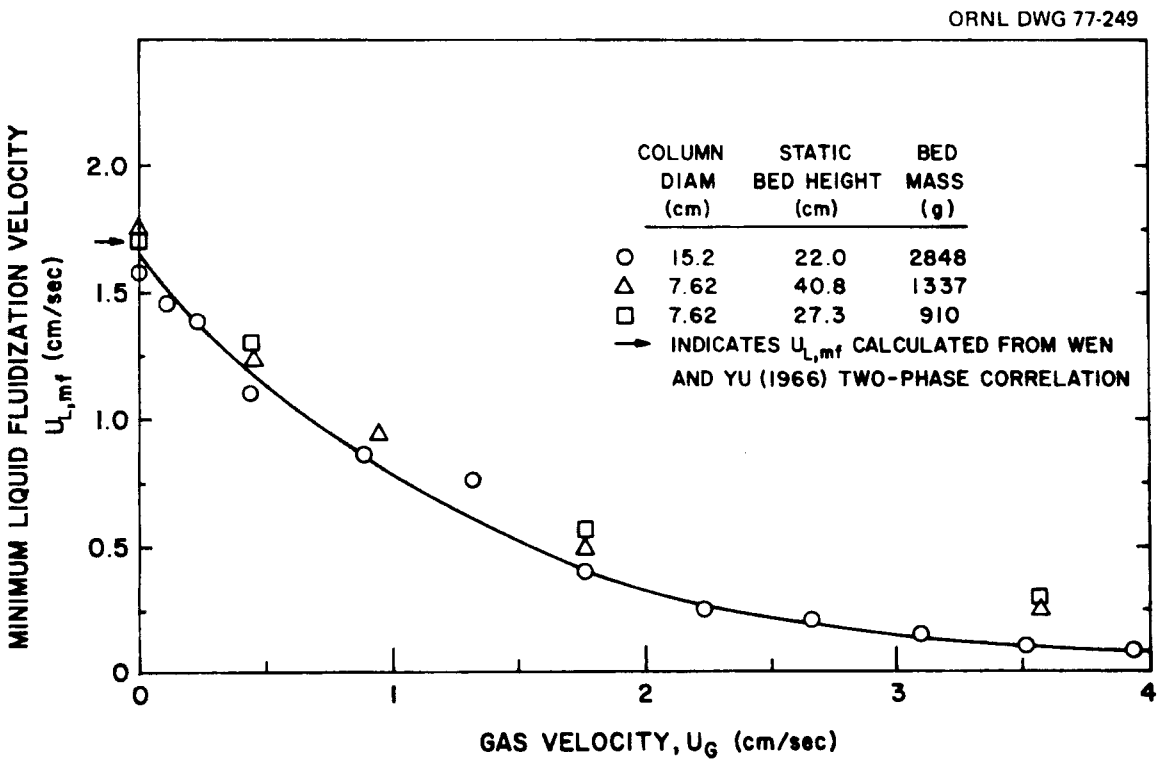

Figure 8. Minimum fluidization velocities for the air-water-plexiglass beads.

density difference between the water and solid phases made the breakpoint in the pressure drop-versus-liquid velocity curve very difficult to determine and subject to error. Since fluidization of a bed is achieved when the upward inertial and drag forces exerted on the particles by the fluids equal the buoyant weight of the bed, an effect of static bed height on the MF velocities would be expected only if end effects were present in the bed. Likewise, one would not expect the MF velocities to be a function of column diameter unless the size of the gas bubbles approached that of the column diameter or unless channeling occurred.

Effect of particle size and density. MF velocities are shown in Fig. 9 for each of the systems studied. Note that the smooth curves of Figs. 7 and 8 correspond to those shown in Fig. 9. As the gas velocity was increased, the minimum liquid velocity required to achieve fluidization in each of the systems decreased. The magnitude of this decrease is considerably different for the plexiglass beads with their small solid/liquid density difference. In their two-phase correlation, Wen and Yu [1966] noted that the MF velocity increases with increasing particle diameter and increasing solid/liquid density difference but decreases with increasing fluid viscosity. Although the plexiglass beads have the same diameter as the alumina particles and one set of the glass beads, they have a much smaller

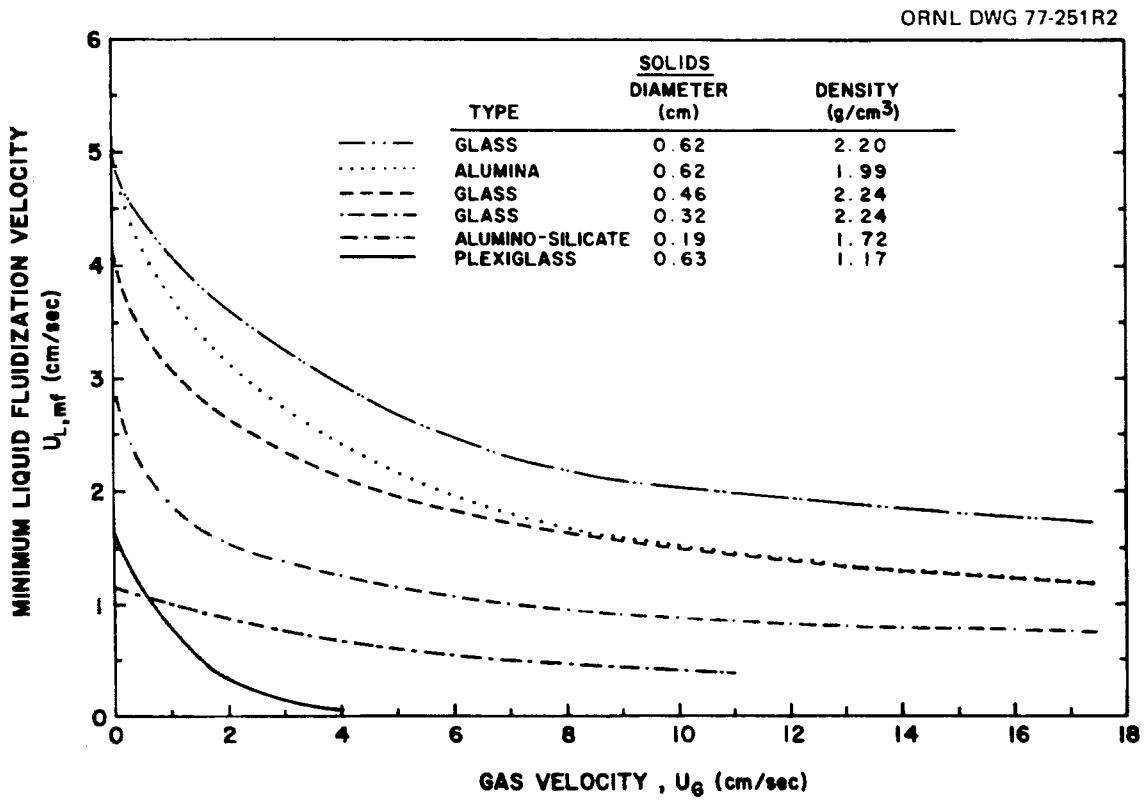

Figure 9. Effect of particle size and density on the minimum fluidization velocities.

solid/liquid density difference; thus, they fluidize at lower velocities. The alumina and alumino-silicate beads have approximately the same density, but the smaller diameter of the latter particles causes them to fluidize at lower velocities.

Likewise, the 3.2-mm-diam glass beads fluidize at lower velocities than do the 4.6-mm-diam glass beads, which in turn fluidize at lower velocities than do the 6.2-mm-diam glass beads. It is of interest to note that the curves of the alumina and 6.2-mm-diam glass beads start at essentially the same point for zero gas velocity; however, as the gas velocities increase, they rapidly diverge until the gas velocities exceed 8 cm/sec. At that point, the curve for the alumina beads merges with the curve of the 4.6-mm-diam glass beads.

Overall Phase Holdups

The assumption of a homogeneous bed may be justified in cases where the fluid velocities are sufficiently low that they result in only slightly expanded fluidized beds. Since the conductivity of the bed and the pressure gradient were measured over the entire column length, an overall, or average, phase holdup could be calculated for each phase in two ways: (a) using the conductivity reading at the center of the bed and Eqs. (1), (2), and (7); and (b) using the average measured pressure gradient over the column to obtain an equivalent homogeneous bed height and substituting that

height in Eqs. (1)-(3). Both of these methods assume that the phase holdups are constant over the entire bed.

Comparison of overall phase holdups. The holdups obtained by the conductivity and pressure gradient methods are compared in Figs. 10-16.

The overall gas holdup determined by each method is shown in Fig. 10 for air-water flow only (i.e., no solids present) in both columns. A least-squares fit of the data yields a line with approximately unity slope and zero intercept.

The glass and plexiglass beads were used in both columns without any difficulty; however, the conductivity readings obtained using the porous alumina beads, which is the likely catalyst support for a coal liquefaction reactor, had to be corrected by a factor approximately equal to the volume fraction of the liquid residing in the internal pores of the solids. This factor, which was found to vary with varying gas or liquid velocities, was determined by assuming that the liquid holdup described by Eq. (7) was the external liquid holdup plus the internal pore volume fraction occupied by the liquid. The average internal pore volume fraction was determined for a particular set of conditions by applying Eq. (7), along with Eqs. (1)-(3), over the 9-cm intervals along the column that both conductivity and pressure were measured. This average internal pore volume fraction was then used in the

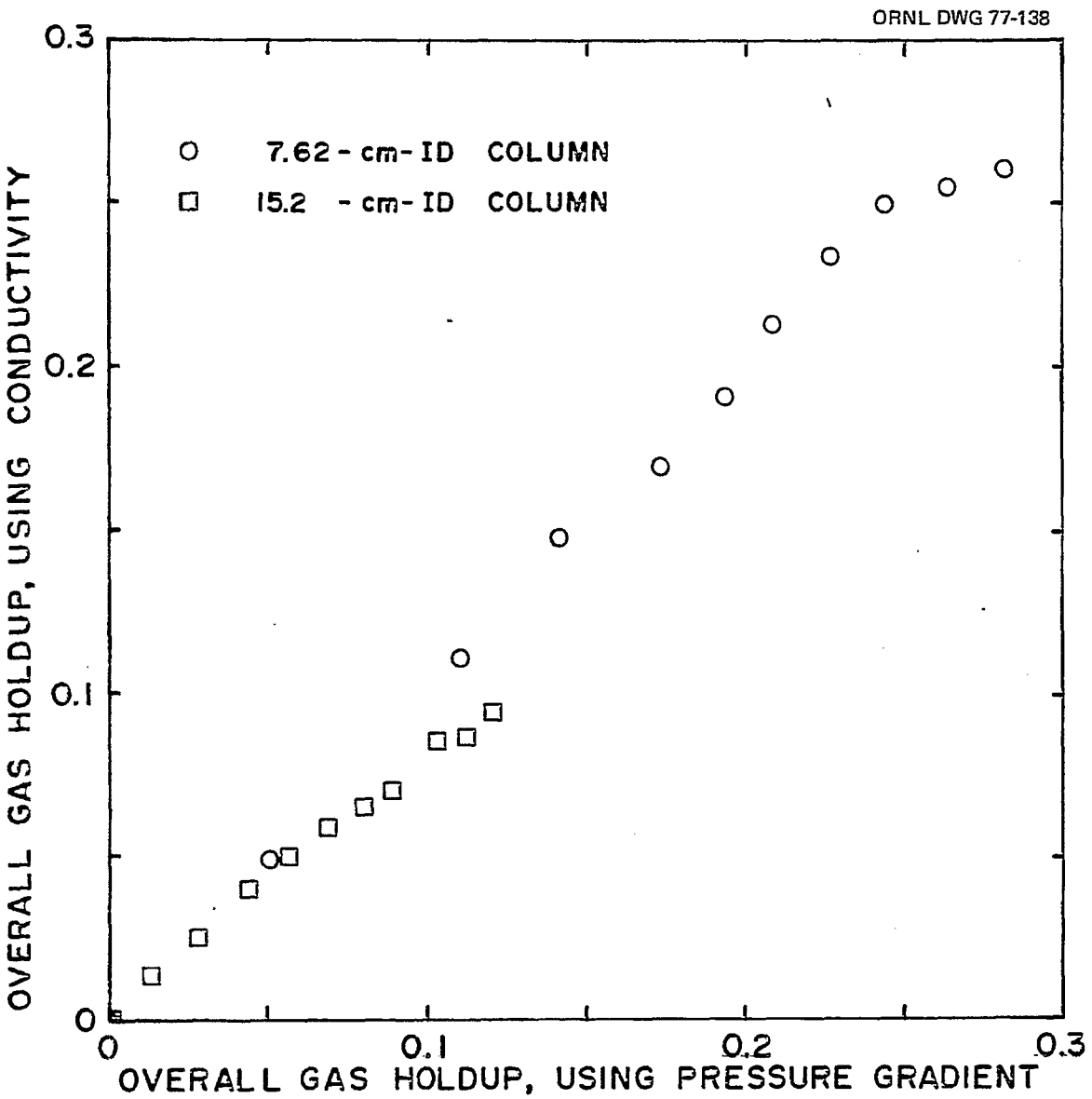

Figure 10. Comparison of overall gas holdups in two bubble columns obtained by two different methods.

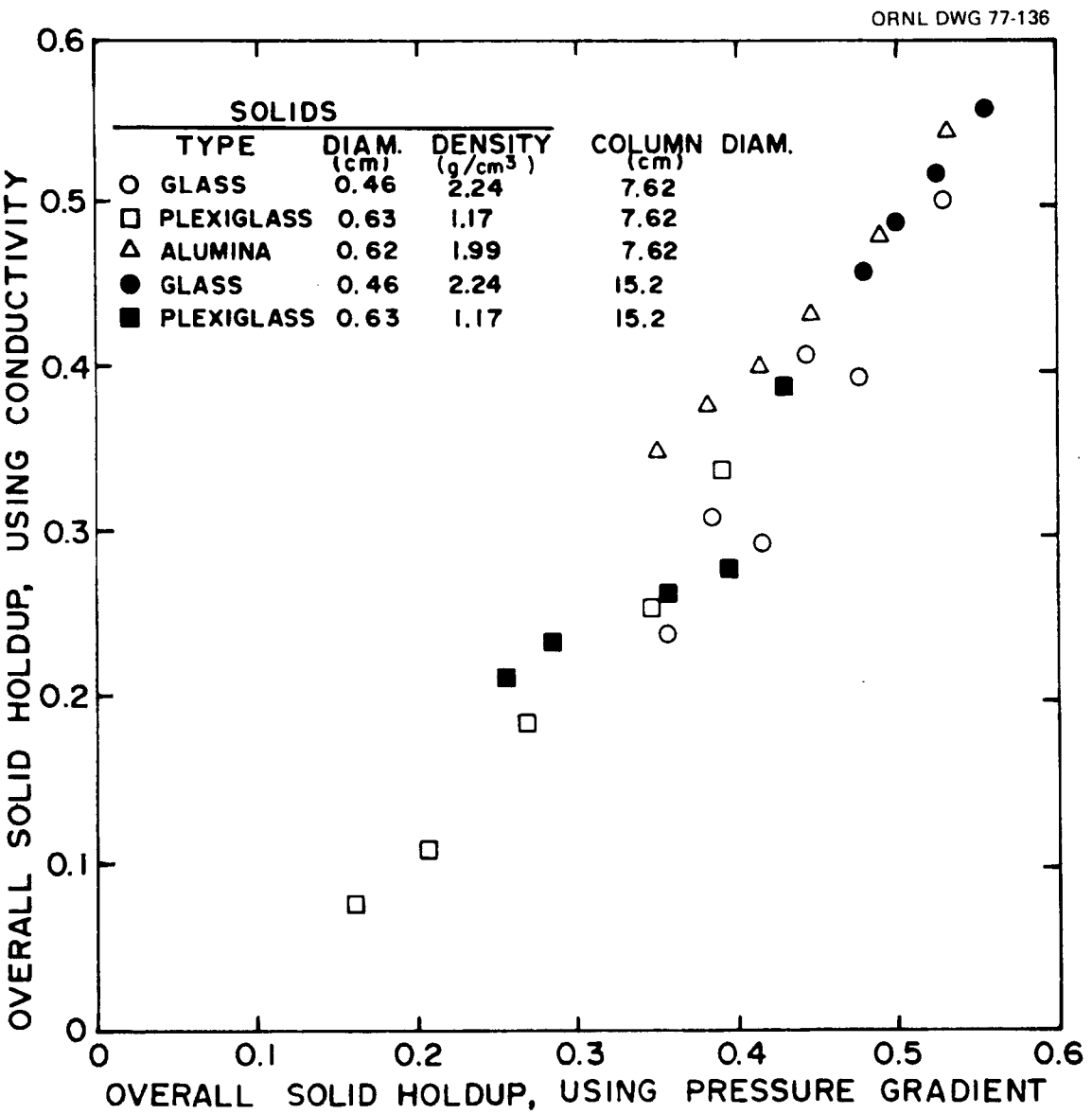

Figure 11. Comparison of overall solid holdups in liquid fluidized beds obtained by two different methods

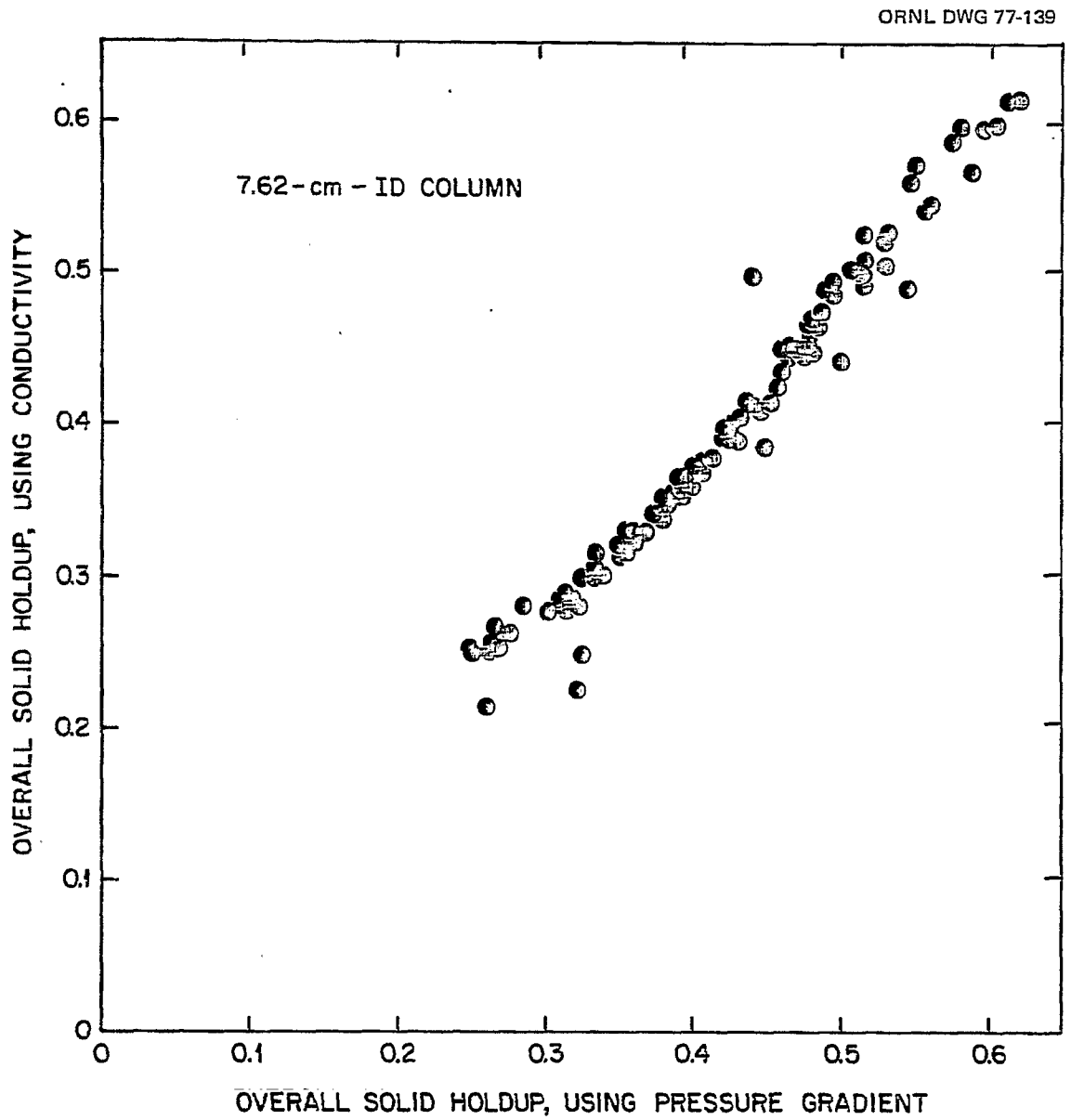

Figure 12. Comparison of overall solid holdups obtained by two different methods in the 7.62-cm-ID column using the air-water-glass beads.

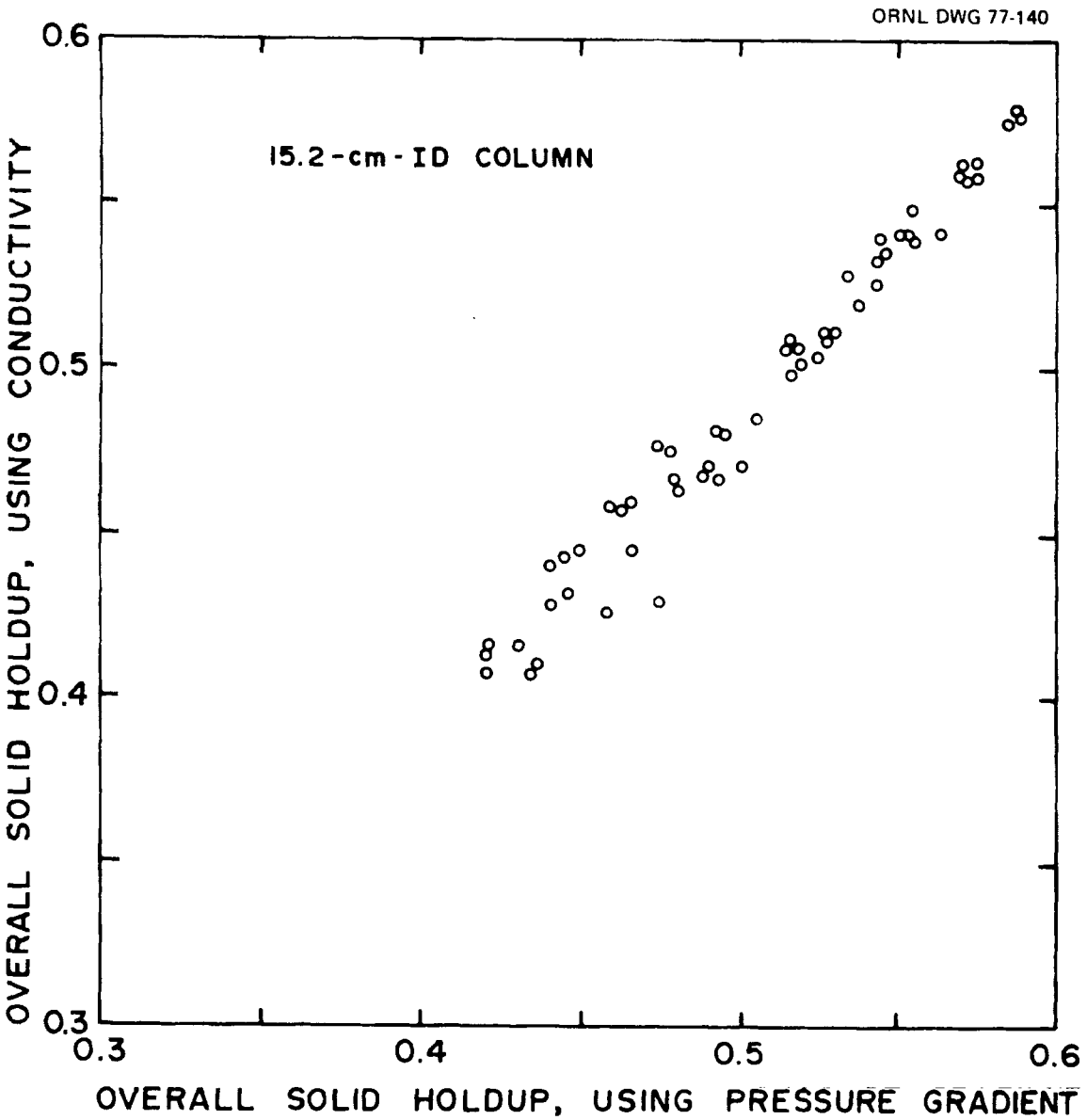

Figure 13. Comparison of overall solid holdups obtained by two different methods in the 15.2-cm-ID column using the air-water-glass beads.

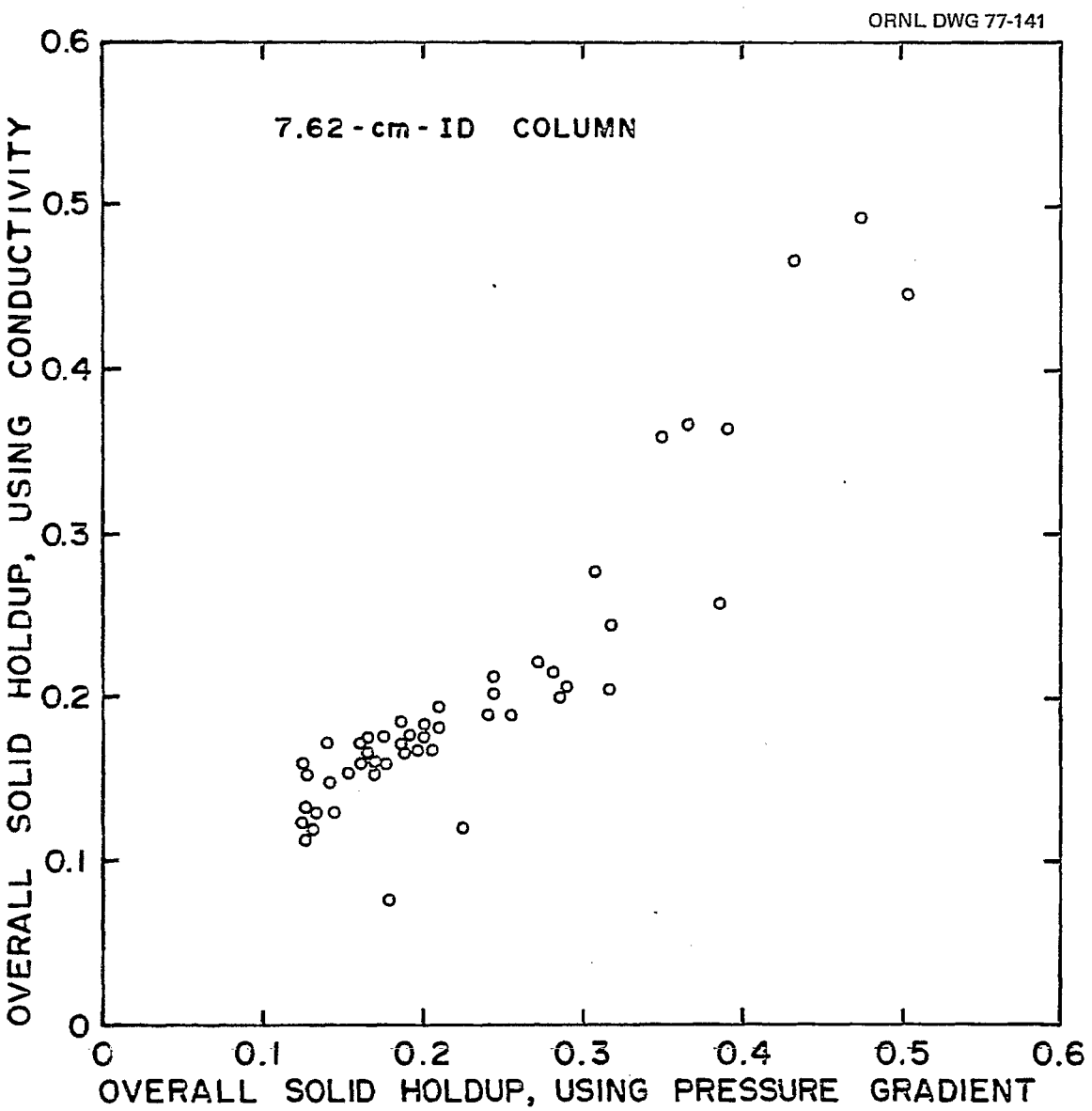

Figure 14. Comparison of overall solid holdups obtained by two different methods in the 7.62-cm-ID column using the air-water-plexiglass beads.

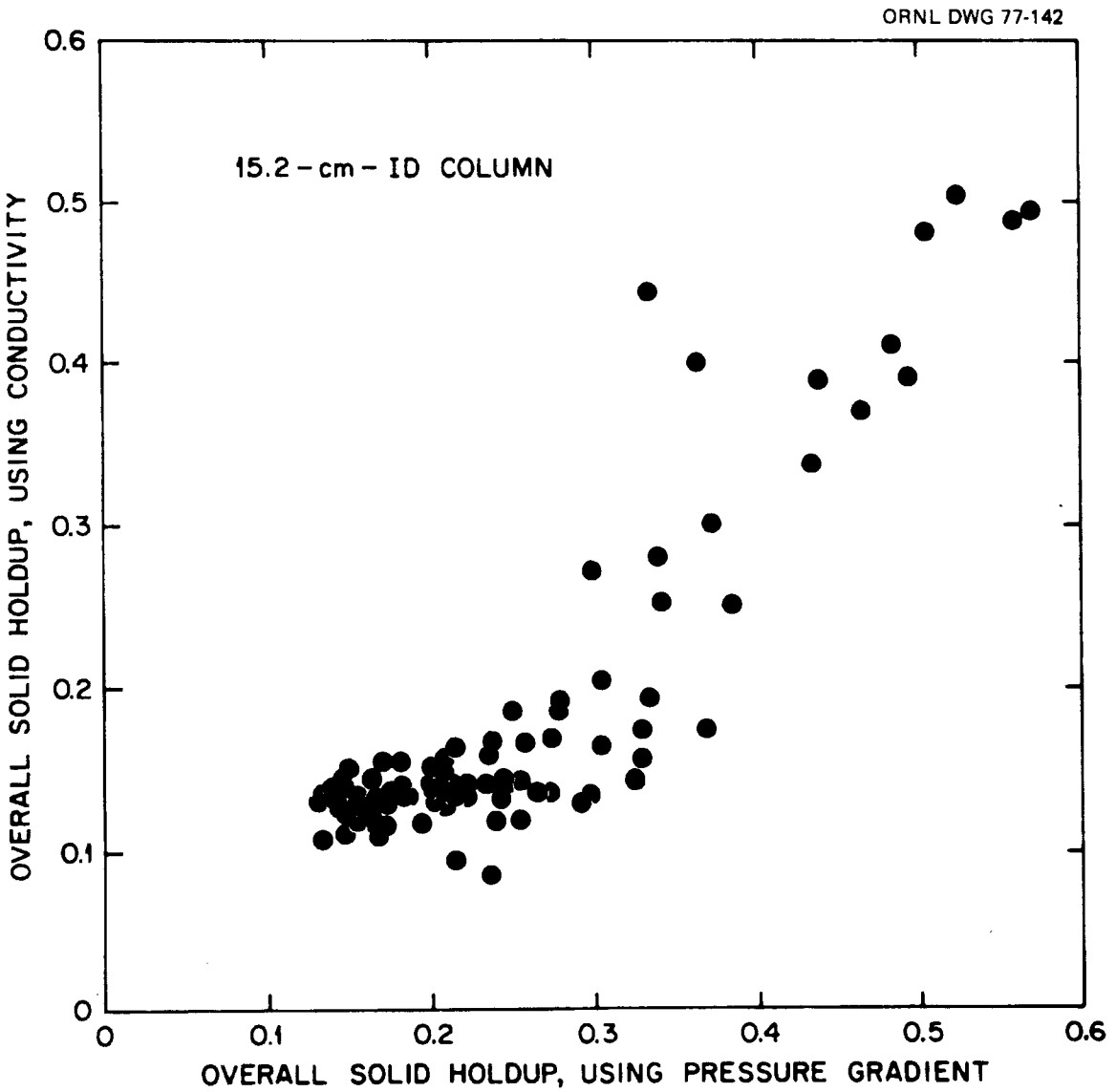

Figure 15. Comparison of overall solid holdups obtained by two different methods in the 15.2-cm-ID column using the air-water-plexiglass beads.

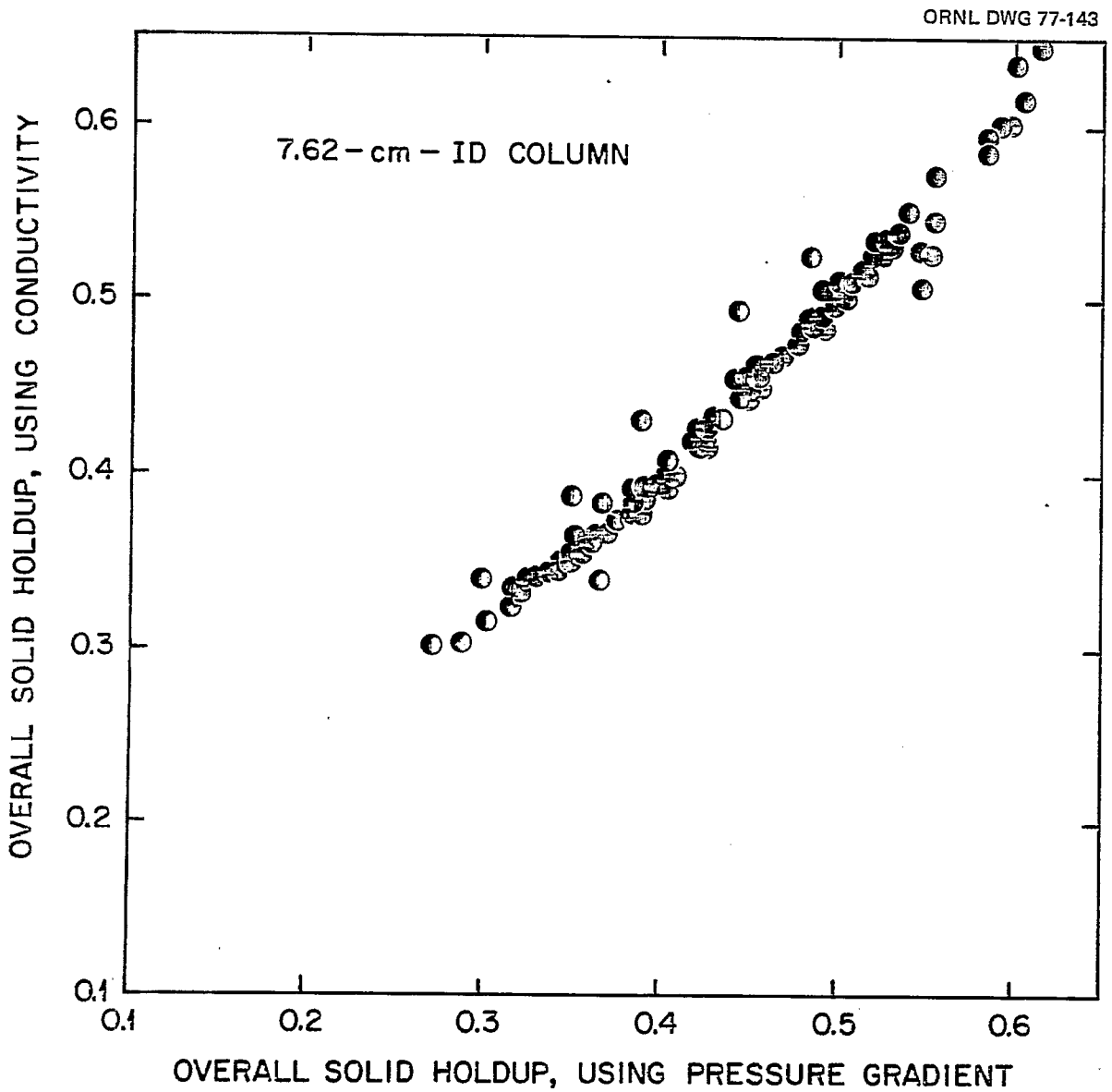

Figure 16. Comparison of overall solid holdups obtained by two different methods in the 7.62-cm-ID column using the air-water-alumina beads.

appropriate equations to solve for the holdups by both the conductivity and pressure gradient methods.

For water fluidization only (i.e., no gas phase present), values of the overall solid holdup determined by the conductivity method are shown in Fig. 11 plotted against values obtained by the pressure gradient method. In Figs. 12-16, similar comparisons are made for air-water fluidization of each of the systems studied. Least-squares fit of these data also results in lines of approximately unity slope and zero intercept, as indicated in Table 4.

As expected, disagreement between the two methods occurs chiefly for low values of solid holdups--that is, where the fluid flow rates are high and the bed height is not distinct. Under such conditions, the pressure gradient method yields a solid holdup based on a uniform bed. The conductivity method, however, yields a solid holdup based on conditions in the middle of the bed. Since the bed really goes from a fairly uniform lower section through a transition region of decreasing solid holdup to a region of only gas and liquid, the solid holdup obtained from measurements of the conductivity at the middle of the bed is lower that that obtained from the pressure gradient method.

Since the homogeneous bed model has been assumed by most of the investigators in the literature, as have Eqs. (1)-(3), the effects of solid characteristics and fluid flow rates on the overall holdups determined by the pressure gradient method will be discussed next.

Table 4. Comparison of overall solid holdup by two different methods

$$\bar{\varepsilon}_{S,C} = a + b\,\bar{\varepsilon}_{S,\Delta P}$$

Solid	Column diameter (cm)	Value of a	Value of b	Correlation coefficient	Number of points
Glass	7.62	-0.052	1.067	0.985	96
Glass	15.2	-0.016	1.005	0.985	56
Plexiglass	7.62	0.005	0.862	0.914	48
Plexiglass	15.2	-0.028	0.841	0.875	84
Alumina	7.62	-0.023	1.054	0.985	98

Effect of fluid flow rates on the overall phase holdups. The effect of fluid flow rates on the overall phase holdups in a typical example with the glass beads system is shown in Fig. 17. As the liquid velocity was increased, the bed expanded, thereby reducing the solid holdup. The gas holdup was not significantly affected by changes in the liquid velocity. Since the holdups of the three phases must sum to unity, the increased liquid velocity in turn increased the overall liquid holdup. At constant liquid velocity, increasing the gas velocity caused the overall gas holdup to increase and the overall solid and liquid holdup to decrease.

Similar behavior is shown in Fig. 18 for the alumina beads. The liquid velocity had a negligible effect on the overall gas holdup; it mainly affected the degree of bed expansion. Increasing the gas velocity again increased the gas holdup; however, its effect on the other two phase holdups is less pronounced, with the solid and liquid holdups showing a range, or band, of values for the gas velocities used.

Increasing the liquid velocity in the plexiglass beads systems, as shown in Fig. 19, decreased the overall solid holdup but had essentially no effect on the gas holdup. Increasing the gas velocity again increased the overall gas holdup while substantially reducing the overall solid holdup. The solid holdup was apparently reduced to a larger

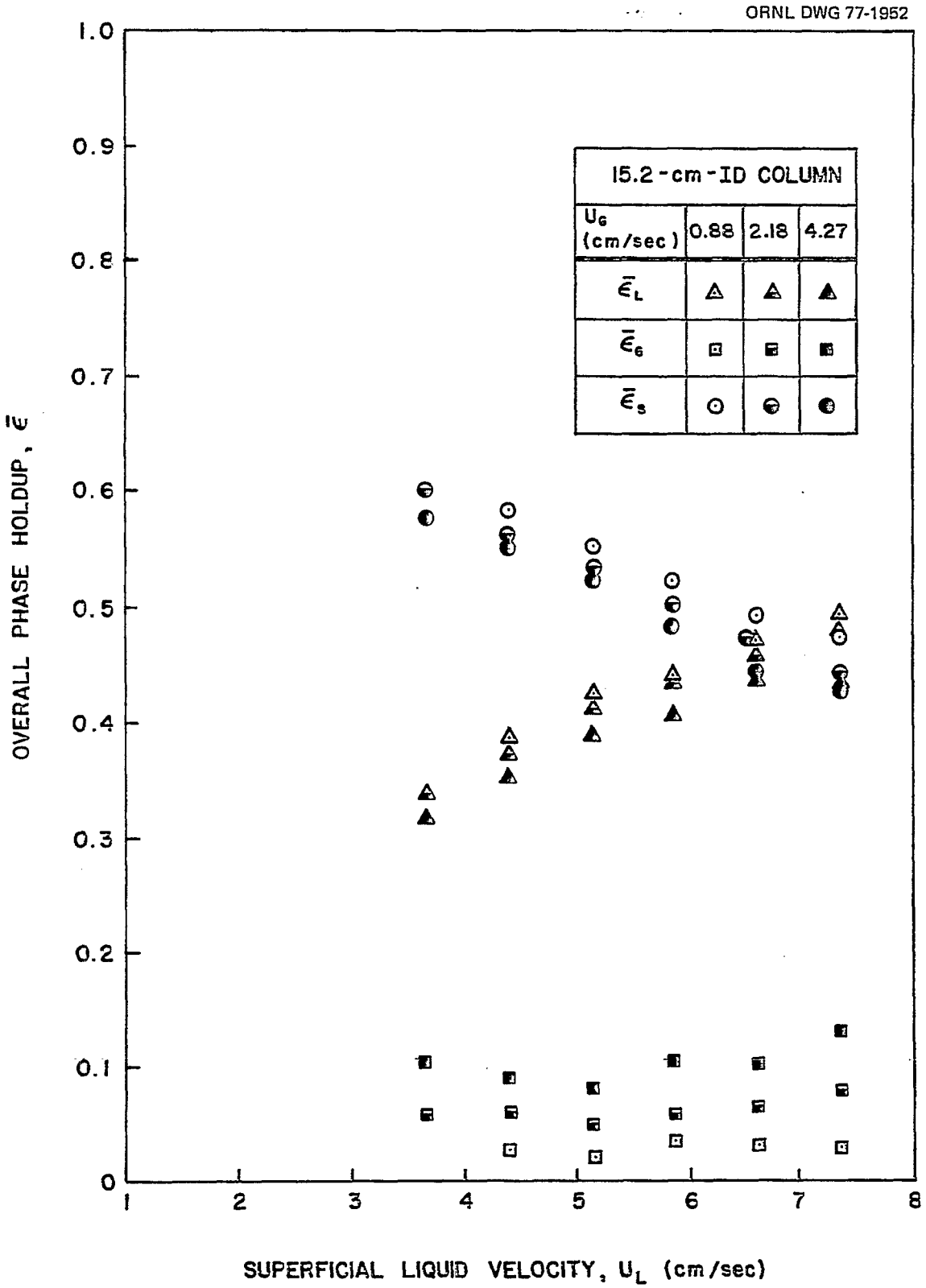

Figure 17. Effect of fluid velocities on the overall phase holdups obtained in the 15.2-cm-ID column using the air-water-glass beads.

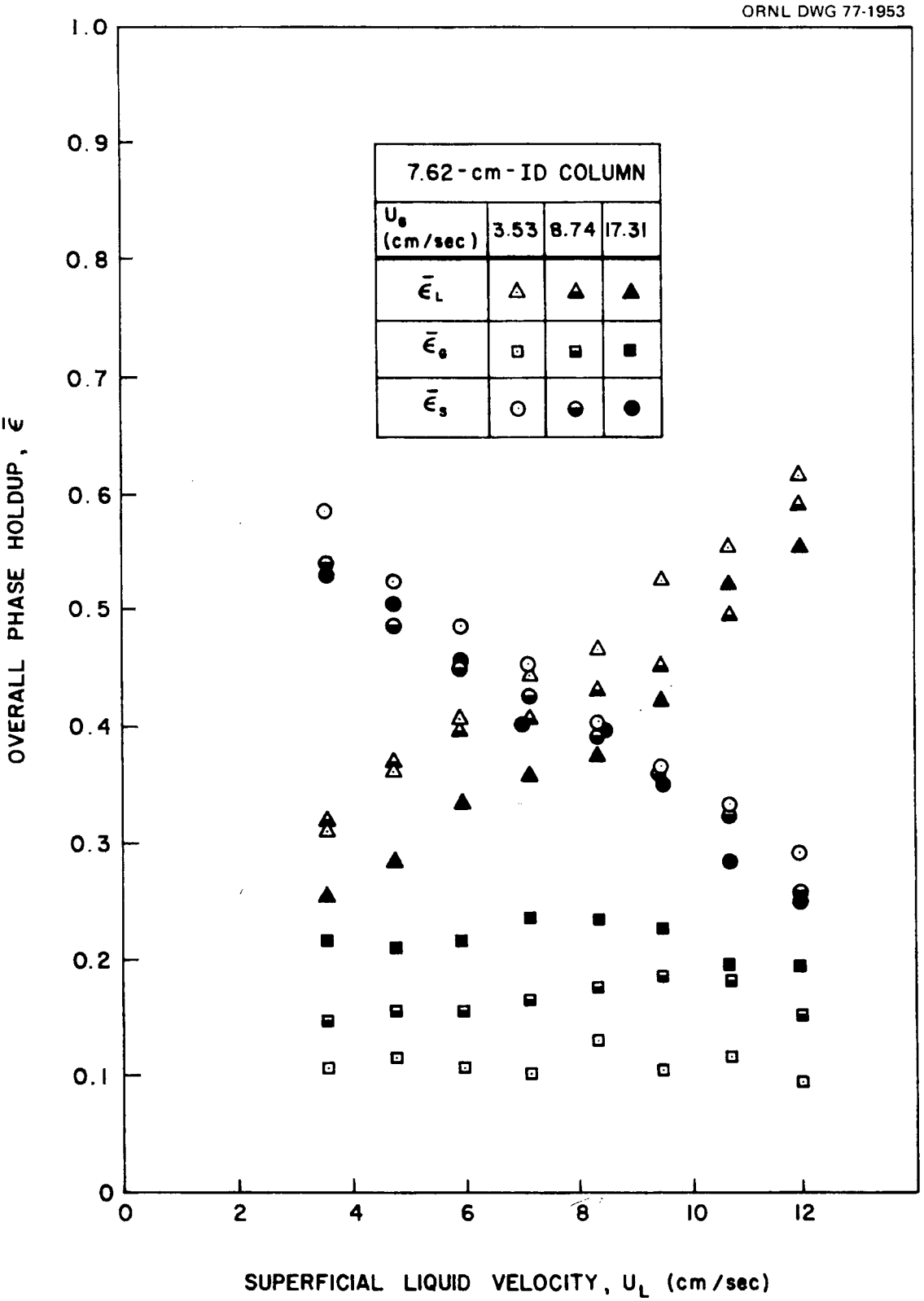

Figure 18. Effect of fluid velocities on the overall phase holdups obtained in the 7.62-cm-ID column using the air-water-alumina beads.

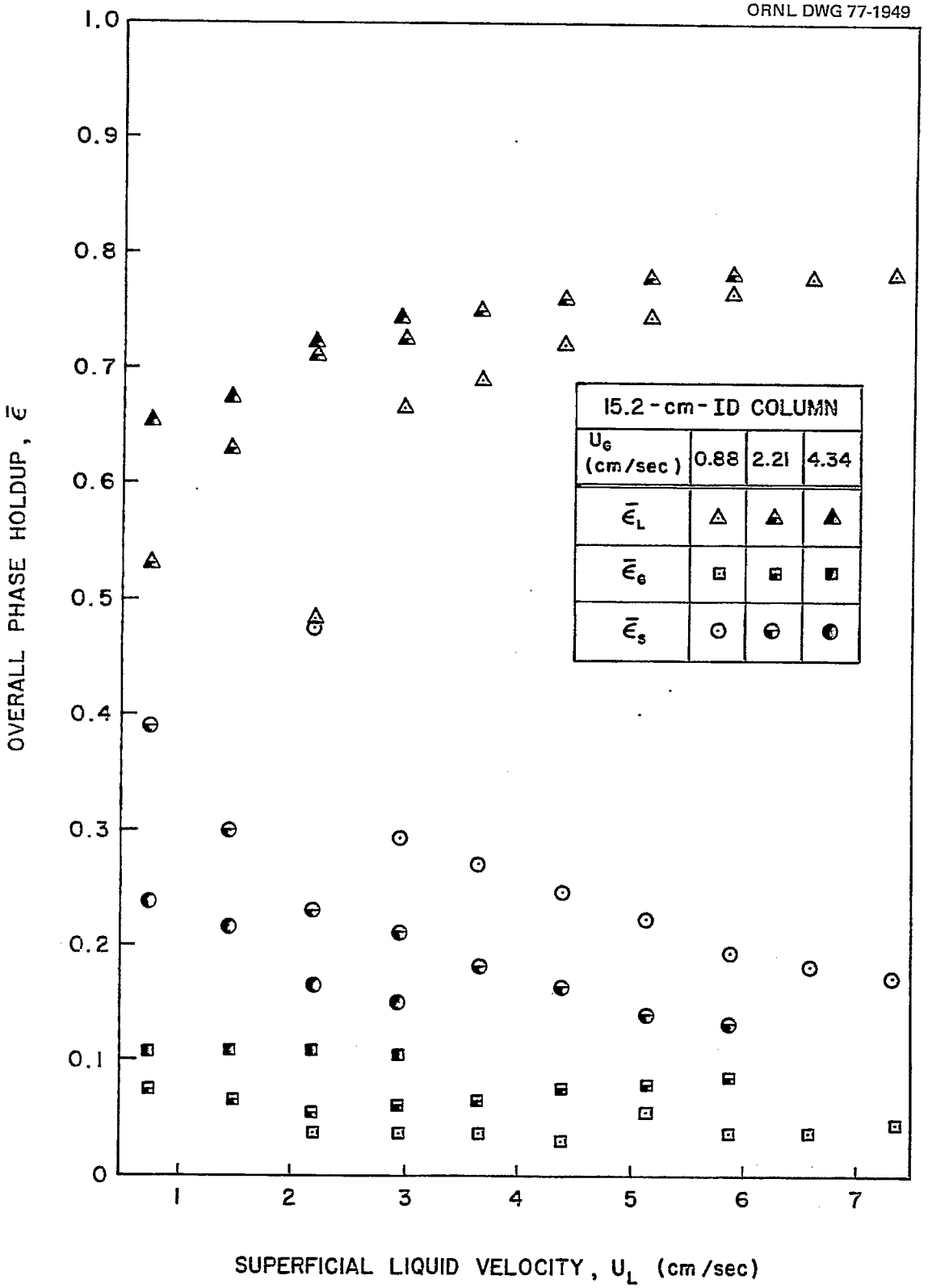

Figure 19. Effect of fluid velocities on the overall phase holdups obtained in the 15.2-cm-ID column using the air-water-plexiglass beads.

extent than the gas holdup was increased, so that the liquid holdup was increased.

Effect of column diameter on the overall phase holdups. The effect of column diameter on the overall phase holdups at a constant gas velocity is shown in Fig. 20 for the glass beads. The overall solid holdup was the same in both columns over the range of liquid velocities tested, while the gas holdup appeared to be slightly decreased in the large column as compared with that in the smaller 7.62-cm-ID column.

Data obtained by using a constant gas velocity of 0.44 cm/sec in the plexiglass beads system shown in Fig. 21 showed that the overall phase holdups followed the same trend with increasing liquid velocity in both columns. The gas holdup was similarly unaffected by column diameter in the same system at a higher gas velocity of 1.77 cm/sec, as shown in Fig 22. However, at this gas velocity and at liquid velocities below 3.5 cm/sec, the overall solid holdup was greater in the 7.62-cm-ID column than in the 15.2-cm-ID column. For liquid velocities in excess of 3.5 cm/sec, the overall solid and liquid holdup curves for the two columns merged into single curves.

Effect of solid characteristics on the overall phase holdups. The three systems used in the 7.62-cm-ID column--glass, plexiglass, and alumina beads--are shown in Fig. 23 as a function of the liquid velocity at a constant

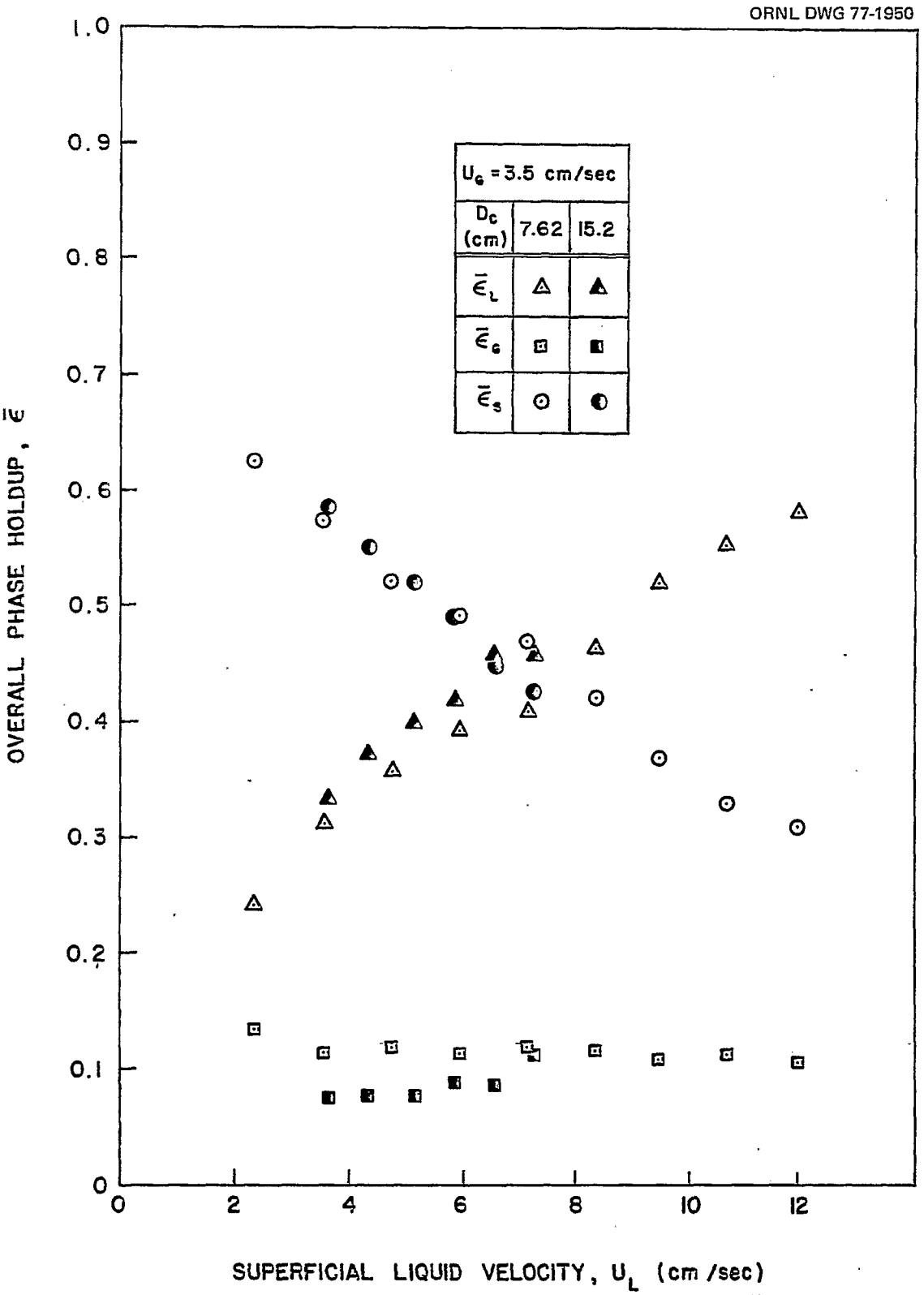

Figure 20. Effect of liquid velocity and column diameter on the overall phase holdups obtained using the air-water-glass beads.

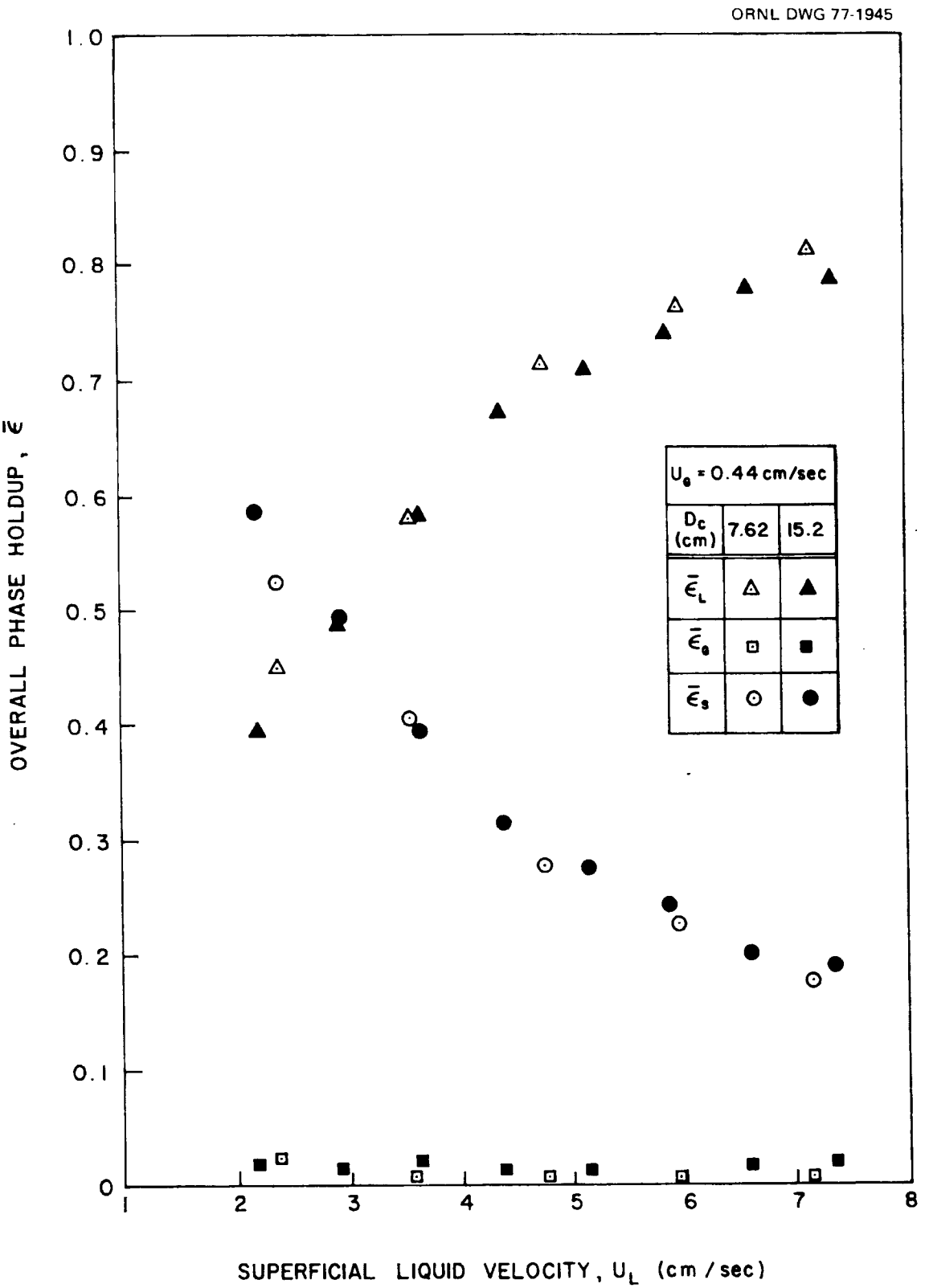

Figure 21. Effect of liquid velocity and column diameter on the overall phase holdups obtained using the air-water-plexiglass beads.

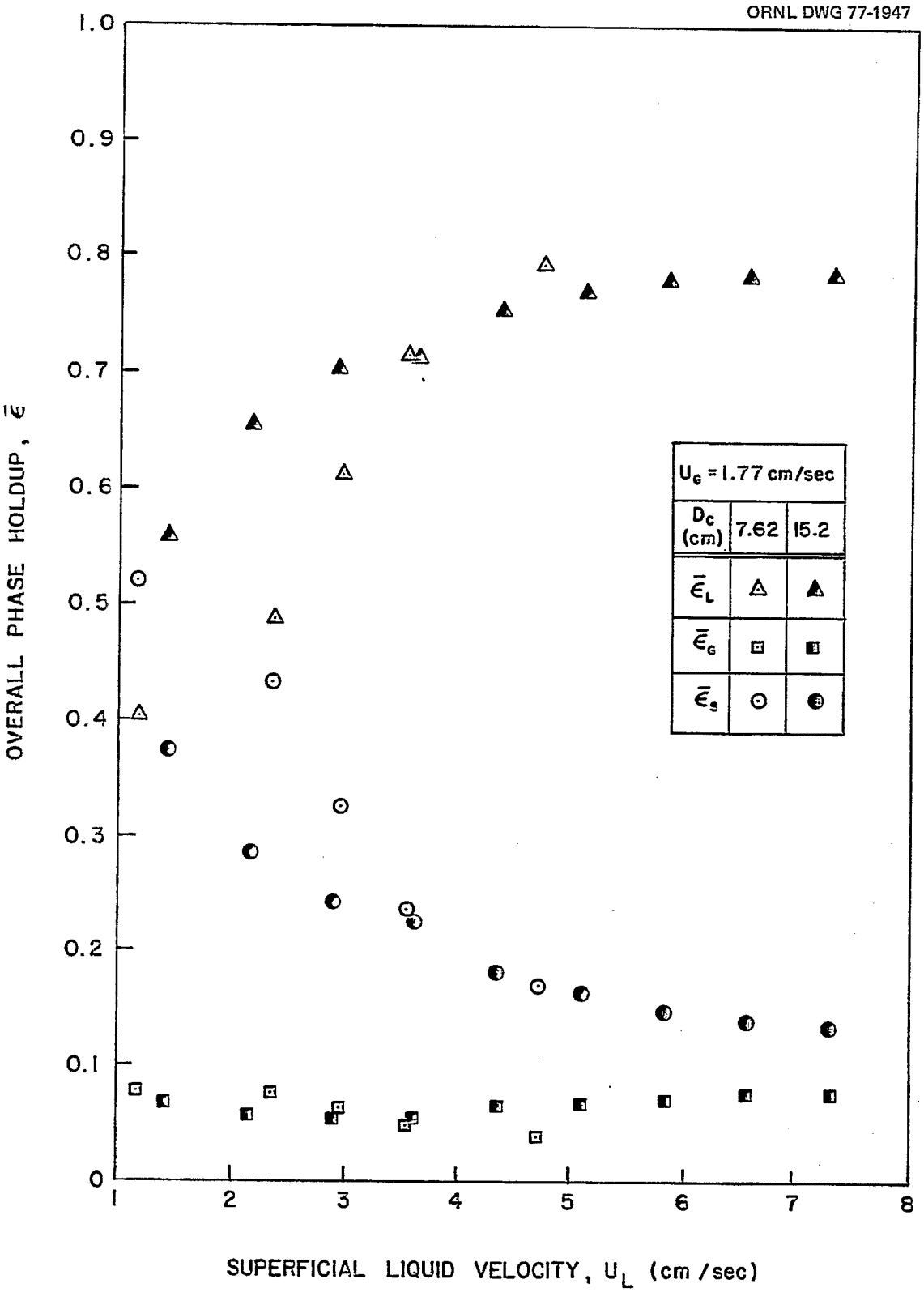

Figure 22. Effect of liquid velocity, column diameter, and a high gas velocity on the overall phase holdups obtained using the air-water-plexiglass beads.

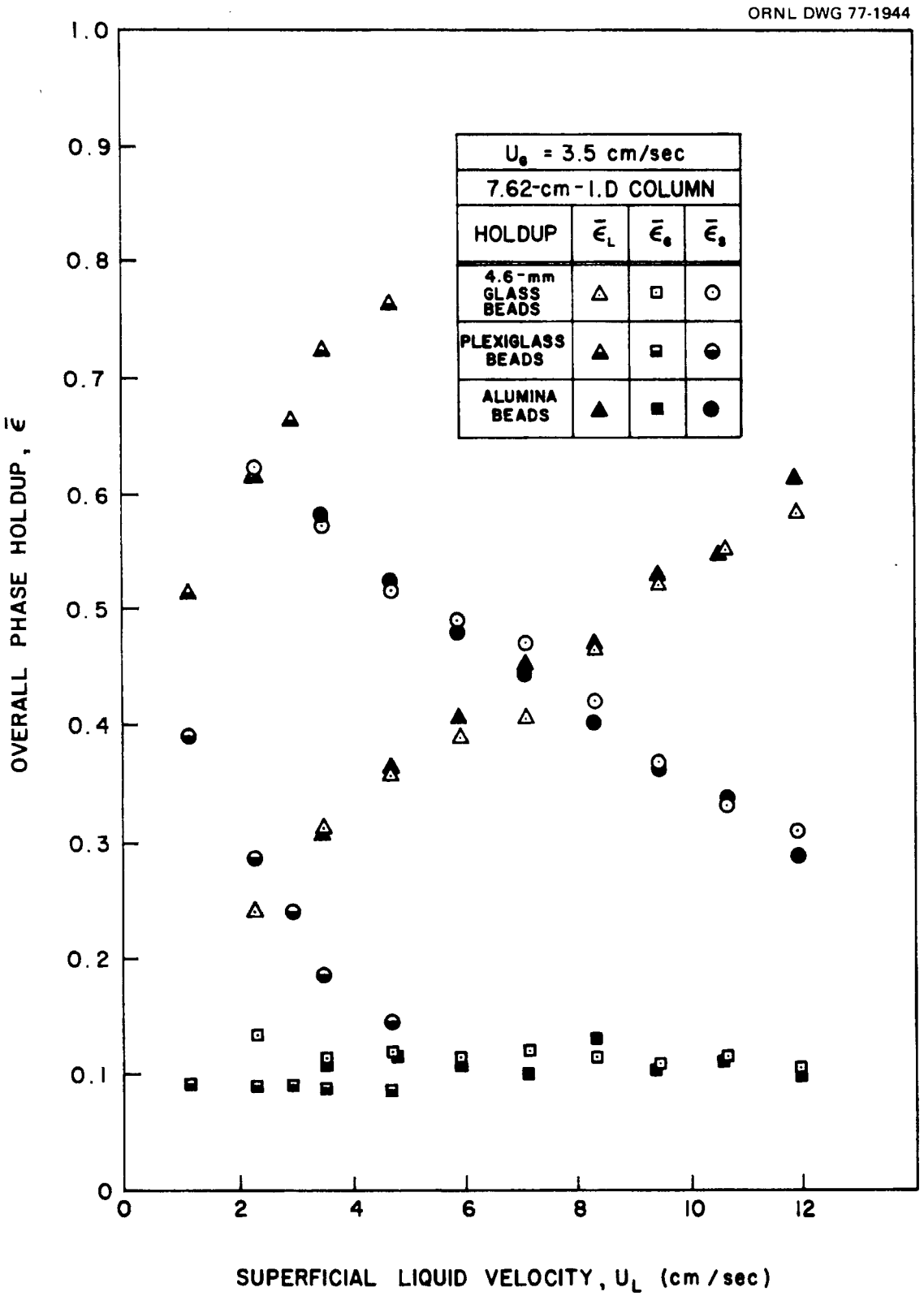

Figure 23. Effect of liquid velocity and solid characteristics on the overall phase holdups obtained in the 7.62-cm-ID column.

gas velocity. The overall gas holdup was essentially the same in all three systems, although use of the plexiglass beads resulted in slightly lower values. The glass and alumina beads gave the same values for the solid and liquid holdups while the plexiglass beads gave significantly lower solid and higher liquid holdups. The higher density of the glass beads, as compared with that of the alumina beads, compensated for their smaller diameter; on the other hand, the much lower density of the plexiglass beads did not compensate for their large diameter. Thus, while the glass and alumina bead beds were expanded to the same degree as the liquid velocity was increased, expansion of the plexiglass bead bed occurred to a considerably greater degree.

Similar behavior can be observed in Fig. 24 for the two systems studied in the 15.2-cm-ID column. For a constant gas velocity of 2.2 cm/sec, the overall gas holdup was nearly identical in the glass and plexiglass bead beds. Again, however, the lower-density plexiglass beads, while fluidized at less than half the liquid velocity needed to fluidize the glass beads, expanded to a considerably greater degree. This yielded a lower overall solid holdup and, in turn, a higher overall liquid holdup.

The overall phase holdup results are in good agreement with those of other investigators mentioned in the literature survey.

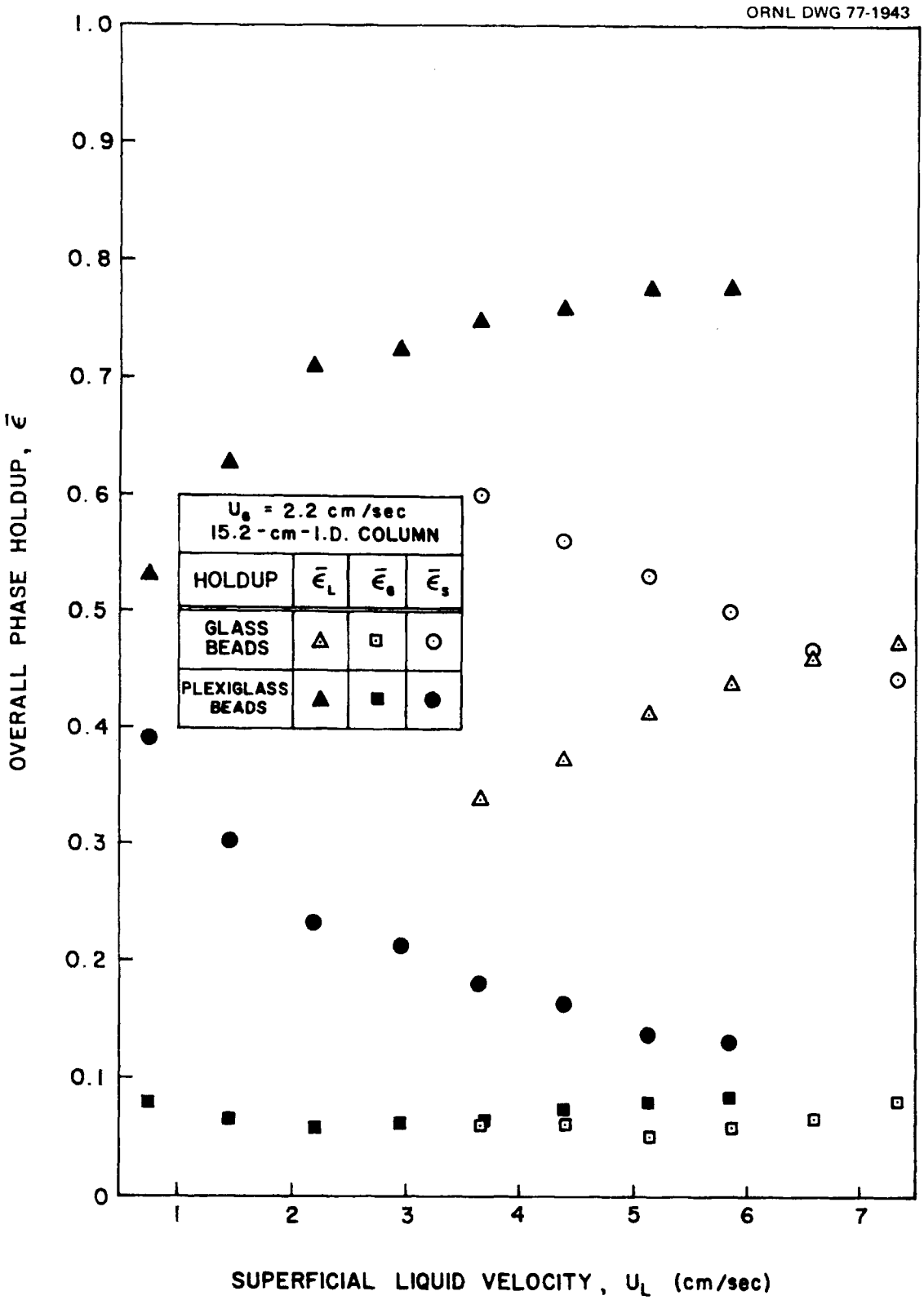

Figure 24. Effect of liquid velocity and solid characteristics on the overall phase holdups obtained in the 15.2-cm-ID column.

Bed Expansion Characteristics

The effects of injecting gas into a liquid-only fluidized bed were studied in several systems. In addition to noting whether the liquid fluidized bed initially expanded or contracted upon injection of gas, pertinent data were recorded so that the criterion of Epstein [1976], Eq. (17), could be applied.

The results, presented in Table 5, show that each of the systems expanded upon the introduction of gas when low liquid velocities were used. As the liquid velocity was increased in a liquid-only fluidized bed, the tendency of the bed to expand upon the introduction of gas decreased in each of the systems studied. Recalling that a positive value for Ψ indicates expansion and a negative value denotes contraction, Eq. (17) correctly predicted the expansion characteristics of each system studied except for the plexiglass beads at the two highest liquid velocities used. At those two liquid flow rates, Eq. (17) predicted that the bed would contract upon injection of gas; experimental observations, on the other hand, indicated that it would expand. The experimental observations were based on the bed heights calculated from the pressure gradients measured before and after gas was introduced into the columns. The plexiglass beads, with their small solid/liquid density difference, yielded a small change in pressure over the column; thus the pressure drop measurements for the plexiglass beads were subject to the

Table 5. Bed expansion characteristics of liquid fluidized beds upon injection of gas

System	U_L (cm/sec)	ε_L at ε_G =0	v_S (cm/sec)	k	Ψ (cm/sec)	Experimental Observation
4.6-mm-diam glass beads, 7.62-cm-ID column, U =41.4 cm/sec, n = 2.39	4.77	0.432	32.5	0.282	9.4	Expansion
	5.96	0.481	32.7	0.389	8.7	Expansion
	8.35	0.553	33.3	0.592	7.4	Expansion
4.6-mm-diam glass beads, 15.2-cm-ID column, U =41.4 cm/sec, n = 2.39	4.77	0.404	45.1	0.231	9.7	Expansion
	5.87	0.456	45.3	0.332	7.8	Expansion
	7.34	0.522	45.6	0.498	3.9	Expansion
6.2-mm-diam alumina beads, 7.62-cm-ID column, U =42.8 cm/sec, n = 2.39	4.77	0.381	32.8	0.194	13.7	Expansion
	5.29	0.411	32.8	0.243	13.0	Expansion
	5.96	0.441	33.0	0.300	12.4	Expansion
	7.16	0.488	33.2	0.407	11.4	Expansion
	8.35	0.526	33.4	0.509	10.5	Expansion
	9.54	0.575	33.6	0.665	7.6	Expansion
	10.74	0.616	33.7	0.818	4.8	Expansion
	11.93	0.649	33.9	0.957	2.5	Expansion
6.3-mm-diam plexiglass beads, 15.2-cm-ID column, U =18.4 cm/sec, n = 2.39	1.83	0.393	25.0	0.212	3.0	Expansion
	3.67	0.558	25.0	0.712	-3.9	Contraction
	5.50	0.698	25.0	1.190	-10.5	Expansion
	7.34	0.785	25.0	1.693	-18.3	Expansion
1.9-mm-diam alumino-silicate beads, U =17.9 cm/sec, n = 2.49	1.22	0.292	31.1	0.087	4.2	Expansion
	2.45	0.470	31.4	0.278	-1.7	Contraction
	4.77	0.621	31.8	0.838	-7.4	Contraction

largest potential relative error of any of the systems studied.

Axial Variation in Holdups

As discussed previously, bed heights are indistinct at high flow rates, and the holdups calculated using Eqs. (1)-(3) are based on an unrealistic homogeneous-bed model. The holdups could be determined as functions of axial position within the column by using the electroconductivity of the bed and the measured pressure gradient

A typical plot of the axial variation of the phase holdups is shown in Fig. 25. The liquid holdup remained essentially uniform near the bottom of the bed but increased with distance from the bottom to a constant value in the gas-liquid region above the bed. The calculated bed height (48 cm) was that obtained from the pressure gradient in and above the bed. This corresponded to the height of a bed with uniform solid holdup as indicated by the horizontal dashed line. However, the actual solid holdup decreased with increasing axial position in the bed, so that the observed upper limit of solids would be between 60 and 70 cm. The area under the solid holdup curve should be equal to the following modification of Eq. (3):

$$\int_0^H \varepsilon_S dh = M_S/\rho_S A \quad . \tag{27}$$

If the solid holdup is not a function of height in the bed, Eq. (27) reduces to Eq. (3).

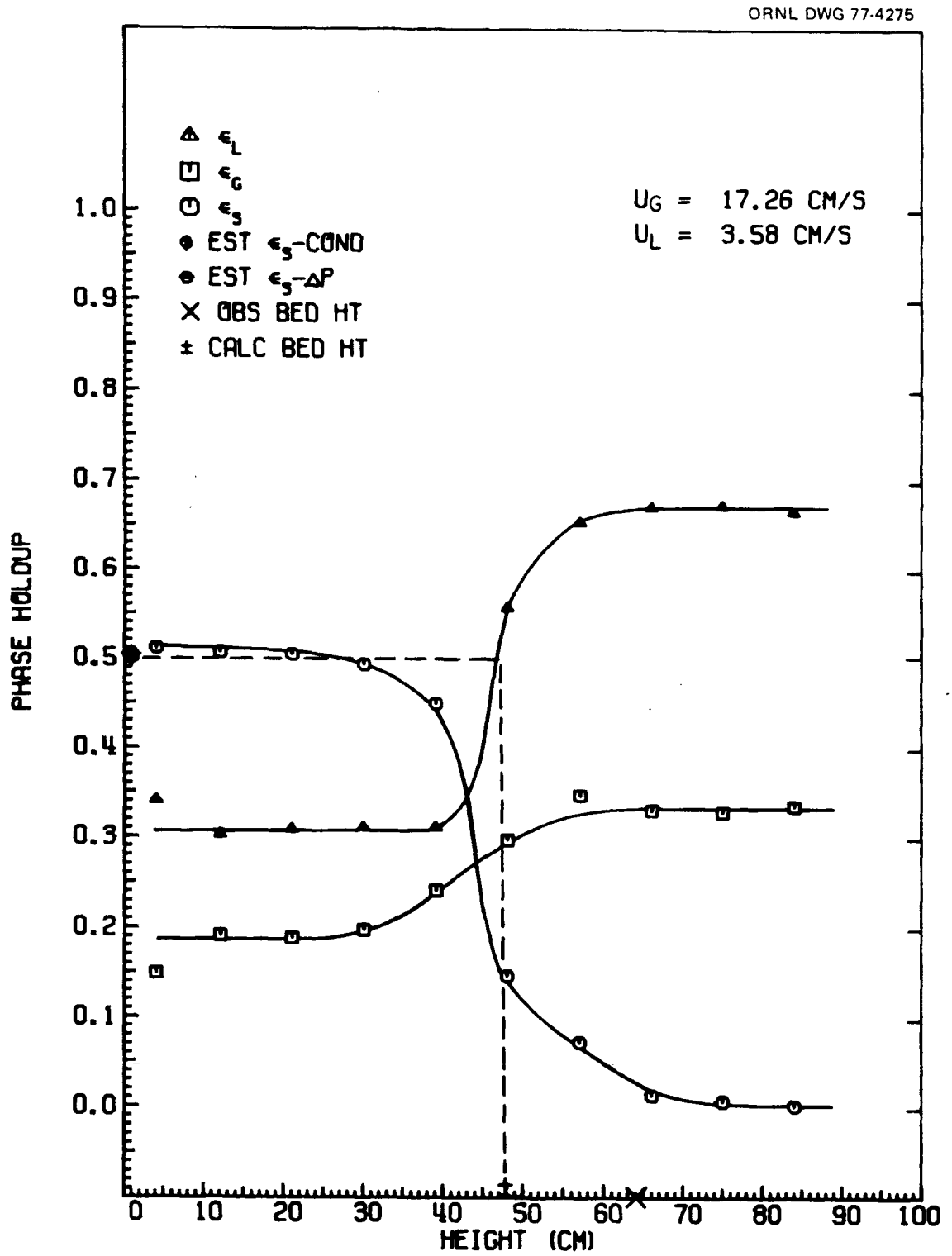

Figure 25. Axial variation of phase holdups in the 7.62-cm-ID column using the air-water-glass beads.

Effect of column diameter. The effect of column diameter on the axial variation of the solid and liquid holdups can be seen in Figs. 26 and 27. These results, typical of most of the data, were obtained in the 7.62- and 15.2-cm-ID columns under identical conditions (i.e., identical gas velocities, liquid velocities, particle type, and static bed height).

Neither figure indicates a dependence of the holdups on column diameter in the lower portion of the beds. However, for the lower liquid velocity used in Fig. 26, the transition region from three phases (gas-liquid-solid) to two phases (gas-liquid) appeared to be broader in the smaller column. The liquid holdup also rose to a slightly lower value in the 7.62-cm-ID column as compared with the 15.2-cm-ID column. These effects are not evident in Fig. 27, where the same relationship between the holdups and height was obtained in both columns.

Effect of liquid velocity. The effect of liquid velocity on the axial variation in the glass bead holdup is shown in Fig. 28 under conditions of constant gas velocity in the 7.62-cm-ID column. The bed expanded, and thus the solid holdup decreased, as the liquid velocity was increased. The calculated bed height, as found from the intersection of the measured pressure gradients in and above the bed, is indicated on the curves for each flow rate. This value corresponds to the height the same bed would have

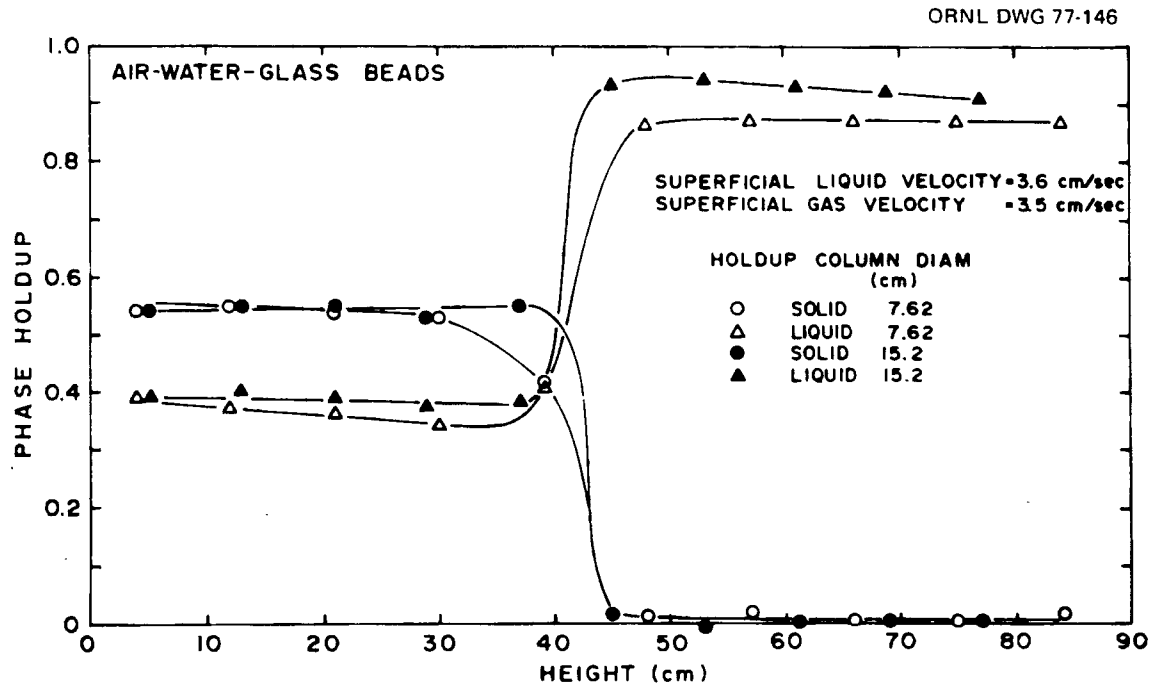

Figure 26. Effect of column diameter on the axial variation of phase holdups using a liquid velocity of 3.6 cm/sec.

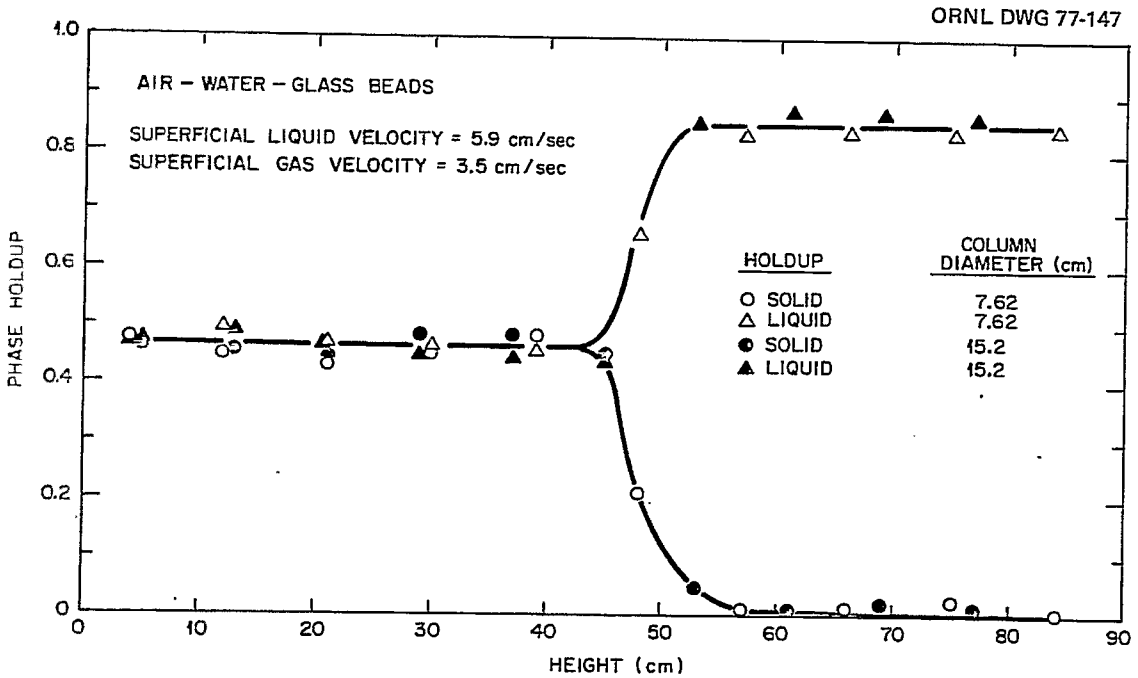

Figure 27. Effect of column diameter on the axial variation of phase holdups using a liquid velocity of 5.9 cm/sec.

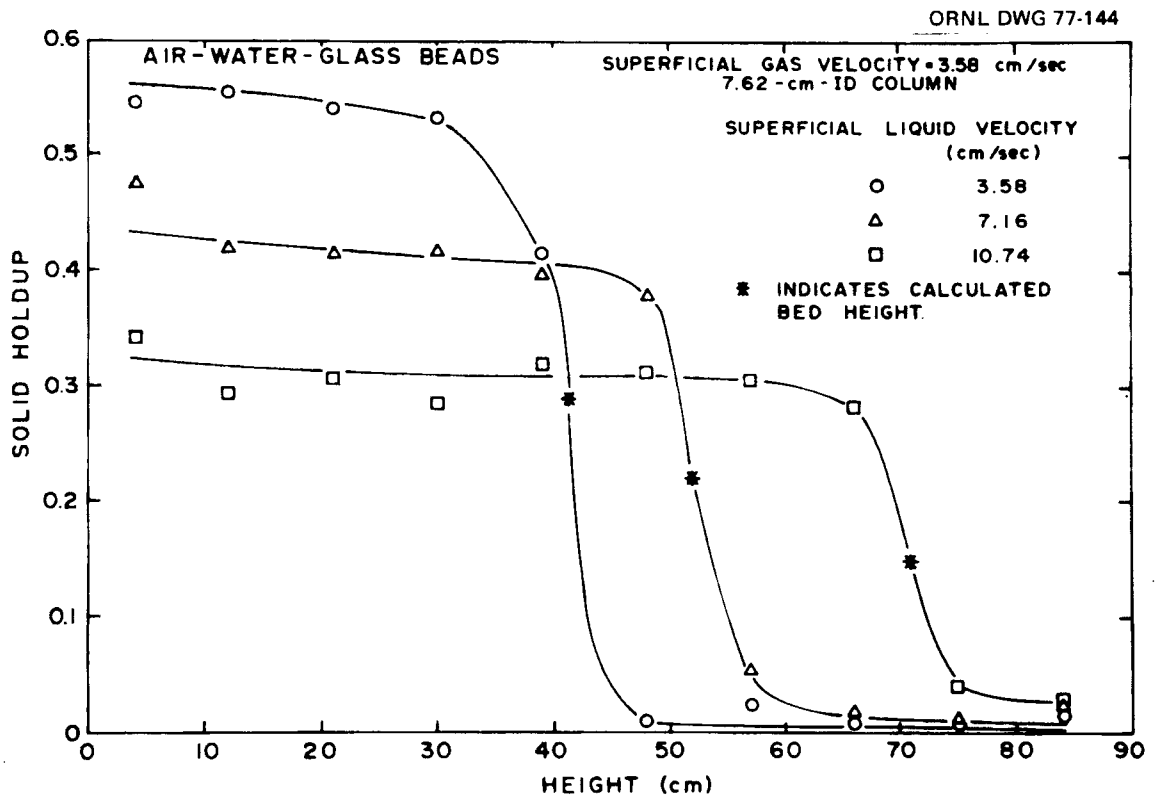

Figure 28. Effect of liquid velocity on the axial variation in the solid phase holdup.

if the solids in the column were uniformly distributed. The highest point at which solids were detected was higher than this calculated bed height, however, since the bed contains a rather wide transition region over which flow changes from a three-phase to a two-phase column. The width of this transition region appeared to remain approximately constant with changing liquid velocity; that is, the solid holdup decreased from the approximately constant value in the bed to zero over about 20 cm of column height.

Effect of gas velocity. When the liquid velocity was held constant and the gas velocity was increased, the width of the transition region increased substantially, as illustrated in Fig. 29. The solid holdup in the lower portion of the bed was decreased slightly by the increase in gas velocity from 3.58 to 17.26 cm/sec; however, the width of the transition region increased from 20 cm to approximately 35 cm. As expected, the calculated bed height for the higher gas velocity indicated a much lower bed height than that observed visually (highest position with solids).

These results demonstrate the shortcomings of assuming a distinct bed height and a uniform bed. The transition region is a significant fraction of the total bed height and must be considered in realistic designs of three-phase systems. If commercial units operate with taller beds, the transition region would become less important; however, the

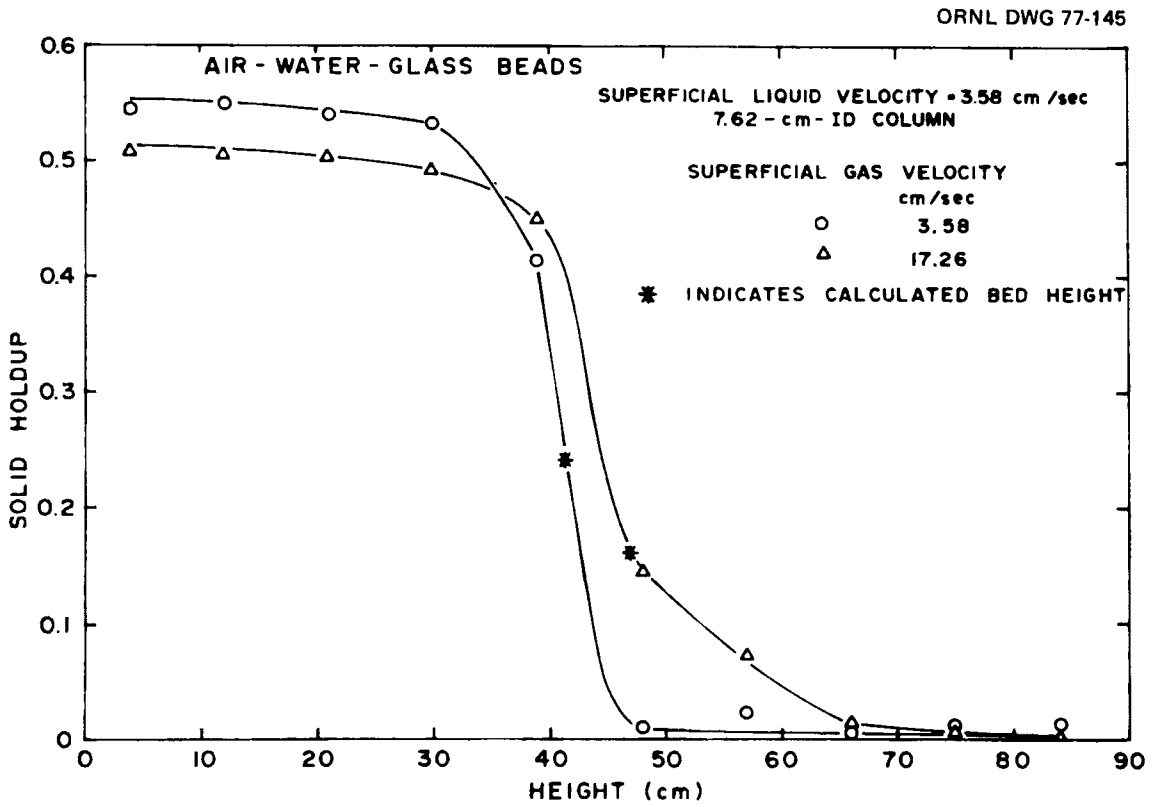

Figure 29. Effect of gas velocity on the axial variation in the solid phase holdup.

higher gas rates often employed by such units could still cause the transition regions to remain a significant fraction of the total bed height.

Discussion of Error

Four runs were performed using the 4.6-mm-diam glass beads in the 7.62-cm-ID column under identical conditions (i.e., gas and liquid flow rates and initial bed heights). Runs G45A13, G46A13, G47A13, and G48A13 were made with no air flow and with initial bed heights of 36 cm. Although the systems consisted of only two phases, it is felt that the errors associated with measuring bed heights and pressure drops and calculating bed heights and holdups are substantially equivalent to those associated with a three-phase system.

At a defined liquid velocity, the pressure and conductivity gradients were measured as described earlier in the section on "Experimental Procedure" (see page 35). The bed height and bed pressure drop were calculated from these data. Then the overall phase holdups were calculated based on either the conductivity method or the pressure gradient method. Finally, the phase holdups were calculated as a function of column position.

Table 6 shows the results obtained in the four runs, which were made with a liquid velocity of 8.35 cm/sec. An average and a standard deviation can be calculated for each variable at this liquid velocity. By using the Student's t

Table 6. Calculated values for four identical runs[1]

Parameter	Run G45A13	G46A13	G47A13	G48A13
Bed height, cm	53.7	52.1	52.2	52.6
Δh_{Bed}, cm water	27.44	28.37	28.56	28.60
$\bar{\varepsilon}_{L,C}$	0.649	0.647	0.647	0.643
$\bar{\varepsilon}_{S,C}$	0.442	0.442	0.442	0.442
$\bar{\varepsilon}_{L,\Delta P}$	0.578	0.548	0.546	0.548
$\bar{\varepsilon}_{S,\Delta P}$	0.431	0.444	0.443	0.443

[1]Conditions for each run: U_L = 8.35 cm/sec; U_G = 0

distribution and a given confidence level, a confidence interval about the mean can be found. For a confidence level of 95%, the average value and its confidence interval for each variable shown in Table 6 are given below:

$$H = 52.6 \pm 1.22, \qquad \bar{\varepsilon}_{S,C} = 0.442 \pm 0,$$

$$\Delta h_{Bed} = 28.24 \pm 0.886, \qquad \bar{\varepsilon}_{L,\Delta P} = 0.555 \pm 0.0244,$$

$$\bar{\varepsilon}_{L,C} = 0.647 \pm 0.0040, \qquad \bar{\varepsilon}_{S,\Delta P} = 0.440 \pm 0.0098.$$

These results are typical of all of those found at each of the six liquid velocities used in these runs.

Taking the average of a variable at each liquid velocity, an overall standard deviation can be found for the variable based on its values at all of the liquid velocities for the four runs. The confidence interval for each variable and a confidence interval percentage based on an average value for the entire set of runs are shown in Table 7 for a confidence level of 95%.

The confidence intervals shown in Table 7, which are based on all six liquid velocities used in the four runs for a total of 24 points, are lower than those calculated at a single liquid velocity of 8.35 cm/sec, which are based only on a total of four points. Regardless of the method of calculation of the confidence interval, it is apparent that the agreement between the four runs was quite good and that each variable could be determined with a small confidence interval at a high degree of certainty.

Table 7. Confidence intervals of calculated values for four identical runs

Variable	Confidence interval	Percent confidence interval	Average value of variable used as basis
H	0.18	0.4	47
Δh_{Bed}	0.260	1.2	22
$\bar{\varepsilon}_{L,C}$	0.0024	0.4	0.60
$\bar{\varepsilon}_{S,C}$	0.0019	0.4	0.48
$\bar{\varepsilon}_{L,\Delta P}$	0.0035	0.7	0.52
$\bar{\varepsilon}_{S,\Delta P}$	0.0016	0.3	0.48

CHAPTER 6

CORRELATION OF RESULTS

The results shown in the previous chapter for minimum fluidization velocities, overall phase holdups, and local phase holdups were correlated with the physical parameters of the systems studied by using multiple linear regression. Dimensional correlations were first tried, followed by dimensionless correlations whenever possible. The predictive equations presented in this chapter represent the best correlations of the many that were attempted.

Minimum Fluidization

The minimum liquid fluidization velocities shown in Fig. 4 and Figs. 7-9 (see pp. 30, 39, 40, and 42) were correlated with the system parameters and resulted in the following dimensionless correlation:

$$Re_{mf} = a\, Ar^{b}\, Fr_{G}^{c} \quad , \tag{28}$$

where the constants and their 95% confidence limits are:

$a = 5.131 \times 10^{-3} \pm 0.002$,

$b = 0.661 \pm 0.034$,

$c = -0.120 \pm 0.025$.

Equation (28) had a correlation coefficient of 0.94 and an F-value of 478, using a total of 135 points, and is shown in Figs. 30-32 as predicted-versus-experimental MF curves.

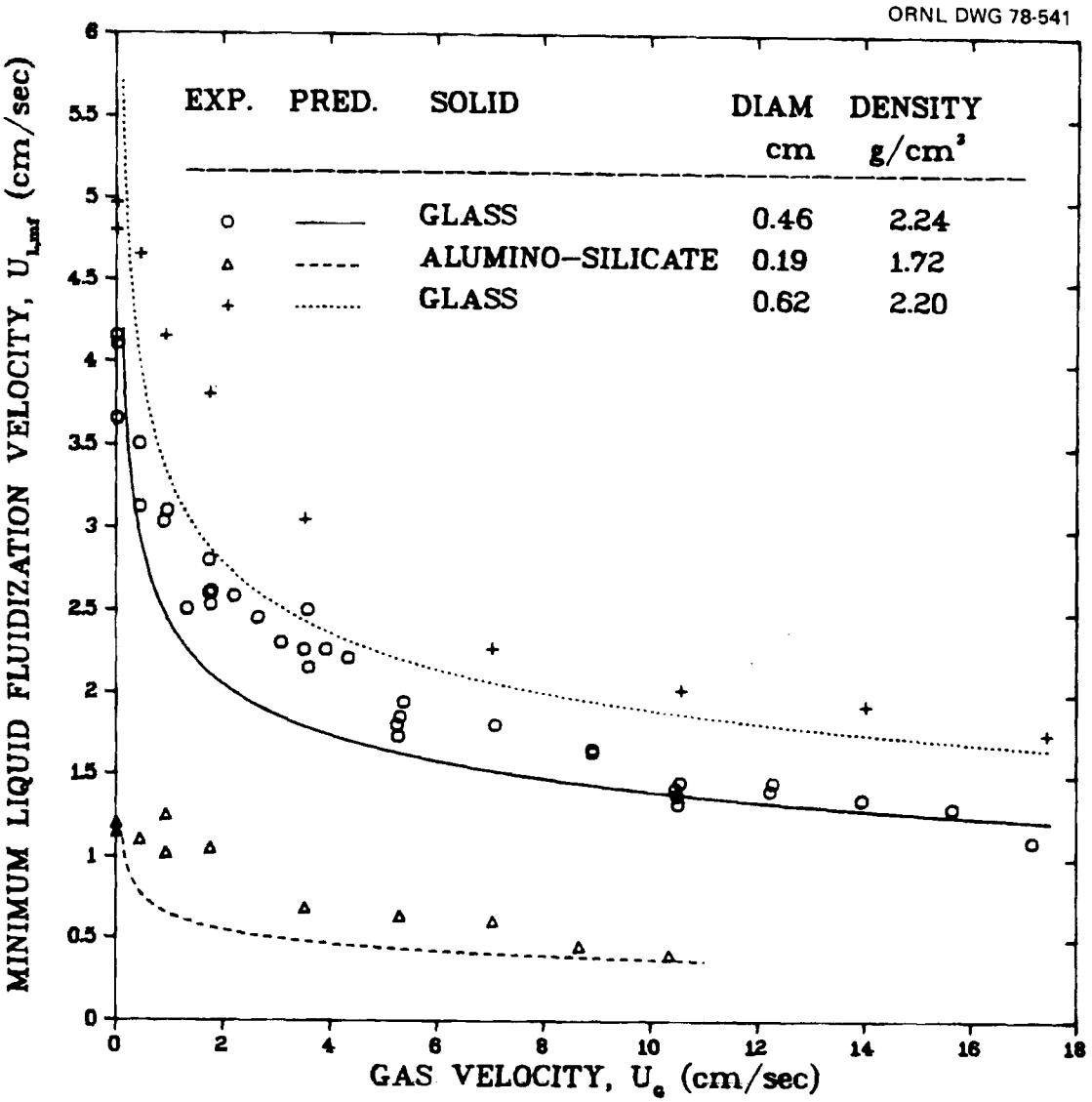

Figure 30. Predicted versus experimental minimum fluidization curves for the glass and alumino-silicate beads.

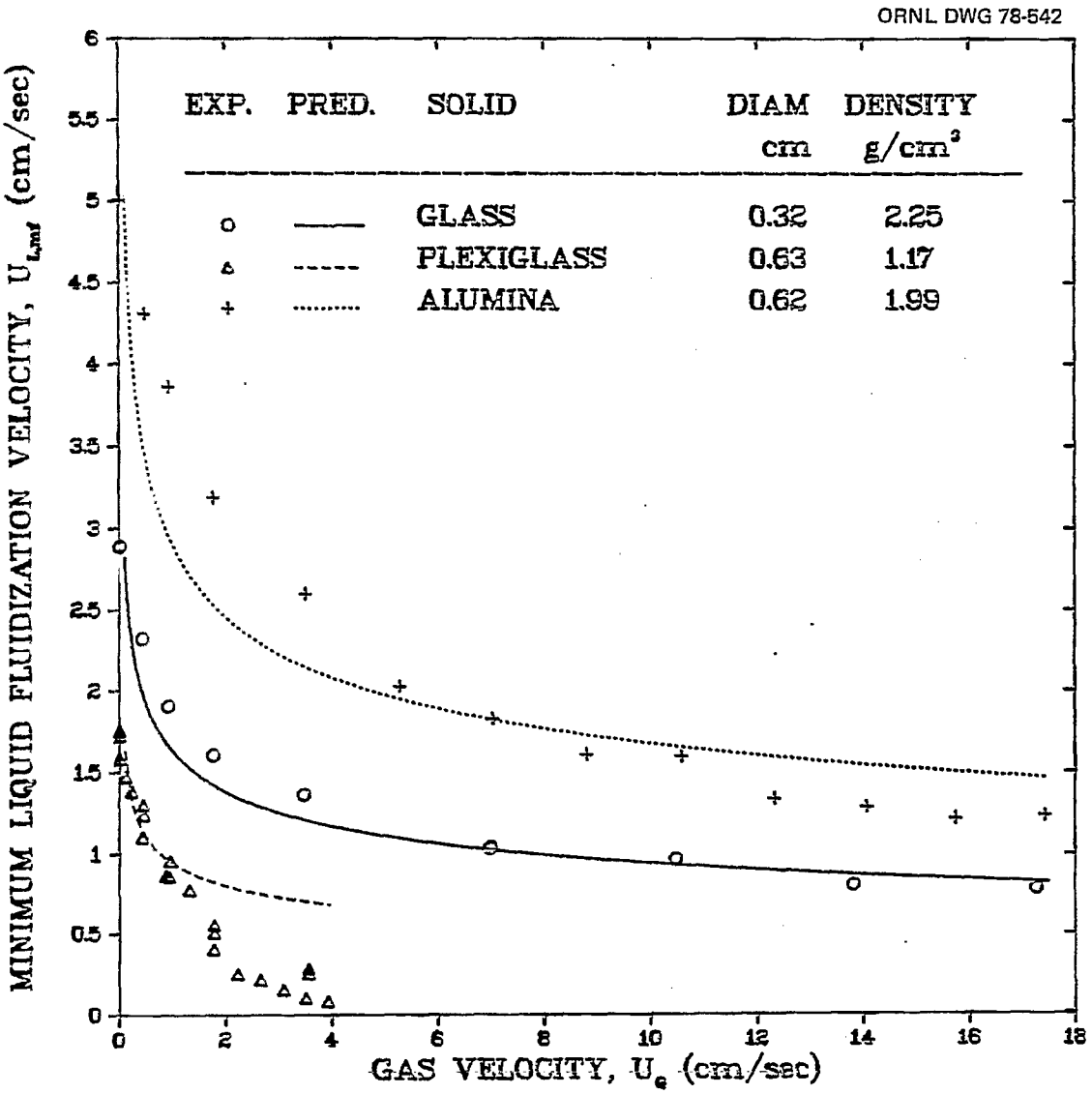

Figure 31. Predicted versus experimental minimum fluidization curves for the glass, plexiglass, and alumina beads.

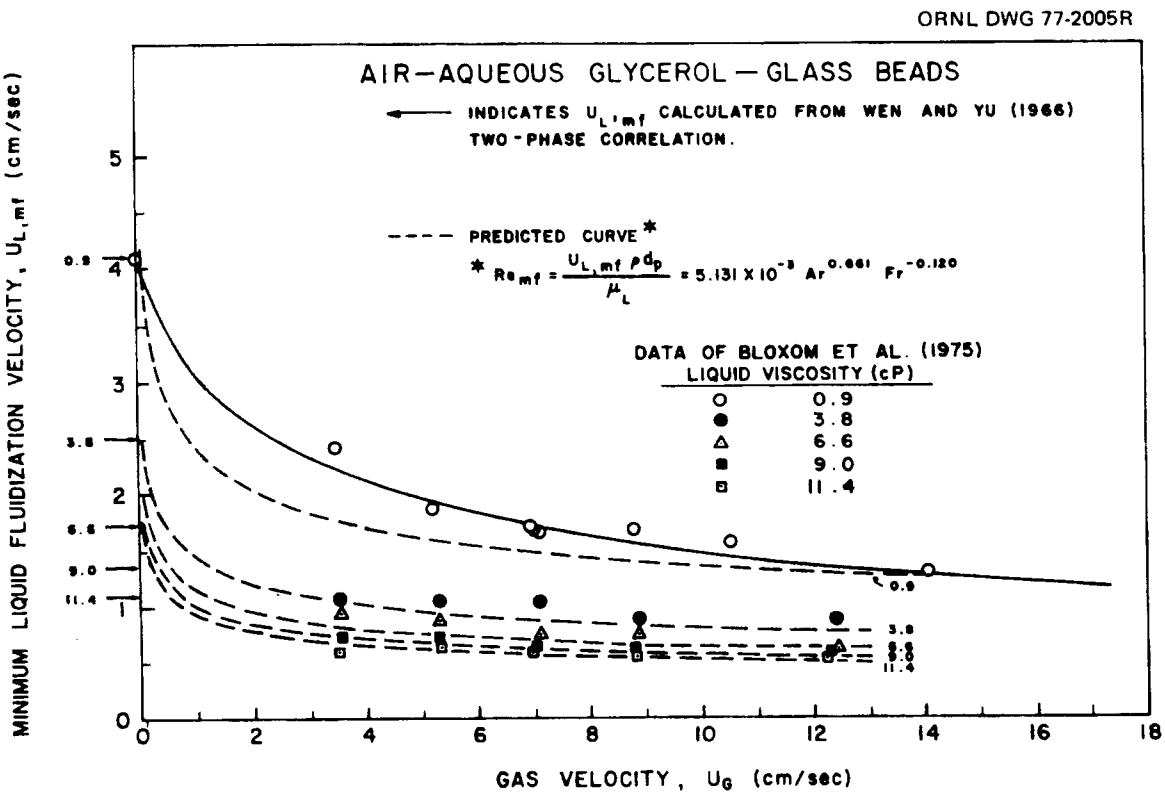

Figure 32. Effect of liquid viscosity on the predicted versus experimental minimum fluidization curves.

It should be noted that Eq. (28) is not valid for a zero gas rate where it would predict a liquid MF velocity of zero. However, Figs. 30-32 show that the MF curves can be reliably extrapolated to zero gas flow rate if a predicted MF curve is generated starting with gas velocities just greater than zero. Alternatively, at zero gas velocity, the two-phase correlation of Wen and Yu [1966], Eq. (26), can be used to predict the MF velocity.

Overall Phase Holdups

The overall solid holdups from this study were combined with 1355 points from the literature [Bhatia and Epstein, 1974; Bruce and Revel-Chion, 1974; Dakshinamurty et al., 1971; Efremov and Vakhrushev, 1970; Kim et al., 1975; Michelsen and Ostergaard, 1970; Ostergaard, 1965; Ostergaard and Michelsen, 1968; Ostergaard and Thiesen, 1966; Rigby and Capes, 1970] to yield the following dimensional correlation:

$$1 - \bar{\varepsilon}_S = a\, U_L^{\,b}\, U_G^{\,c}\, (\rho_S - \rho_L)^d\, d_p^{\,e}\, \mu_L^{\,f}\, D_c^{\,g} \quad , \qquad (29)$$

where the constants and their 95% confidence limits are:

$a = 0.371 \pm 0.013$, $e = -0.268 \pm 0.008$,

$b = 0.271 \pm 0.008$, $f = 0.055 \pm 0.006$,

$c = 0.041 \pm 0.004$, $g = -0.033 \pm 0.010$,

$d = -0.316 \pm 0.008$,

and centimeter-gram-second (CGS) units are used for each parameter. Equation (29), shown as a parity plot in Fig. 33, has a correlation coefficient of 0.87 and an F-value of

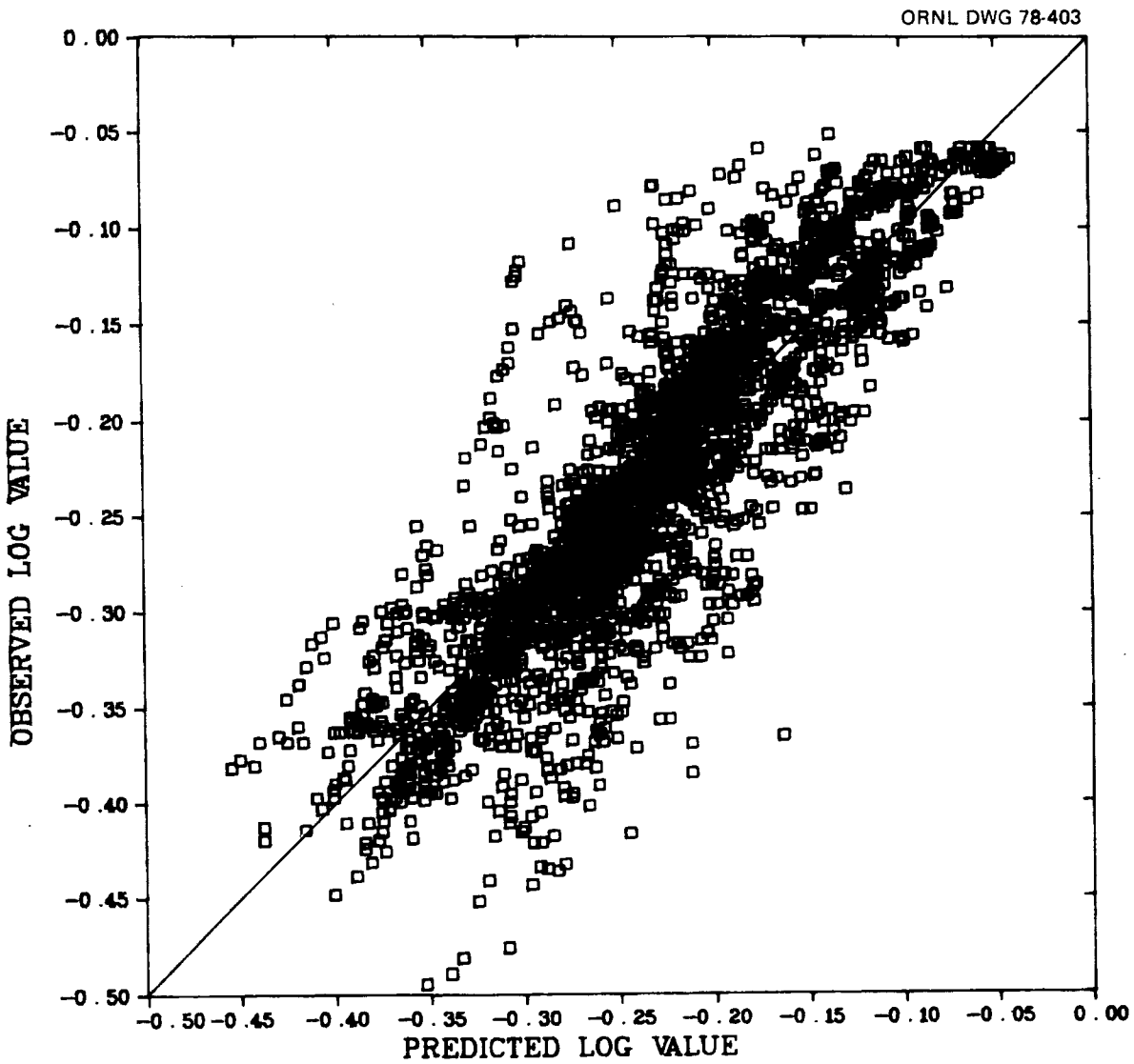

Figure 33. Predicted versus experimental overall solid holdup values.

1178; it was based on a total of 2381 points.

Combining the gas holdup with 169 points available from the literature [Bhatia and Estein, 1974; Efremov and Vakhrushev, 1970; Kim et al., 1975; Michelsen and Ostergaard, 1970; Ostergaard and Michelsen, 1968] resulted in the following correlation:

$$\bar{\varepsilon}_G = a\, U_G^{\,b}\, d_p^{\,c}\, D_c^{\,d} \quad , \tag{30}$$

where the constants and their 95% confidence limits are:

$a = 0.048 \pm 0.008$, $c = 0.168 \pm 0.046$,

$b = 0.720 \pm 0.021$, $d = -0.125 \pm 0.067$,

and, again, CGS units are used for each parameter. Equation (30), based on a total of 913 points, had a correlation coefficient of 0.93 and an F-value of 1793; it is shown as a parity plot in Fig. 34.

Local Holdups

Figures 25-29 (see pp. 68, 70, 71, 72, and 74) clearly indicated that each of the holdups is approximately constant in two regions: (a) the lower portion of the bed, and (b) the gas-liquid region above the bed. The transition region between these two extremes was seen to depend on the gas velocity and the physical characteristics of the solid particles. An inflection point was observed on each curve with a spread about that point proportional to the width of the transition region. If each curve were differentiated, these two parameters would correspond to the mean and the

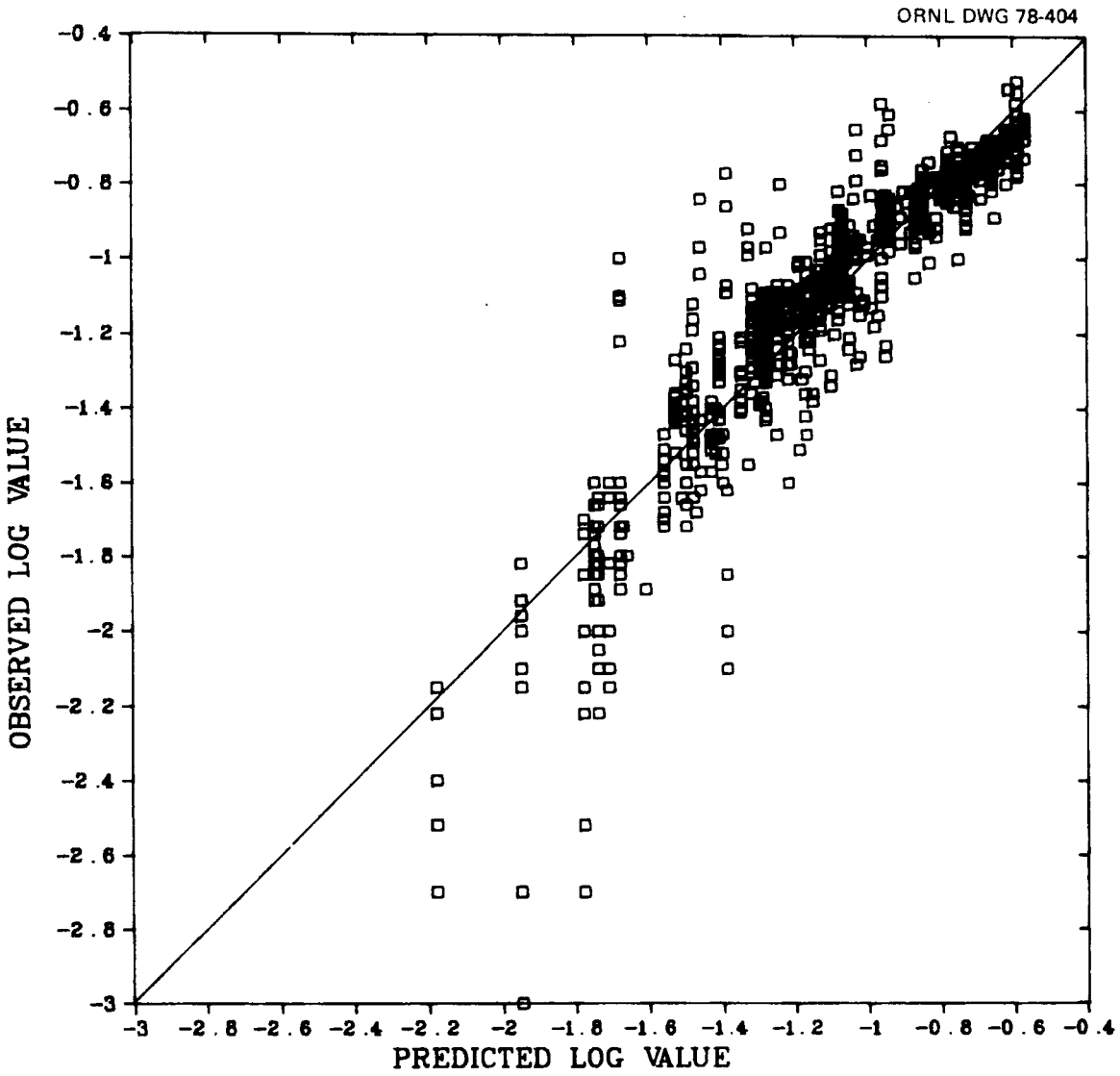

Figure 34. Predicted versus experimental overall gas holdup values.

standard deviation of the normalized Gaussian curves. The error function was used to fit the gas and solid holdup curves, and the liquid holdup curve was determined as the residual of Eq. (1). Use of the error function was essentially equivalent to use of the probability integral since the two are related by the following:

$$\text{erf}(x) = 2\Phi\ (\sqrt{2}\ x) \quad . \tag{31}$$

Thus, the gas holdup curves were fitted by the following:

$$\varepsilon_G = [(P_G - 1)/-2]\varepsilon_G^{'''} + [(P_G + 1)/2]\varepsilon_G^{''} \quad , \tag{32}$$

where

$$P_G = \text{erf}\ [(h - I_G)/\sigma_G] \quad . \tag{33}$$

The solid holdup was fitted in a similar manner using the error function and the knowledge that the solid holdup in the gas-liquid region of the column is zero:

$$\varepsilon_S = [(P_S + 1)/2]\varepsilon_S^{'''} \quad , \tag{34}$$

where

$$P_S = -\text{erf}\ [(h - I_S)/\sigma_S] \quad , \tag{35}$$

and

I = inflection point in local holdup-versus-height curve,

σ = standard deviation in local holdup-versus-height curve.

The liquid holdup at each point was obtained from the residual of Eq. (1).

Thus, knowledge of seven parameters--ε_G''', ε_G'', ε_S''', σ_S, σ_G, I_S, and I_G--allows one to construct each of the curves showing phase holdup versus axial column position. An example of such a fit in shown in Fig. 35. For the system shown, the seven parameters are:

$\varepsilon_G''' = 0.072$, $I_G = 45.7$ cm,

$\varepsilon_G'' = 0.129$, $\sigma_S = 2.83$ cm,

$\varepsilon_S''' = 0.511$, $\sigma_G = 2.64$ cm.

$I_S = 44.8$ cm,

Treatment of the experimental data in this way and correlation of the seven parameters with fluid and solid properties and experimental conditions using least-squares multiple linear regression analysis resulted in a predictive equation for each parameter.

The gas holdup in the three-phase region of the column was successfully correlated by the following:

$$\varepsilon_G''' = a\,[U_G^5(\rho_S-\rho_L)/U_L\, g\, \sigma_{LV}]^b \quad , \qquad (36)$$

where the constants and their 95% confidence limits are:

$a = 0.159 \pm 0.008$,

$b = 0.150 \pm 0.006$.

Equation (36), shown as a parity plot in Fig. 36, had a

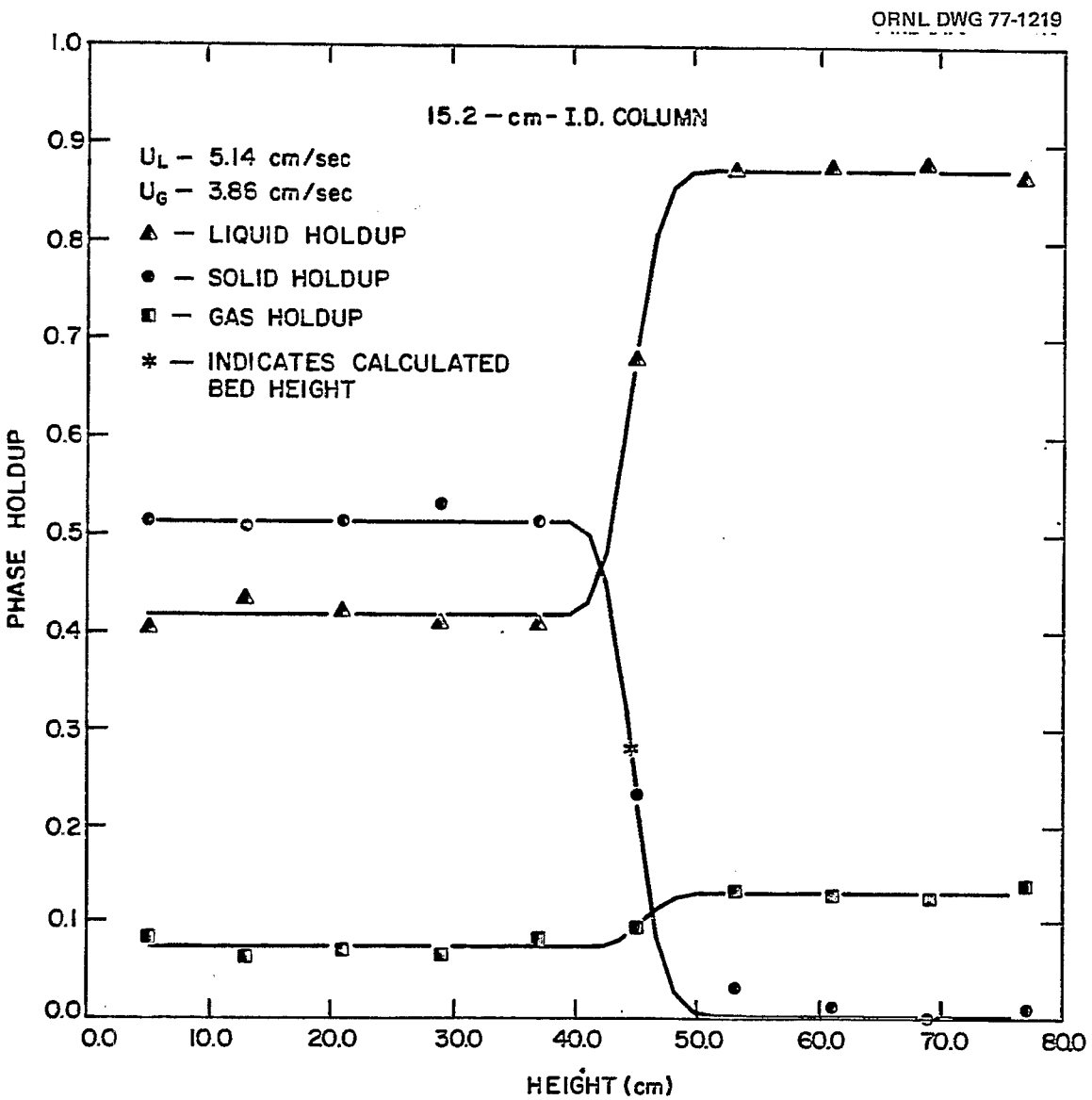

Figure 35. Fit of local holdup profiles for the air-water-glass beads.

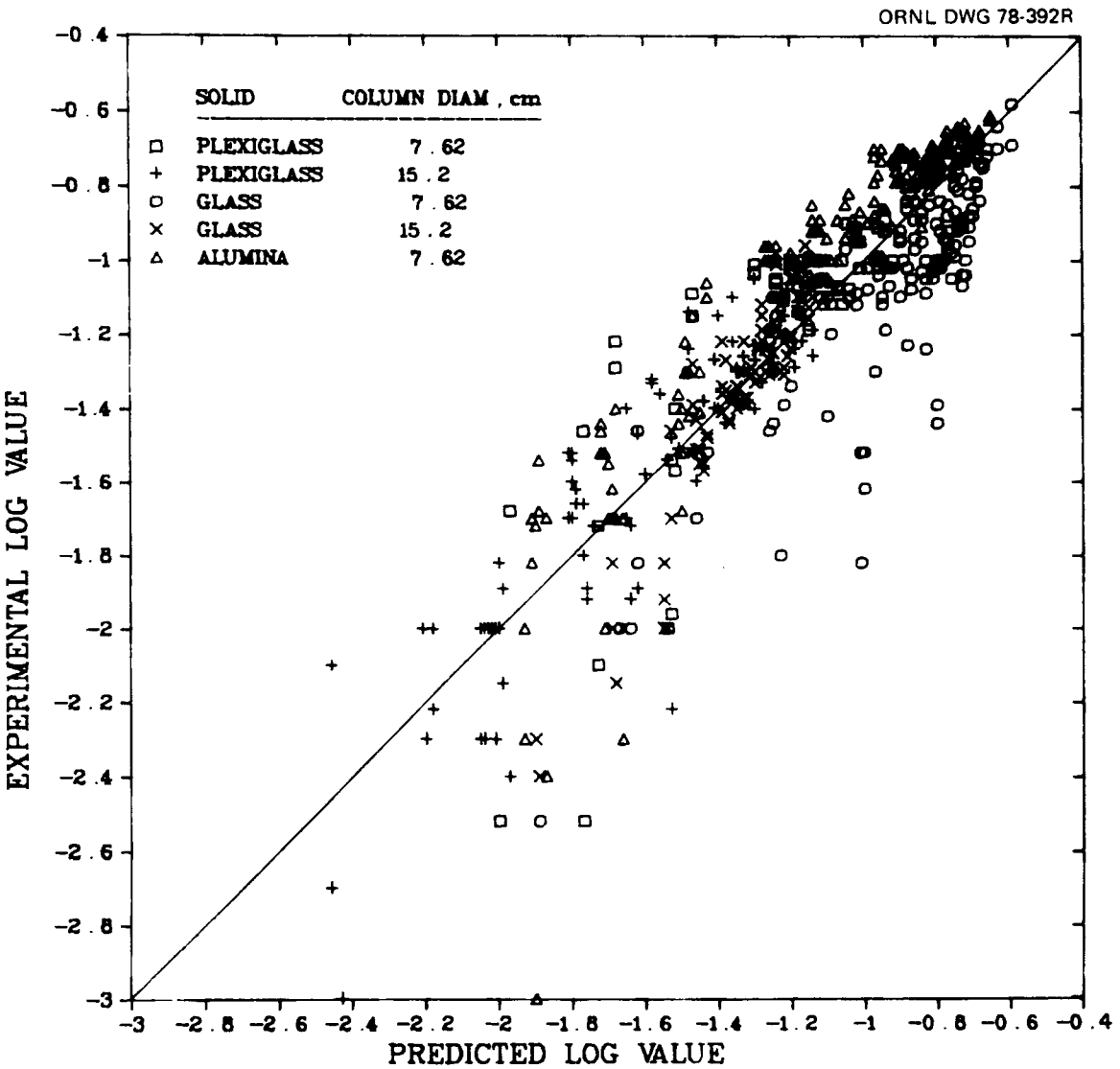

Figure 36. Predicted versus experimental values of the gas holdup in the three-phase region.

correlation coefficient of 0.89 and an F-value of 2155, and was based on a total of 555 points.

The gas holdup in the two-phase portion of the column can be predicted using the following dimensionless correlation:

$$\varepsilon_G'' = a\,[U_G^4(\rho_S-\rho_L)/g\,\sigma_{LV}]^b \quad , \tag{37}$$

where the constants and their 95% confidence limits are:

$a = 0.237 \pm 0.010$,

$b = 0.185 \pm 0.006$.

Equation (37) had a correlation coefficient of 0.93 and an F-value of 4266. The 634 points on which it was based are shown as a parity plot in Fig. 37.

The solid holdup in the bed was correlated as the bed porosity as follows:

$$1-\varepsilon_S''' = a\,Ar^b\,Re_L^c\,(H/H_o)^d \quad , \tag{38}$$

where the constants and their 95% confidence limits are:

$a = 1.990 \pm 0.273$, $c = 0.197 \pm 0.011$,

$b = -0.178 \pm 0.012$, $d = 0.298 \pm 0.018$.

A parity plot of Eq. (38) is shown in Fig. 38. The equation had a correlation coefficient of 0.95 and an F-value of 2529, and was based on 762 points.

The expanded bed height used in Eq. (38) was also correlated with the system properties and resulted in the following:

$$H/H_o = a\,Fr_G^b\,Re_L^c\,Ar^d\,[(\rho_S-\rho_L)/\rho_L]^e \quad , \tag{39}$$

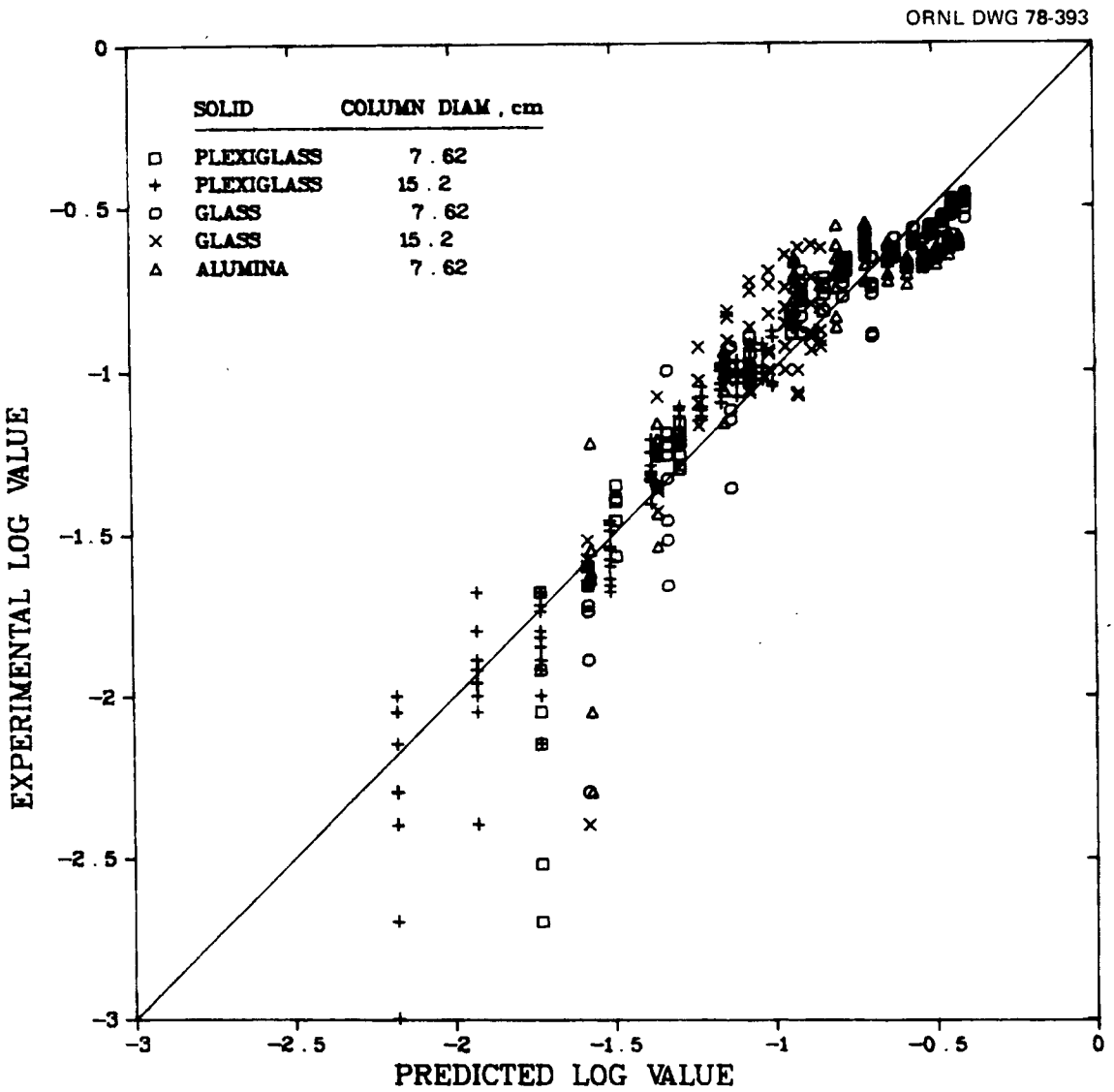

Figure 37. Predicted versus experimental values of the gas holdup in the two-phase region.

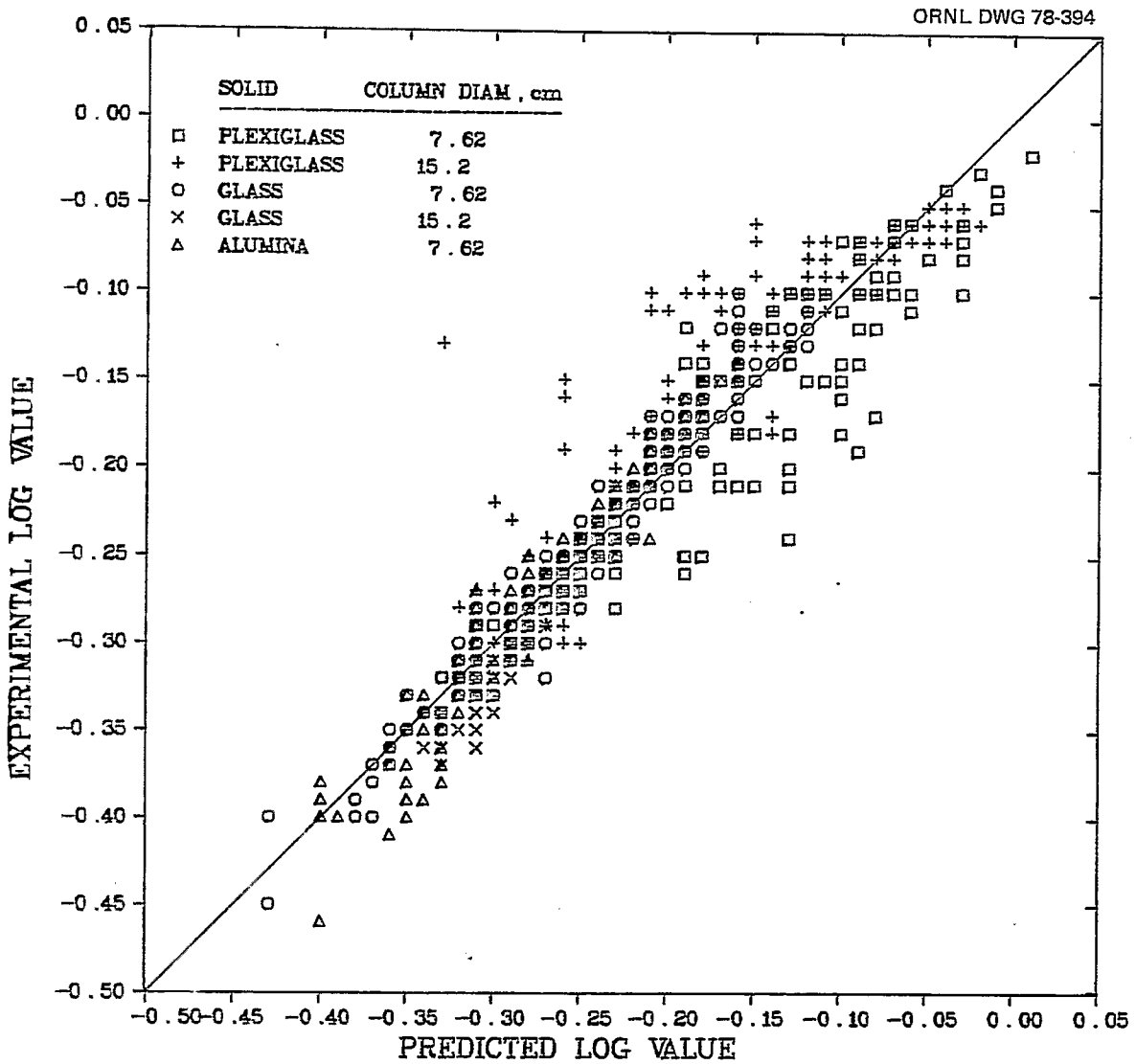

Figure 38. Predicted versus experimental values of the solid holdup in the three-phase region.

where the constants and their 95% confidence limits are:

$a = 10.483 \pm 5.7$, $d = -0.295 \pm 0.039$,

$b = 0.069 \pm 0.005$, $e = -0.305 \pm 0.027$.

$c = 0.429 \pm 0.025$,

Equation (39), based on a total of 706 points, had a correlation coefficient of 0.90 and an F-value of 762; it is shown as a parity plot in Fig. 39.

The inflection point in the solid holdup curve followed the calculated bed height fairly closely and could be correlated by the following:

$$I_S = a\, U_G^{\,b}\, U_L^{\,c}\, D_c^{\,d}\, H^e \quad , \tag{40}$$

where the constants and their 95% confidence limits are:

$a = 2.354 \pm 0.440$, $d = 0.061 \pm 0.031$,

$b = 0.017 \pm 0.008$, $e = 0.628 \pm 0.045$.

$c = 0.247 \pm 0.017$,

Equation (40), which is shown as a parity plot in Fig. 40, had a correlation coefficient of 0.92 and an F-value of 875; it was based on a total of 689 points.

Similarly, the inflection point in the gas holdup curve followed that in the solid holdup curve, yielding the following correlation:

$$I_G/H_o = a\, (\rho_S-\rho_L)^b\, d_p^{\,c}\, D_c^{\,d}\, I_S^{\,e} \quad , \tag{41}$$

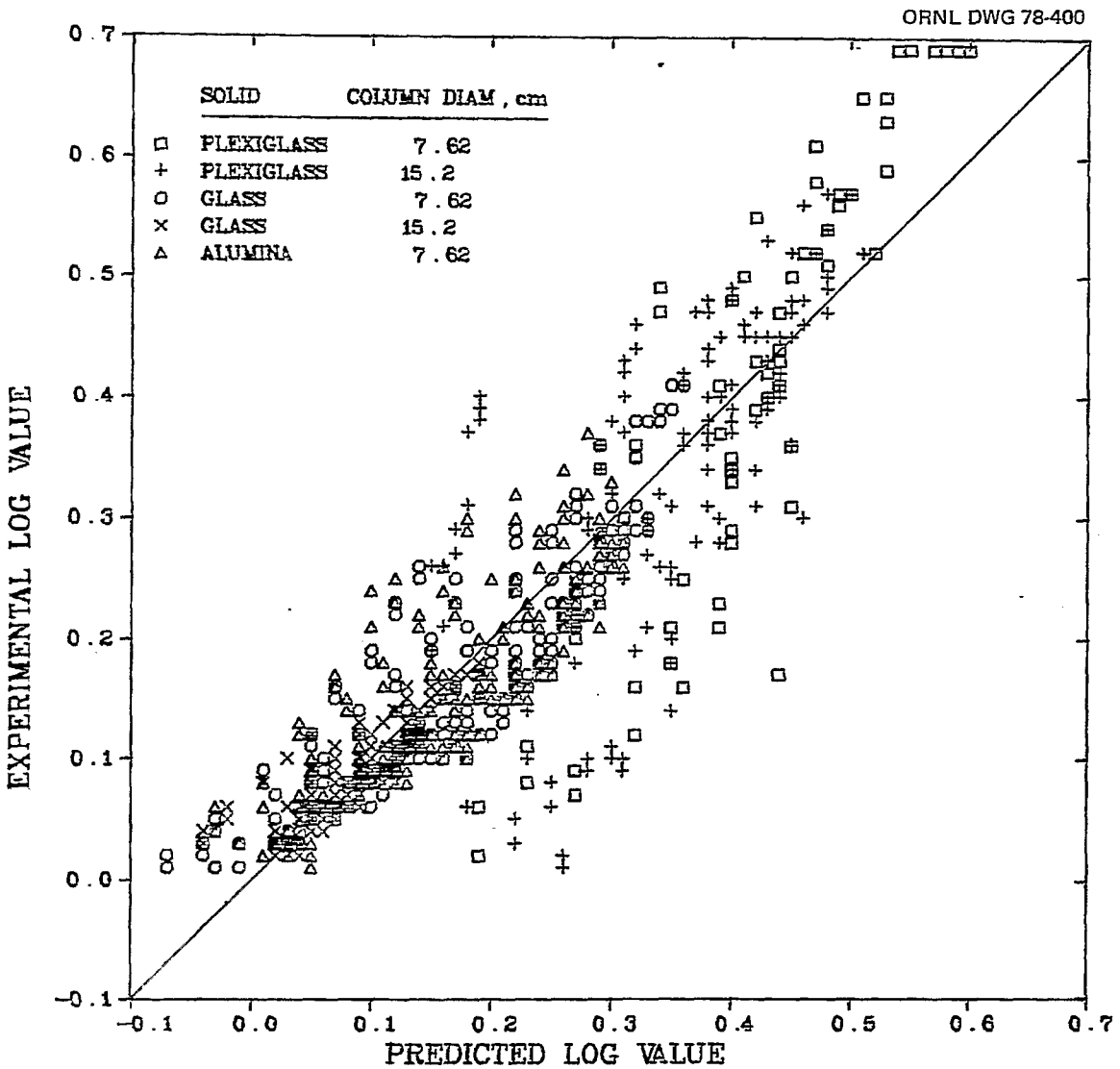

Figure 39. Predicted versus experimental expanded bed height values.

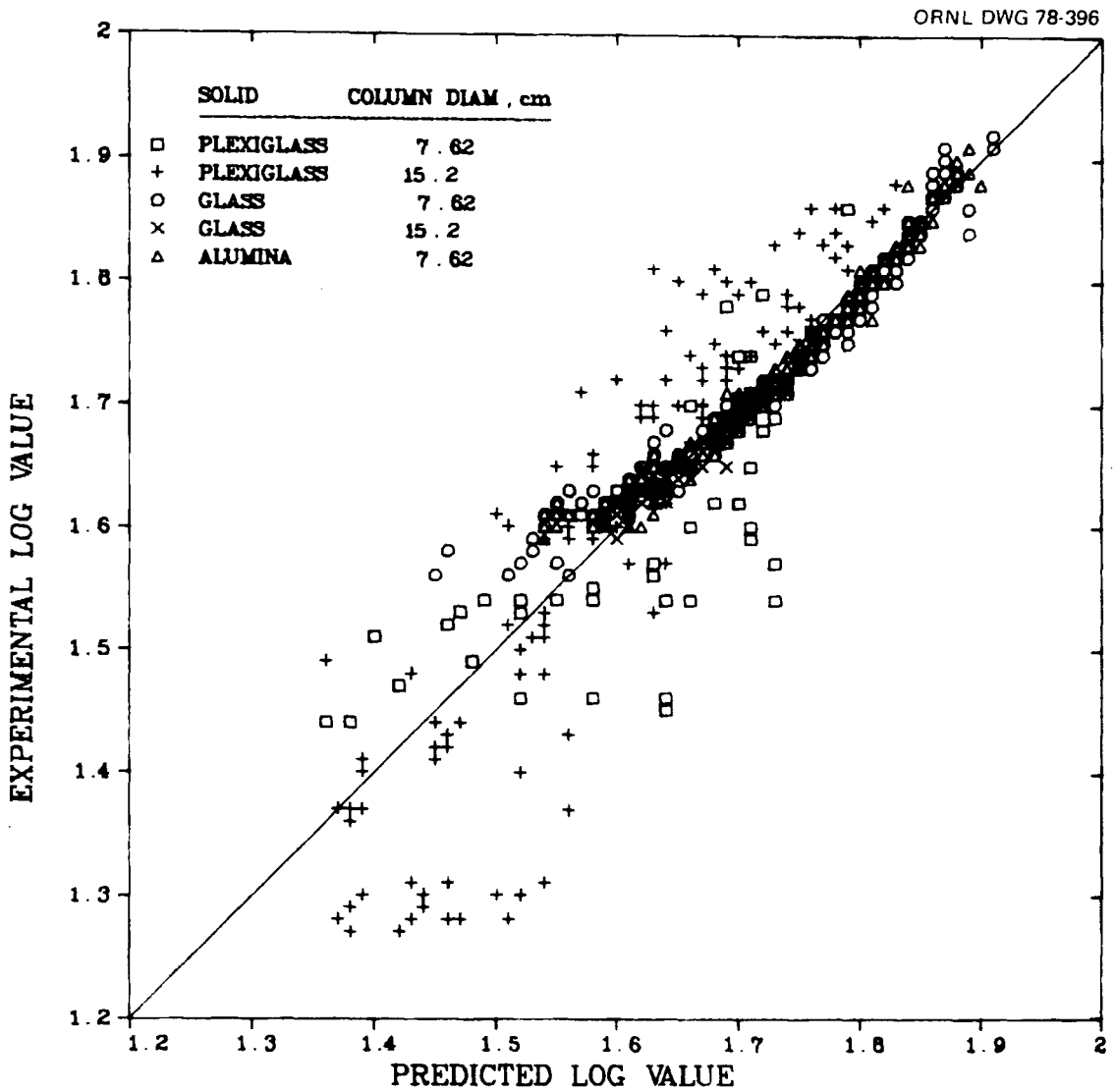

Figure 40. Predicted versus experimental values of the inflection points in the solid holdup curve.

where the constants and their 95% confidence limits are:

$a = 0.027 \pm 0.006$, $d = 0.170 \pm 0.045$,

$b = -0.250 \pm 0.026$, $e = 0.875 \pm 0.049$.

$c = -0.145 \pm 0.123$,

Equation (41), based on a total of 635 points and shown in Fig. 41 as a parity plot, had a correlation coefficient of 0.85 and an F-value of 408.

The standard deviations in the local holdup-versus-height curves were the most difficult parameters to measure (a slight variation in the local holdup affected the standard deviation considerably) and hence to correlate. The standard deviation in the solid phase holdup curve can be estimated from the following:

$$\sigma_S/H_o = a\, C_D^{\,b}\, Fr_H^{\,c} \quad , \qquad (42)$$

where the constants and their 95% confidence limits are:

$a = 5.510 \times 10^{-6} \pm 3.3 \times 10^{-6}$,

$b = -1.015 \pm 0.052$,

$c = -0.840 \pm 0.048$,

and

$$C_D = (\rho_S - \rho_L) d_p / \rho_L U_G^{\,2} \quad ,$$

$$Fr_H = U_G^{\,2}/gH \quad .$$

Equation (42), shown in Fig. 42 as a parity plot, had a correlation coefficient of 0.84 and an F-value of 752; it was based on a total of 635 points.

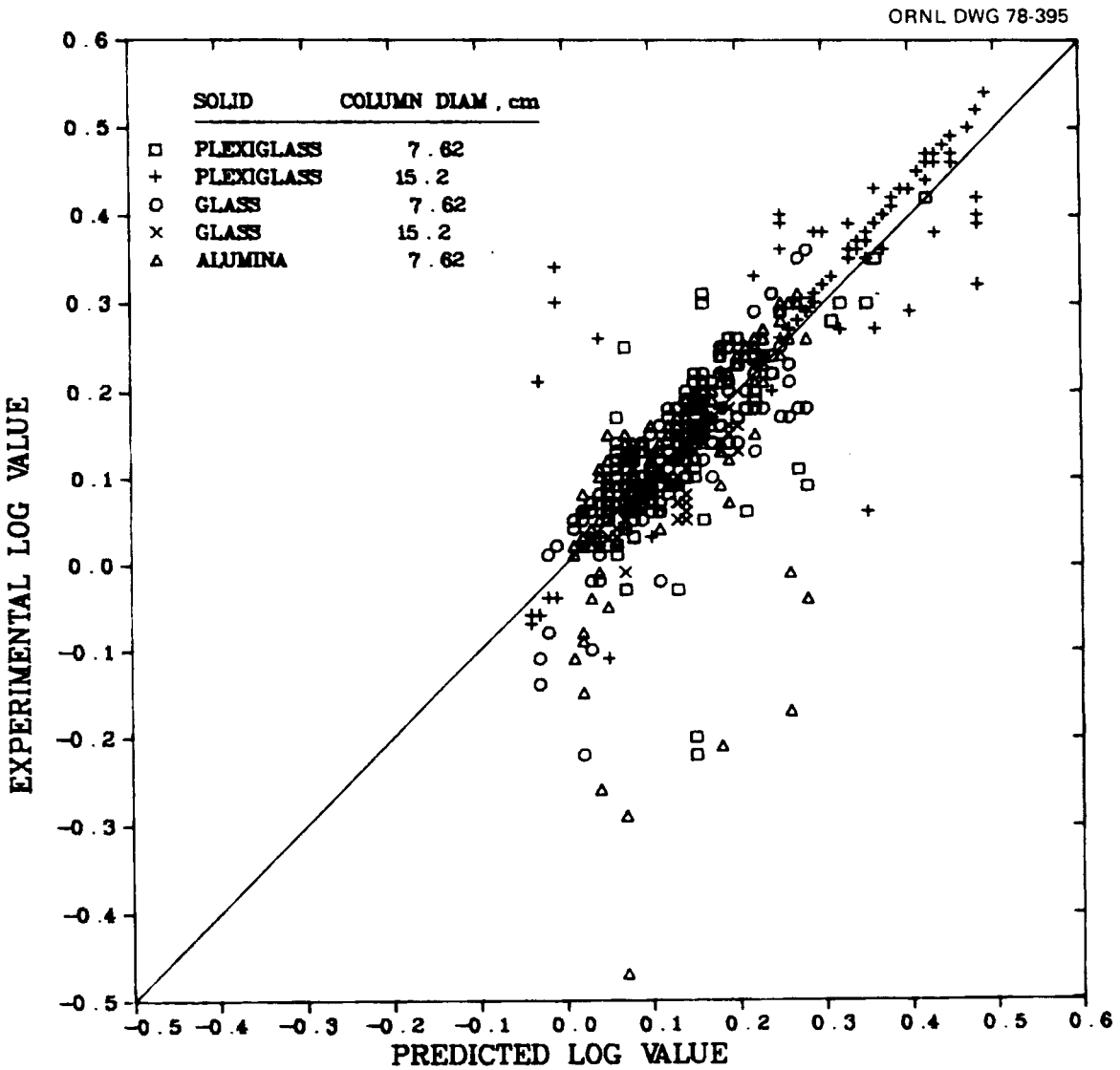

Figure 41. Predicted versus experimental values of the inflection points in the gas holdup curve.

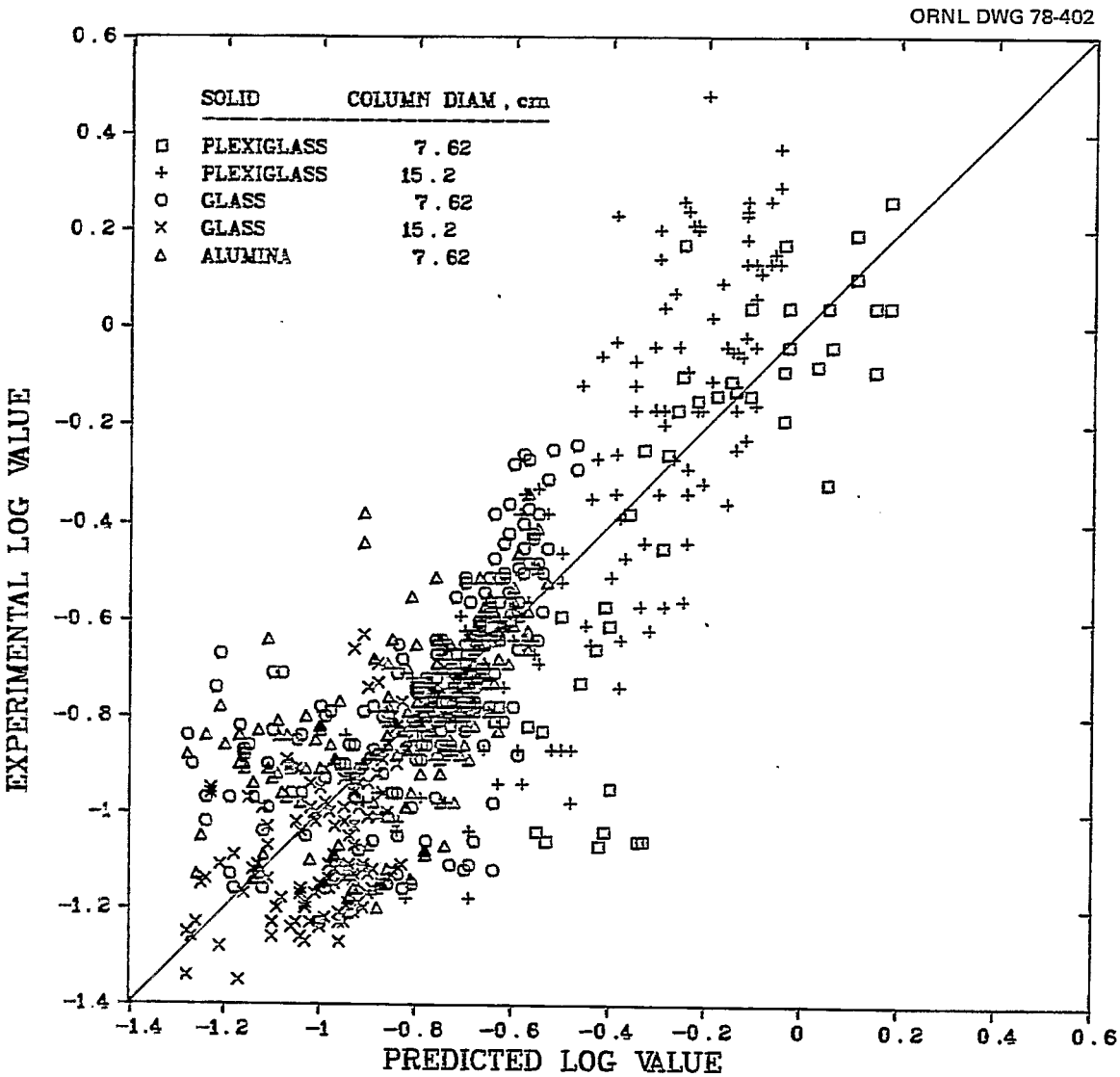

Figure 42. Predicted versus experimental values of the standard deviations in the solid holdup curve.

The standard deviation in the gas phase holdup curve, unfortunately, was even more difficult to correlate than σ_S. A very rough estimate of σ_G can be obtained from the following:

$$\sigma_G/H_o = a\,(\varepsilon_G'' - \varepsilon_G''')^b\,(\rho_S-\rho_L)^c\,d_p^{\,d}\,H^e\,\sigma_S^{\,f}\quad , \qquad (43)$$

where the constants and their 95% confidence limits are:

$a = 0.005 \pm 0.004$, $\quad d = -0.861 \pm 0.461$,

$b = 0.132 \pm 0.061$, $\quad e = 0.693 \pm 0.242$,

$c = -0.362 \pm 0.094$, $\quad f = 0.429 \pm 0.090$.

Equation (43), which was based on a total of 609 points, had a correlation coefficient of 0.66 and an F-value of 93. The parity plot, shown in Fig. 43, indicates that a large amount of the variation between the measured and calculated values of σ_G was due to the two plexiglass beads systems. These beads, with their small solid/liquid density difference, made the pressure gradient (and thus the holdups) difficult to measure--hence the large amount of scatter in the parity plot. However, in the fitting of the local holdup-versus-height curves, it was noted that smoother fits resulted when the gas and solid phase inflection points and standard deviations were similar. Therefore, it might be more appropriate if the inflection point and the standard deviation in the gas phase curve were estimated by equating them to the predicted solid phase values rather than by using Eqs. (41) and (43).

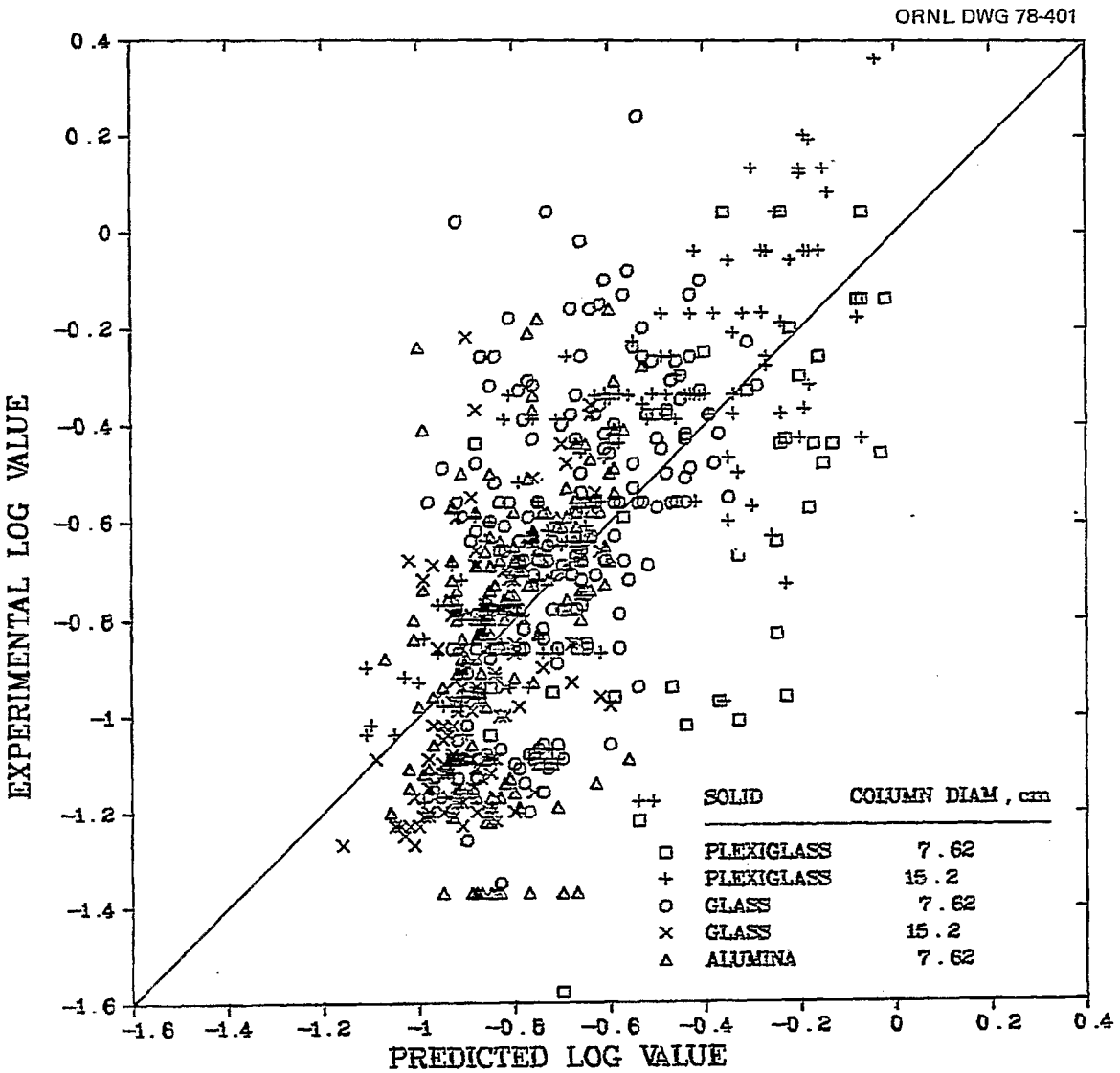

Figure 43. Predicted versus experimental values of the standard deviations in the gas holdup curve.

Figure 44 shows the inflection points in the gas phase holdup curves plotted against the solid phase holdup inflection points. Similarly, the standard deviations in the gas phase holdup curves are plotted against those in the solid phase holdup curves, as shown in Fig. 45. Although a fair amount of scatter is evident in Fig. 44 and especially in Fig. 45, the data in Figs. 41 and 43, which represent least-square fits, are also scattered. In fact, because of the scatter in the correlated fits, it is recommended that both the inflection point and the standard deviation of each of the three holdup curves be estimated by a single equation. Equation (42) should be used for the standard deviation in the holdup curves.

A further simplification can be made for the inflection point in the holdup curves. As mentioned previously, the inflection point in the solid holdup curve followed the calculated bed height closely. The two parameters are shown plotted against each other in Fig. 46. The agreement between the two is quite good, as expected, since the calculated bed height represents that height in the column of an equivalent homogeneous bed. Disagreements occurred chiefly in beds of plexiglass beads, particularly those that were highly expanded.

An example of an expanded bed of plexiglass beads is shown in Fig. 47. Under the set of conditions indicated, the concentration of solids decreased very gradually to zero, giving a solid phase inflection point of 36 cm.

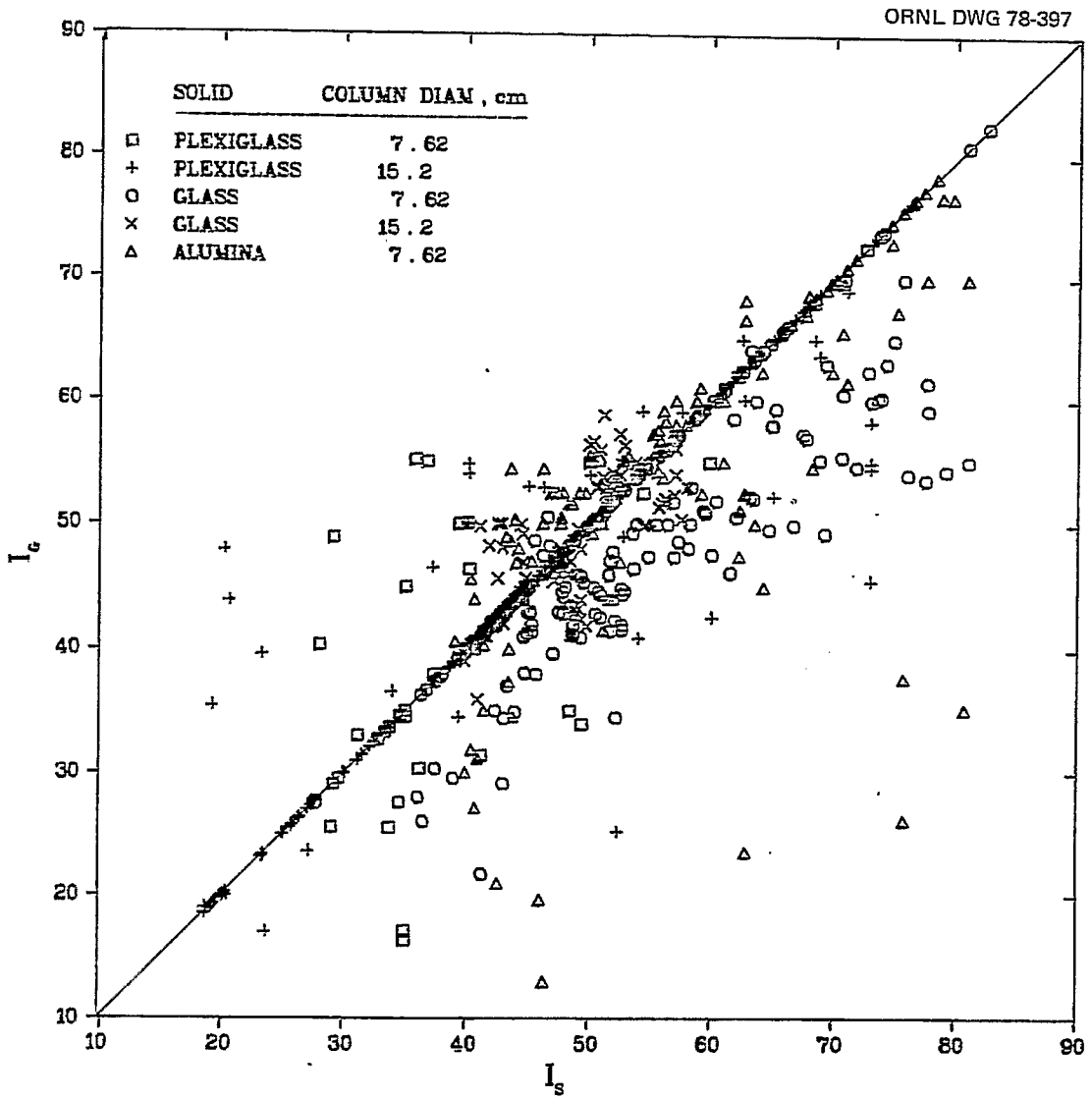

Figure 44. Gas-holdup-curve inflection points versus solid-holdup-curve inflection points.

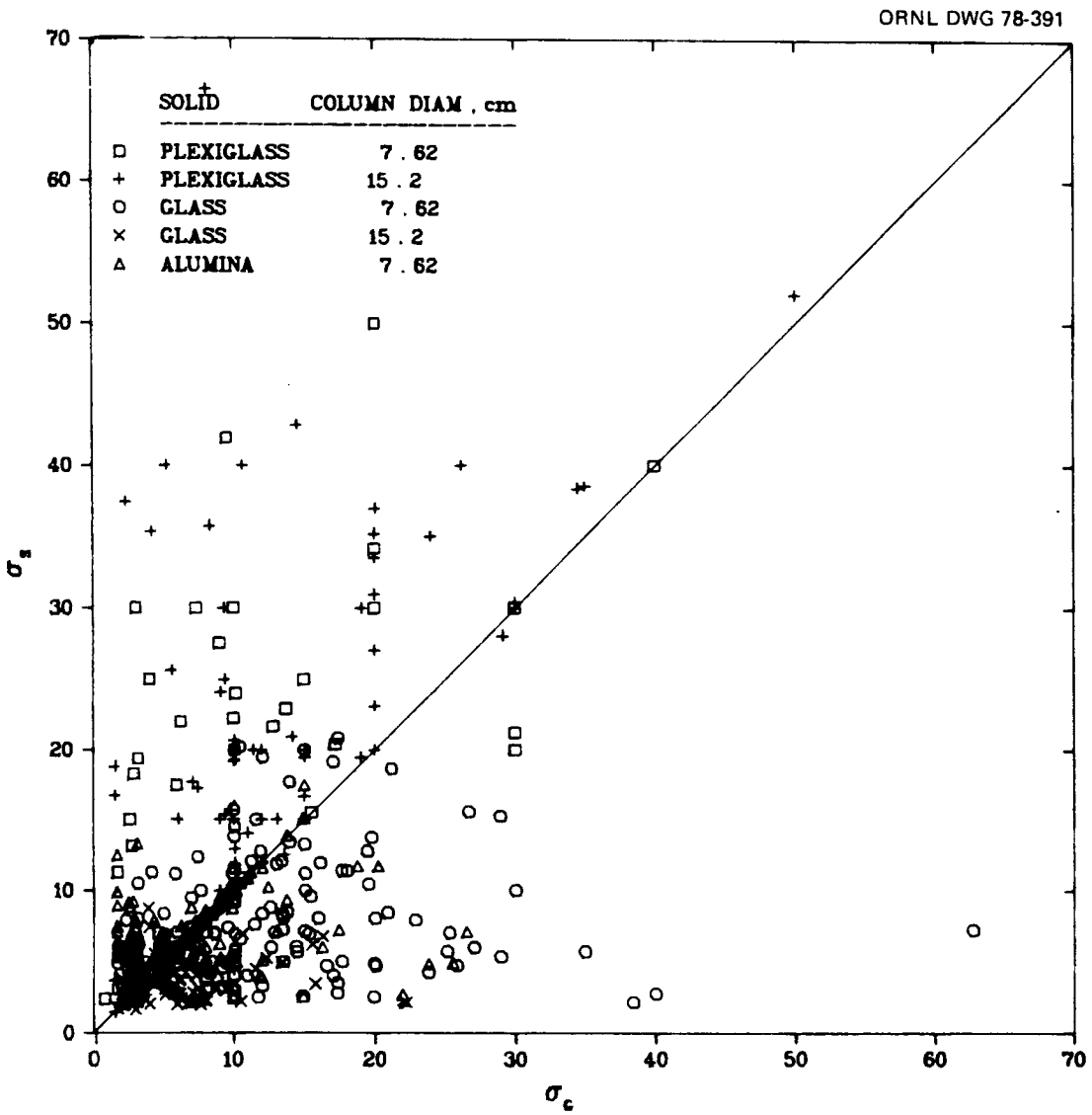

Figure 45. Standard deviations for the gas holdup curve versus those for the solid holdup curve.

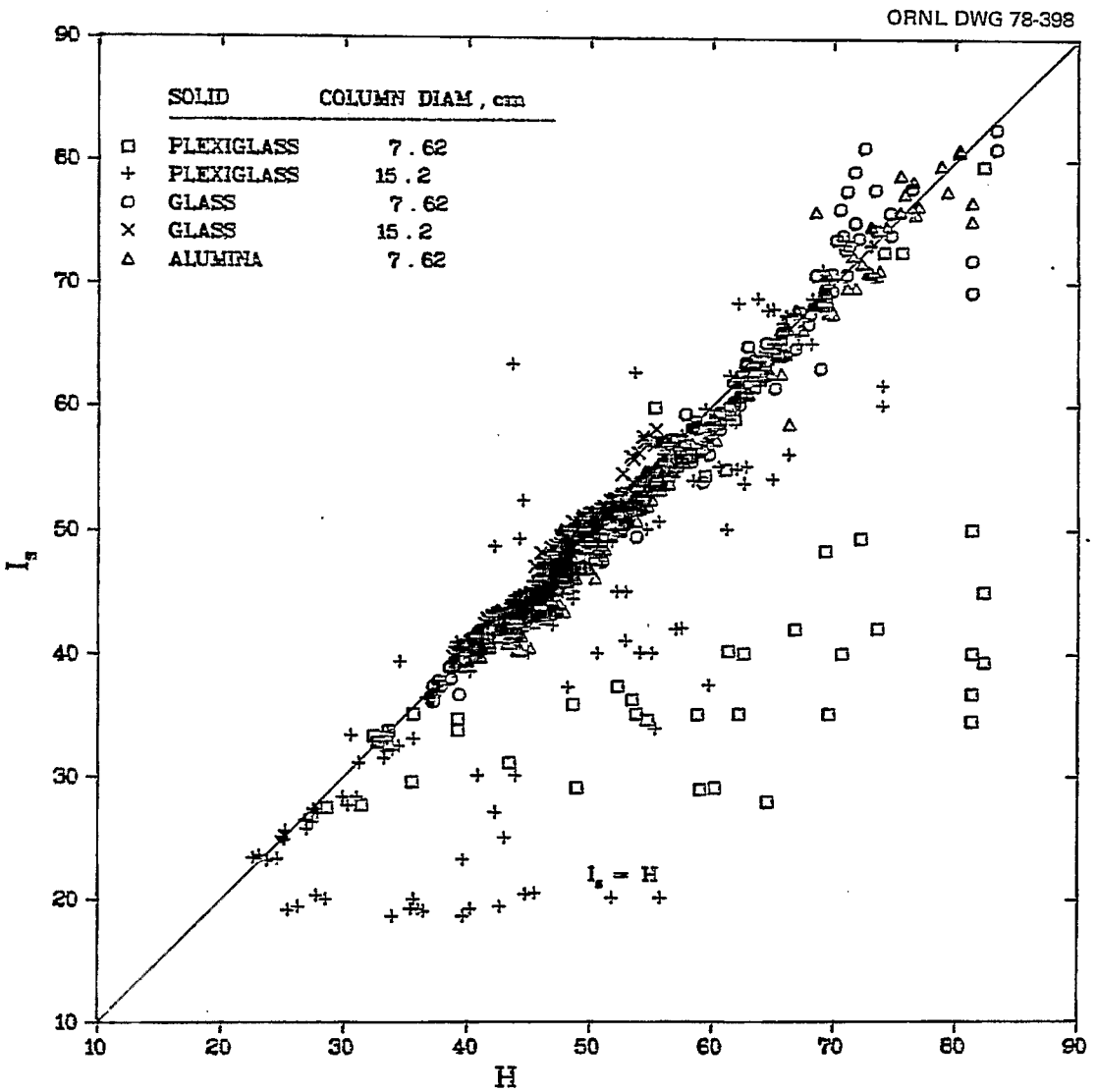

Figure 46. Inflection points in the solid holdup curve versus the calculated bed heights.

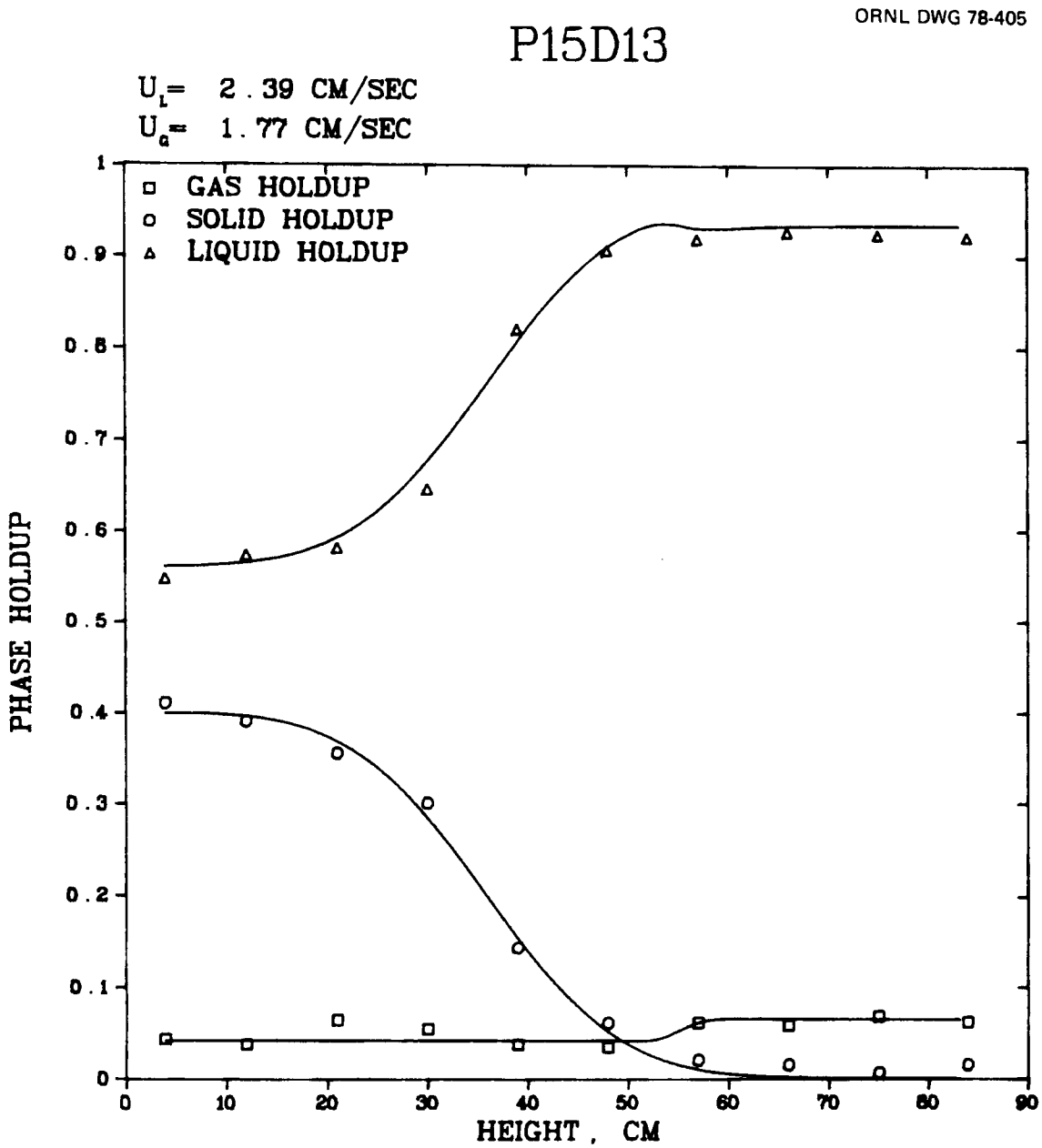

Figure 47. Axial variation of phase holdups in a bed of plexiglass beads.

However, the pressure gradient over the two- and three-phase regions yielded a calculated bed height of 49 cm. It has been mentioned several times that the low solid/liquid density difference of the plexiglass beads made calculation of the bed heights and pressure drops subject to larger potential errors than those associated with the other solids studied. Thus, with the possible exception of very low solid/liquid density difference systems, it is recommended that Eq. (39) be used to predict both the expanded bed heights and the inflection points in the three holdup curves.

In summary, then, it is recommended that the following dimensionless correlations be used to construct phase holdup versus column position curves: (a) Equations (36)-(38) for estimating the gas and solid phase holdups in the two- and three-phase regions, (b) Equation (39) for determining the inflection point in each of the three phase holdup curves; and (c) Equation (42) for calculating the standard deviation in each of the three phase holdup curves.

All of the parameters employed in these correlations [Eqs. (36)-(43)] are expressed in CGS units. The correlations were based on a varying number of total points, depending on how many of the points used were zero (i.e., ε_G''', ε_G'', σ_G, and I_G) and how many were associated with zero gas flow rates. Such points could not be logarithm transformed and hence could not be used in the multiple linear regression analysis. Also, a number of experimental

conditions were used such that the bed height was above the highest manometer tap. The transition between the three- and two-phase regions could not be determined under such conditions; therefore, only the solid phase holdup was measured.

Care should be exercised when applying these correlations to systems with physical parameters far removed from those used in this study. All of the beads used herein were spherical, and the remaining physical parameters covered in these correlations are given in Tables 1 and 2 (see page 34).

CHAPTER 7

CONCLUSIONS

The minimum gas and liquid velocities required to fluidize various types of solids were determined and correlated as a function of particle size, particle density, and liquid viscosity; no effect of the initial bed height or column diameter was found.

Overall phase holdups determined from a homogeneous bed model were combined with similarly determined literature data to yield correlations for the overall solid and gas phase holdups. The overall solid holdup, which was primarily a function of the liquid velocity, solid/liquid density difference, and the particle diameter, varied proportionally with the latter two parameters and inversely with the liquid velocity. The overall gas holdup was primarily a function of the gas velocity and was almost proportional to it.

An electroconductivity technique was adapted for use in three-phase fluidized beds and permitted measurement of the local phase holdups to be determined as a function of position in the columns. This technique has shown the existence of a transition region as the bed goes from a three-phase to a two-phase system. The transition region where the solids concentration drops to zero was found to increase in width with increasing gas velocity, but was unaffected by changes in liquid velocity or column diameter.

One disadvantage of the technique is that it can only be applied to systems with electroconductive liquids. However, since most real or prototype systems either use water or can be simulated with a fluid capable of being made electroconductive, this handicap is not overly restrictive. The technique can be successfully applied to a number of systems, including porous alumina beads if a correction is made for their internal porosity.

Using the seven parameters determined from the local gas and solid holdup profiles, it was possible to fit each of the holdup-versus-column height curves. Use of the dimensionless correlations of just five of these parameters-- ε_G''', ε_G'', ε_S''', σ_S , and H-- should give a reactor designer more information concerning important phase distributions than is available from the simpler homogeneous bed model, and thus aid in the rational design of reactors in which local conditions throughout the bed must be considered. Of course, the correlations should not be used for conditions far beyond the range on which they are based.

LIST OF REFERENCES

LIST OF REFERENCES

Achwal, S. K. and J. B. Stepanek (1975), "An Alternate Method of Determining Holdup in Gas-Liquid Systems," Chem. Eng. Sci. 30, 1443.

Achwal, S. K. and J. B. Stepanek (1976), "Holdup Profiles in Packed Beds," Chem. Eng. J. 12, 69.

Adlington, D. and E. Thompson (1965), "Desulphurization in Fixed and Fluidized Bed Catalyst Systems," Proc. 3rd European Symp. Chem. React. Eng., Pergamon Press, Oxford, p. 203.

Begovich, J. M. (1978) in Advanced Technol. Sect. Semiannu. Progr. Rep. for Period Sept. 1, 1976 to Mar. 31, 1977; Engineering Science Programs, ORNL/TM-6012 (in preparation).

Bhatia, V. K. and N. Epstein (1974), "Three-Phase Fluidization: A Generalized Wake Model," Proc. Int. Symp. on Fluidization and Its Applications, Cepadues Editions, Toulouse, p. 380.

Bhatia, V. K., K. A. Evans, N. Epstein, and P. Dakshinamurty (1972), "Effect of Solids Wettability on Expansion of Gas-Liquid Fluidized Beds," Ind. Eng. Chem. Proc. Des. Dev. 11(1), 151.

Bloxom, S. R., J. M. Costa, J. Herranz, G. L. MacWilliam, and S. R. Roth (1975), Determination and Correlation of Hydrodynamic Variables in a Three-Phase Fluidized Bed, Part IV, ORNL-MIT-219, Mass. Inst. Technol., School of Chem. Eng. Practice, Oak Ridge, Tennessee.

Blum, D. B. and J. J. Toman (1977), "Three-Phase Fluidization in a Liquid Phase Methanator," AIChE Symp. Ser. 73(161), 115.

Bruce, P. N. and L. Revel-Chion (1974), "Bed Porosity in Three-Phase Fluidization," Powder Technol. 10, 243.

Burck, G. M., K. Kodama, R. G. Markeloff, and S. R. Wilson (1975), Cocurrent Three-Phase Fluidized Bed, Part II, ORNL-MIT-213.

Buyevich, Y. A. (1974), "On the Thermal Conductivity of Granular Materials," Chem. Eng. Sci. 29, 37.

Dakshinamurty, P., K. V. Rao, R. V. Subbaraju, and V. Subrahmanyam (1972), "Bed Porosities in Gas-Liquid Fluidization," Ind. Eng. Chem. Proc. Des. Dev. 11(2), 318.

Dakshinamurty, P., V. Subrahmanyam, and J. N. Rao (1971), "Bed Porosities in Gas-Liquid Fluidization," Ind. Eng. Chem. Proc. Des. Dev. 10(3), 322.

Efremov, G. I. and I. A. Vakhrushev (1970), "A Study of the Hydrodynamics of Three-Phase Fluidized Beds," Int. Chem. Eng. 10(1), 37.

Epstein, N. (1976), "Criterion for Initial Contraction or Expansion of Three-Phase Fluidized Beds," Can. J. Chem. Eng. 54, 259.

Francl, J. and W. D. Kingery (1954), "Thermal Conductivity: IX, Experimental Investigation on the Effect of Porosity on Thermal Conductivity," J. Am. Ceram. Soc. 37, 99.

Hellwig, K. C., M. C. Chervenak, E. S. Johanson, H. H. Stotler, and R. H. Wolk (1968), "Convert Coal to Liquid Fuels with H-Coal," Chem. Eng. Prog. Symp. Ser. 64(85), 98.

Khosrowshahi, S., S. R. Bloxom, C. Guzman, and R. M. Schlapfer (1975), Cocurrent Three-Phase Fluidized Bed. Part III, ORNL-MIT-216.

Kim, S. D., C. G. J. Baker, and M. A. Bergougnou (1972), "Holdup and Axial Mixing Characteristics of Two and Three Phase Fluidized Beds," Can. J. Chem. Eng. 50, 695.

Kim, S. D., C. G. J. Baker, and M. A. Bergougnou (1975), "Phase Holdup Characteristics of Three-Phase Fluidized Beds," Can. J. Chem. Eng. 53, 134.

Maxwell, J. C. (1881), A Treatise on Electricity and Magnetism, 2nd ed., Vol. 1, Clarendon Press, Oxford, p. 398.

Meredith, R. W. and C. W. Tobias (1962), "Conduction in Heterogeneous Systems," Advances in Electrochemistry and Electrochemical Engineering, 2, Interscience, New York, p. 15.

Michelsen, M. L. and K. Ostergaard (1970), "Holdup and Fluid Mixing in Gas-Liquid Fluidized Beds," Chem. Eng. J. 1, 37.

Mukherjee, R. N., P. Bhattacharya, and D. K. Taraphdar (1974), "Studies on the Dynamics of Three-Phase Fluidization," Proc. Int. Symp. on Fluidization and Its Applications, Cepadues Editions, Toulouse, p. 372.

Ostergaard, K. (1965), "On Bed Porosity in Gas-Liquid Fluidization," Chem. Eng. Sci. 20, 165.

Ostergaard, K. (1971), Chapter 18, Fluidization, ed. by J. F. Davidson and D. Harrison, Academic Press, New York.

Ostergaard, K. and H. L. Michelsen (1968), "Holdup and Axial Dispersion in Gas-Liquid Fluidized Beds," Preprint 31d, 2nd Joint AIChE-IIQPR Meeting, Tampa, Florida, May 19-22.

Ostergaard, K. and P. I. Thiesen (1966), "The Effect of Particle Size and Bed Height on the Expansion of Mixed Phase (Gas-Liquid) Fluidized Beds," Chem. Eng. Sci. 21, 413.

Pichler, H., H. C. Chervenak, C. A. Johnson, M. C. Sze, and J. F. Campagnolo (1957), "The 'H-Oil' Process," Oil Gas J. 55(39), 109.

Razumov, I. M., V. V. Manshilin, and L. L. Nemets (1973), "The Structure of Three-Phase Fluidized Beds," Int. Chem. Eng. 13(1), 57.

Richardson, J. F. and W. N. Zaki (1954), "The Sedimentation of a Suspension of Uniform Spheres Under Conditions of Viscous Flow," Chem. Eng. Sci. 3, 65.

Rigby, G. R. and C. E. Capes (1970), "Bed Expansion and Bubble Wakes in Three-Phase Fluidization," Can. J. Chem. Eng. 48, 343.

Saad, E. T., H. D. Ayala, W. M. Burke, and D. K. Clarkson (1975), Cocurrent Three-Phase Fluidized Bed, Part I, ORNL-MIT-209.

Schugerl, K. (1967), "Experimental Comparison of Mixing Processes in Two- and Three-Phase Fluidized Beds," Proc. Int. Symp. on Fluidization, Netherlands University Press, Amsterdam, p. 782.

Scott, C. D. et al. (1976), Experimental Engineering Sect. Semiannu. Progr. Rep. (Excluding Reactor Programs), March 1, 1975 to August 31, 1975, ORNL-TM-5291, Section 4.3.

Sherrard, A. J. (1966), "Three-Phase Fluidized Beds," Dissertation, University College of Swansea, Wales.

Stewart, P. S. B. and J. F. Davidson (1964), "Three-Phase Fluidization: Water, Particles, and Air," Chem. Eng. Sci. 19, 319.

Turner, J. C. R. (1976), "Two-Phase Conductivity: The Electrical Conductance of Liquid Fluidized Beds of Spheres," Chem. Eng. Sci. 31, 487.

Vail, Y. K., N. K. Manakov, and V. V. Manshilin (1970), "The Gas Contents of Three-Phase Fluidized Beds," Int. Chem. Eng. 10(2), 244.

Viswanathan, S., A. S. Kakar, and P. S. Murti (1964), "Effect of Dispersing Bubbles into Liquid Fluidized Beds on Heat Transfer and Holdup at Constant Bed Expansion," Chem. Eng. Sci. 20, 903.

Watson, J. S. (1975), Oak Ridge National Laboratory, personal communication.

Wen, C. Y. and Y. H. Yu (1966), "Mechanics of Fluidization," Chem. Eng. Prog. Symp. Ser. 62(62), 100.